A Genetic Algorithm for Automatic Optical Inspection

Syamsiah Mashohor

A thesis submitted for the degree of Doctor of Philosophy.
The University of Edinburgh.
26th September 2006

Abstract

In high and medium production lines, conveyor belts are usually employed to speed up the manufacturing process. Therefore, placing a Printed Circuit Board (PCB) on a conveyor belt in high precision for visual inspection is very tedious and costly with aid of hardware. As a consequence, a robust image registration technique is crucial in order to register images of inspected PCBs with high quality but in low computational time.

This thesis investigates the ability of Genetic Algorithm (GA) in optimising the image registration of whole PCBs to offer linearity in positioning whole board of PCBs on a conveyor belt during acquisition stage of an inspection process. A novel GA based image registration is developed and tailored for accuracy, speed and reliability.

The performance of the GA based image registration determines the success of a special defect detection procedure which employs a combination of image processing functions. The procedure produces excellent results in detecting absence component defect and open solder joints on the whole inspected PCBs in any shape and size. The performance of this procedure is presented in this thesis implies the potential of this system integration between GA based image registration and the defect detection procedure.

The system proves that it is able to register images in high accuracy and consequently manage to produce high quality of defect detection results in low computing time which is 1 minute. Further experiments on a number of PCB types indicate the system flexibility to inspect different types of board especially the high-density layout.

Declaration of originality

I declare that the work presented in the thesis is, to the best of my knowledge and belief, original and my own work, except as acknowledged in the text, and that the material has not been submitted, either in whole or in part, for a degree at this or any other university.

Acknowledgements

I am very grateful to my supervisor, Professor Tughrul Arslan, for providing excellent assistance and unwavering support during my study period, without which it would not have been realised.

I also wish to thank several other people who have been instrumental in making this work a reality by providing helpful comments and assistance. Foremost among these stands Dr. Jonathan R. Evans and Dr. Robert Thompson, my mentors who introduced me to the exciting world of genetic algorithms in 2002, and of course my colleagues at the laboratory especially the members of Evolvable group.

Special appreciations to my sponsor, Ministry of Science, Technology and Innovations (MOSTI) and my employer, University Putra Malaysia (UPM) in Malaysia for giving me a chance to further my study. My biggest thanks go to my husband, Khairulmizam Samsudin for his understanding, support, encouragement and patience over the years. To my daughter, Amatullah Nazirah, thank you for your motivation in your special way. Finally, thanks to my family in Malaysia who always pray for my success.

Contents

List of Figures

List of Tables

Acronyms and abbreviations

AOI	Automatic Optical Inspection
ASMs	Active Shape Models
CAD	Computer Aided Design
CCA	Circuit Card Assemblies
CCD	Charge-Coupled Device
DNA	Deoxyribonucleic Acid
DSA	Digital Subtraction Angiographies
E	Elitism
GA	Genetic Algorithm
HC	Hill-Climbing
HGA	Hybrid Genetic Algorithm
IC	Integrated Circuit
ID	Identification Data
MRI	Magnetic Resonant Imaging
PC	Personal Computer
PCB	Printed Circuit Board
p_c	Probability of Crossover
p_m	Probability of Mutation
RMS	Root Mean Square
SGA	Simple Genetic Algorithm
SMD	Surface Mount Device
SOC	System-On-Chip
3-D	3-Dimensions

Publications

The work presented in this thesis has been published in four major conferences and submitted to one transaction.

1. S. Mashohor, J. R. Evans and T. Arslan, "Genetic Algorithm based Printed Circuit Board (PCB) Inspection System", IEEE International Symposium on Consumer Electronics, p 519 - 522, 2004.

2. S. Mashohor, J. R. Evans and T. Arslan, "Elitist Selection Schemes for Genetic Algorithm based Printed Circuit Board Inspection System", IEEE Congress on Evolutionary Computation, Volume 2, p 974 - 978, 2005.

3. S. Mashohor, J. R. Evans and T. Arslan, "Image Registration of Printed Circuit Boards using Hybrid Genetic Algorithm", IEEE Congress on Evolutionary Computation, 2006.

4. S. Mashohor, J. R. Evans and Ahmet T. Erdogan, "Automatic Hybrid Genetic Algorithm Based Printed Circuit Board Inspection", First NASA/ESA Conference on Adaptive Hardware and Systems (AHS 2006), p 390 - 400, 2006.

5. S. Mashohor, J. R. Evans and T. Arslan, "An Image Registration using Hybrid Genetic Algorithm", submitted to IEEE Transactions on Evolutionary Computation, 2006.

Chapter 1
Introduction

1.1 Introduction

The inspection of manufactured products is an important industrial activity and most expensive stage. To fulfil the demand of productivity and quality in industries, vision-based inspection offers low-cost, high-speed, and high-quality detection of defects. Automated Optical Inspection (AOI) is one of the most explored application fields of computer vision for its importance in the automation of industrial production lines. Many researchers have proposed different algorithms to reduce the cost and space restrictions, while improve the throughput and range of defects that can be detected.

There are many commercially available automatic optical inspection systems that have been produced for different types of inspection but they are very costly for low and medium industries. The ongoing research focused on giving more options to the manufacturers in solving more problems in inspection with reduction in cost. There are numerous algorithms, techniques and approaches in the area of automated visual PCB inspection. Recently, many research works are carried out to produce low-cost inspection system such as image analysis with the assistance of structured lighting [1], artificial neural network with back propagation [2], Haar wavelet and coarse resolution for defect localisation [3]. Each work focused on different scope of problem including inspection of solder joints [4–9], lead displacement, PCB pattern's defects [2, 3, 10–13] or all type of cosmetic defects [14, 15].

The remainder of this chapter is structured as follows: in Section 1.2, the motivation of this work is presented; the main contributions of this work is presented in Section 1.3; Section 1.4 describes the details of prototype system of this work and the description of structure of this thesis is presented in Section 1.5.

1.2 Motivations

Due to higher expectation of productivity in today's manufacturing environment, the PCB manufacturers particularly high-volume production employ conveyor belts in most of the manufacturing process. A correct alignment of the completed PCBs on a conveyor belt is very crucial in order to capture PCB images for inspection purposes especially in reference-based method [16]. Therefore, a common solution is to place the inspected PCBs in high precision on a conveyor belt by utilising high cost hardware such as mechanical jigs and X-Y tables. In most cases, industrial automation systems are designed to inspect only known objects at fixed positions [17]. Due to these practises, automatic image registration offers enormous advantage in reducing the cost of inspection that also will benefit the end users.

In reference-based visual inspection technique, every image of inspected PCB (test image) is compared with a reference image to find the differences between both images which may become the possible defects. The technique is accurate only when the condition that both images are aligned. Image registration attempts to find the relative transforms in the test image with respect to the reference image by searching a correct combination of transformation parameters in large search space.

For small spaces, classical exhaustive methods usually suffice; for larger spaces special artificial intelligence techniques such as Genetic Algorithm (GA) must be employed [18]. GA are stochastic algorithms whose search methods model some natural phenomena such as genetic inheritance and Darwinian strife for survival. GA are a class of general purpose (domain independent) search methods which strike a remarkable balance between exploration and exploitation of the search space.

While most of the registration techniques employ linear search over the sampling of search scope, some researchers have attempted to apply GA to assist searching over the complex search scope [19]. A hardware parallel GA has been studied for vision systems which require processing techniques which are robust, fast and capable of dealing with large quantities of data in [20]. In contrast, relatively little work has been done to implement the GA in industrial inspection, and in particular the PCB inspection due to high computation time which is a major drawback for real-time application. This

thesis addresses the question of whether GAs can be used to register PCB images robustly to facilitate defect detection procedure in real-time inspection environment with low cost implementation.

1.3 Contributions

The main objective of this thesis can be summarised by the following statement:

To develop a specially-tailored GA based image registration for whole completed PCBs that are placed arbitrarily on conveyor belt to facilitate a novel defect detection procedure in order to produce high accuracy, reliable and fast inspection system.

This can be split into four key areas:

1. To demonstrate the use of GA for the image registration of whole PCBs placed arbitrarily on a conveyor belt.
2. To improve the performance and capabilities of GA for this application by implementing several significant enhancements.
3. To investigate the robustness of the novel defect detection procedure that employed a number of image processing operations.
4. To demonstrate the performance of the complete automatic system that integrate GA based image registration and defect detection procedure in real-time perspective for detecting missing component defects including open solder joints.

1.4 System prototype

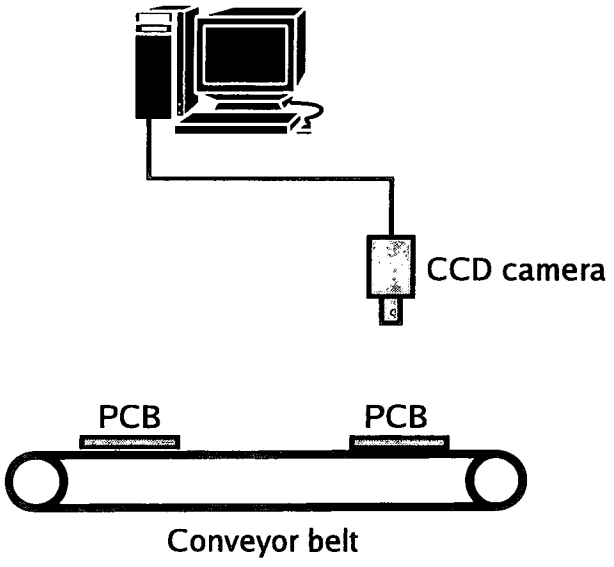

Figure 1.1: *System diagram*

This research aims to produce a low-cost automatic visual inspection system for PCBs using a specially-tailored GA and a novel defect detection procedure. It consists of a PC without the assistance of CAD data (CAD data specifies which components are on the board and their positions) and a CCD camera as shown in Figure 1.1.

PCB production lines require a whole inspected board positioned correctly on a conveyor belt under the camera during the image of the board is captured. Referential method requires particularly accurate alignment to analyse the captured image of inspected PCB [21]. For that, this system offer a linearity on board's positioning which can reduce production time and can cut the labour cost. The flow of this system is described in detail in Figure 1.2. The GA is used to find most optimum rotation and displacement values for every inspected board to aid the defects recognition process.

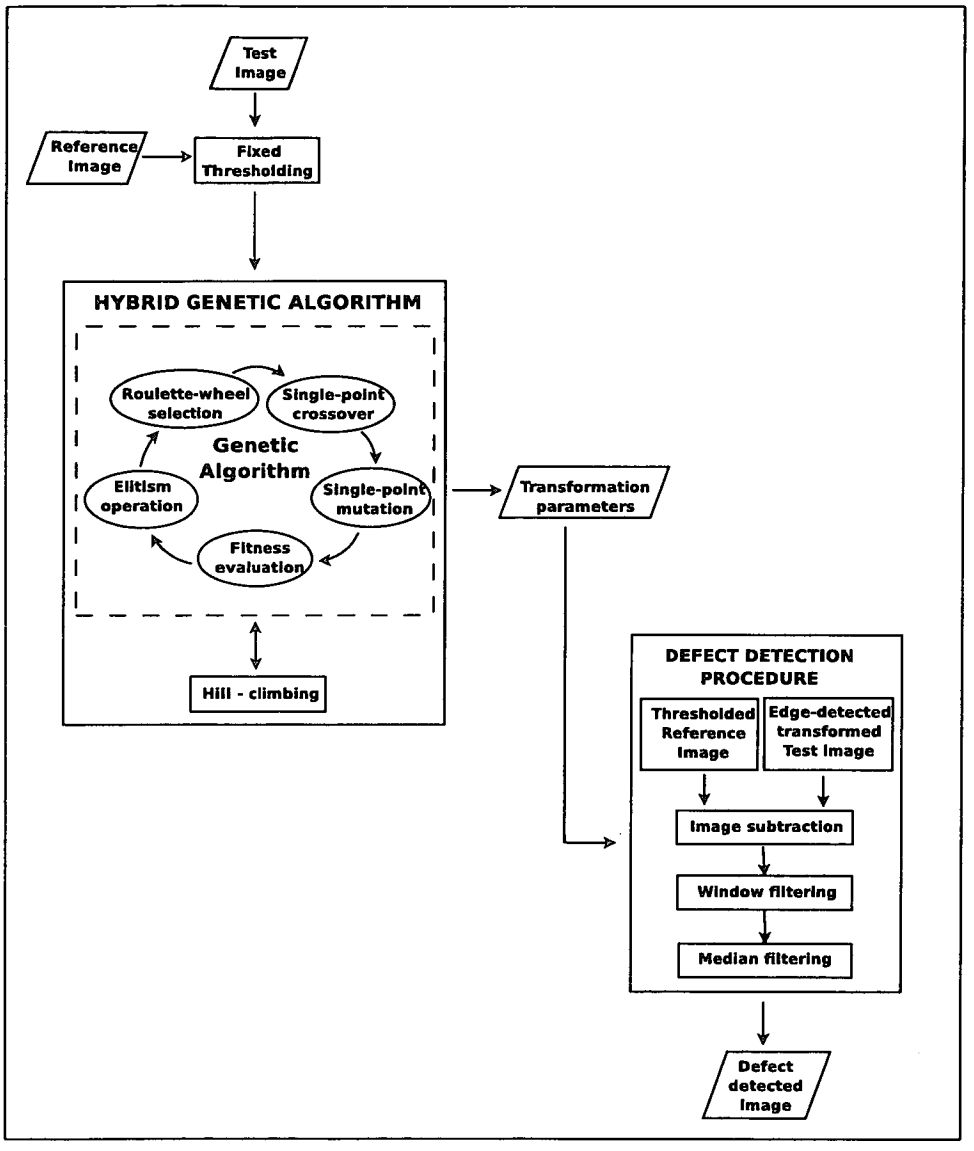

Figure 1.2: *Flow of the system*

Extended study of GA operations are required to ensure that the selected value of parameters will give the most optimum and reliable results for this application. The enhancement work are essential in order to speed up the GA operations and to improve the level of accuracy in finding the transformation values. This process will determine the success of the defect detection procedure to locate the existence of possible physical defects.

The defect detection procedure is designed as robust as possible using low complexity image processing operations such as thresholding, edge-detection, image subtraction and noise elimination. The procedure is able to detect the missing component defects in varying shape and size including open solder joints. The flexibility of the procedure is very important to be implemented for any types of PCB and any inspection environments.

With regard to the above features, the system can be used for many types of PCB with the same settings without hardware assistance in registration. This will prove the concept of flexibility and least complicated visual inspection system using PC but robust enough to detect the possible defects of missing components and open solder joints.

1.5 Structure

This thesis is structured as follows.

Chapter 2 contains description of literature reviews related to this work including the existing PCB visual inspection systems, concept of GA, image processing operations which are widely used in inspection methods and types of PCB defects that are normally investigated.

Discussion on the original framework of GA based PCB inspection system is described in Chapter 3. The framework is using a specially-tailored GA with careful selection of GA parameter values based on independent experiments. The chapter also presents the preliminary results on the performance of GA in registering the inspected PCBs.

Chapter 4 investigates several significant enhancement work to improve the performance of the specially-tailored GA in previous chapter. The enhancement includes a new image rotation function

which contributes to the level of maximum fitness found by the GA. The implementation of block matching algorithm also improves the speed of the whole image registration process. The studies on GA parameters tuning, elitist selection schemes and hybrid methods are also presented in the chapter. The enhancement work produced more accurate and reliable results in big reduction of computational time.

Chapter 5 presents 4 different approaches of defect detection procedure which consist of novel combinations of several image processing operations. The approaches are evaluated on a test sample in terms of detection accuracy and level of noise. The test sample with addition of different artificial defects of missing components and open solder joints is transformed from wrong geometric position to the same alignment of the reference image for these experiments.

Chapter 6 investigates the performance of the system integration which combines the image registration framework with defect detection procedure. Various types of PCBs with different types of missing defect and misalignment are used in the system testing. The analysis focuses on the ability of the system to produce high accuracy detection with low processing time. The chapter also presents a quantitative study which gives good overview of the developed system in order to be implemented in real-time inspection environments.

Finally, chapter 7 concludes the whole thesis.

Chapter 2
Background

2.1 Introduction

This chapter introduces the background literature relevant to the work in this thesis. The chapter commences with the machine vision methods in existing PCB inspection systems. There are three types of inspection which are referential-based, non referential-based and hybrid-based. The advantages and disadvantages of each method are discussed in details.

In this chapter, the image processing techniques such as block matching algorithm, image segmentation, image subtraction and noise filtering used in this work are discussed in details. Examples on these image processing implementation on PCB inspection by other researchers are also given.

The types of PCB physical defects are described in this chapter. This description will give good knowledge on types of defects that are studied in this work.

The concept of image registration is explained and research works on image registration using GA are described in this chapter. Other optimisation techniques for image registration are also given including cross-correlation and heuristic search.

The conceptual overview of GA is given next by explaining every important genetic operations used such as crossover, selection and mutation.

The organisation of this chapter is as follows: Section 2.2 describes the methods used in existing PCB inspection systems, Section 2.3 gives overview on block matching algorithm, Section 2.4 discussed the techniques on image segmentation which focused on thresholding and Sobel edge-detection, defect localisation using image subtraction is introduced in Section 2.5, methods on image noise filtering

are described in Section 2.6, Section 2.7 detailed on types of physical PCB defects that are mainly investigated, in Section 2.8 concept of image registration is given, Section 2.9 gives the concise description of the principles of GA and Section 2.10 concludes the chapter.

2.2 AOI methods for existing PCB inspection

Machine vision plays an important role in automatic inspection for PCBs which demands flexibility, accuracy, speed, stability and cost [22]. The researcher in [22] also suggested that the primary goals in many studies of PCB inspection is to minimise the inspection time and inspection errors.

Nowadays, there exist numerous algorithms, techniques and approaches in order to fulfil the demands. A survey of the state-of-the-art of PCB inspection can be found in [23]. Each operation in the inspection task needs different information such as setup instructions, tool and equipment lists, inspection procedures, measurement locations and sequence, quality standards, and disposition instructions [24].

Flexibility and stability are rarely used to evaluate the performance of an inspection system because they deal with the qualitative aspects of the system. However, they are also important criteria in determining the effectiveness of an inspection system. An inspection function should be flexible in detecting multiple defect types, since there might be more than a single non conforming condition and the defect types of current interest can be changed. Finally, the inspection system should be stable and reliable. The inspection device should not require frequent recalibration and system operators should not be subjected to stress. These criteria are useful to assess the effectiveness of alternative inspection systems [24].

The idea to apply GA in optimisation of image reistration and implemented for PCB inspection has been presented in [25]. The research is focus on registering individual ICs placed om completed PCBs and able to to check the positions of the inspected ICs are in the fault tolerance. The proposed work is implemented on SOC which is expensive and complicated to be implemented. An automatic inspection of assembled PCB using three unique methodologies is proposed in [14], which are normal vector equalisation, dual-channel processing and proximity measure-based. The proposed solution

is able to detect the most frequently arising defects on components such as missing, tilted and not properly-seated components on average PCBs. However, this system needs a fine mechanical jig to control the locations of PCBs.

Surface-spectral reflectance property of an object has been exploited in [26] to inspect raw circuit board using multi-spectral imaging and material classification has been implemented using a special algorithm to classify the objects into circuit elements pixel-by-pixel. The classification algorithm uses the shape features of spectral reflectance based on typical spectral curves of the estimated reflectance for five element materials. The system requires accurate information of spectral reflectance characteristics of each element and the location of detected defects are not provided.

The challenge in solder joint inspection due to the variability in the appearance of acceptable solder joints has raised many interest among researchers [4, 5, 7, 27, 28]. They have applied many techniques to locate and classify the solder joint defects such as Hough curve detection, 3-D pattern recognition supported by Gray-level operations, connectivity preserving shrinking and minimum distance classification for purposes of optimising the inspection process. Most of the systems are using high complexity techniques which will increase the computational time. They also need more hardware such as more than one camera in order to produce 3D images.

The system presented in [10] introduces the application of neural networks and fuzzy logic in printed circuit board inspection. The proposed method is highly parallel and works at the subpattern level. It gives an advantage of not affected by inaccurate alignment of the inspected board but needs rich data information in learning stage. Combination of three types of imaging sensors which are range camera, colour camera and high-resolution camera for development of a multi-sensor system for recognition of electronic components on PCBs with an exemplary approach towards the estimation of uncertain probabilistic information is presented in [29]. The system offers better fault detection quality due to the employment of these multi-sensor but it gives a drawback of high cost implementation. Figure 2.1 based on [30] outlined the two main categories of inspection method in detail.

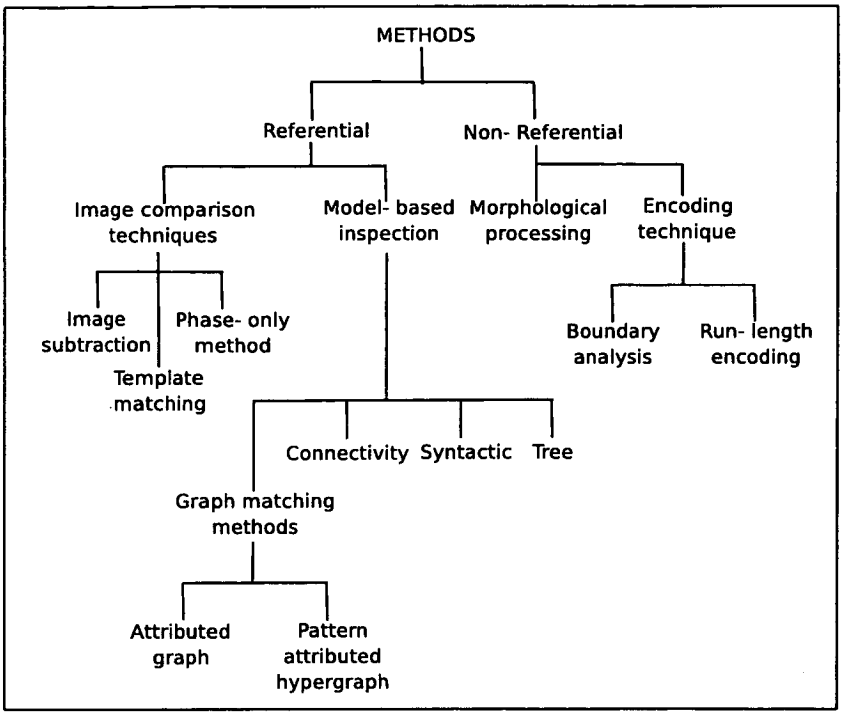

Figure 2.1: *Visual inspection algorithm classification*

2.2.1 Referential inspection

The conventional referential comparison method is very effective in detection of small defects, but it is difficult to detect large defects and missing patterns due to precision of image alignment. It is very difficult to judge whether the model is completely matched with the inspected image or not [11].

However, this method can achieve high throughput when it is implemented on simple hardware [12], even though it may require large memory size to store the image of the reference board or model descriptions. It is also difficult to match templates in the presence of tolerances in specifications. Few examples of work done using this method is presented in [3, 12, 16, 21, 31, 32].

2.2.2 Non-referential inspection

The non referential method requires rich information environment to perform an inspection. It relies on learning process or samples of defected PCBs that the system has found in order to recognise the existence of defects.

Obviously it does not need any reference materials to evaluate the inspected PCBs. In this method, missing patterns are never detected [11]. Furthermore, a special pattern of particular shape is difficult to judge its abnormality. On the other hand, this method is free from precise alignment requirement which simplify the acquisition stage. Response time is generally a major concern about non referential based systems compared to referential method [12].

Few examples of inspection system that used design-rules are Bayesian framework [13], low level morphology [12, 33], content based retrieval [15] and connectivity comparison [9, 34].

The system in [6] utilises a tiered-colour illumination arrangement consisting of coloured ring lights which aid the detection and classification using image processing operations such as windowing, threshold selection, run length code generation and connectivity analysis. An automated 3-D image detection using confocal microscope and several sensors to detect reflected light at different focusing positions simultaneously is developed in [8]. An artificial neural network based PCB inspection system which is trained to distinguish between correct and faulty PCB assembly boards has been proposed in [2]. The system has many beneficial characteristics including fault tolerance, speed of response and more important ability to learn. These systems have many advantages in capability of detecting faults with less error but the complexity of the techniques requires high-cost hardware and complicated process.

2.2.3 Hybrid inspection method

The hybrid method combines both above-mentioned methods to solve the drawbacks and gain benefit from the advantages. Therefore, a PCB inspection system using hybrid method by employing topological comparison which gives flexible conditions with tolerance is proposed in [11].

2.3 Image matching algorithm

Comparison of two images can be performed in many ways depending on the preference of speed, accuracy and complexity. The comparison aims to detect any difference between these images which

will give many information such as the geometric transformation of the studied image referring to the reference image.

Full image matching is the simplest way to match two compared images by comparing every pixel in the images. The main drawback of this approach is the computational time that it requires to perform the whole match. However, this approach gives very high accuracy since there is no modifications are done on the original pixels intensities.

Much faster option is using block matching algorithm that divides an image into a fixed number of usually square blocks. For each block, a comparison is made in the reference image over an area of the studied image. This technique normally employed in motion estimation works such as [35–37]. Block matching algorithm will perform more successfully if the features in the matched block have enough information to compare with and the right size of block is chosen.

2.4 Image segmentation

Image segmentation is the process when an image is segmented into a group of homogeneous regions according to characteristics such as colour and texture [38]. Segmentation of nontrivial images is one of the most difficult tasks in image processing [39]. The existing automatic image segmentation methods can be classified into four approaches, namely, 1) thresholding, 2) boundary-based, 3) region-based, and 4) hybrid [40]. In this literature, thresholding and boundary-based approaches are highlighted since they will be used in this work.

Thresholding is still one of the most commonly used methods of image segmentation. From review by [41], apart from its use as a stand-alone segmentation method, thresholding may yield a good initial estimate from which more advanced methods can proceed and a correct selection of the threshold is the key issue. Generally, the methods may be broadly categorised in techniques employing the histogram, moment preserving, entropy coding, and locally adaptive methods [42].

Edge-detection or also known as boundary based segmentation involves locating and highlighting local discontinuities in an image. This is usually achieved by convolving the image with an operator

to produce an edge-detected image. There are many types of edge-detectors including Sobel, Prewitt, Roberts and Susan. Sobel operator has been widely used in research such as [43, 44].

In [29], the algorithm developed by Tsai [45] is used in multi-level automatic thresholding to segment the electronic components from the background. A machine-vision based on Gray relational theory has also been developed in [46], which is applied for Integrated Circuit (IC) marking inspection. In this inspection procedure, few image processing operations are also implemented before the Gray relational analysis such as segmentation, thresholding and thinning algorithm.

In addition, when the image is interrupted by noise and other artifacts the performance of these thresholding techniques will be poor or even fail. To compensate this drawback, the output of thresholding is combined with the output image from edge-detection operation. A segmentation method that utilises histogram-based edge-detection and thresholding in segmenting Surface Mount technology Devices (SMD) on PCB during inspection process has been proposed in [47].

An effective and computationally efficient colour indexing technique for segmentation and edge-detection of objects with background whose colour appears to be very close to the objects has been studied in [48]. A robust colour image segmentation has been studied in [49], which can can be used extensively on PCB inspection. The proposed segmentation technique employed vectoral imaging approach with low computational effort. It is also a non-parametric solution that is invariant to changes of light and colour of the inspected components.

2.5 Defect localisation using image subtraction

The difference between two images *f(x,y)* and *h(x,y)* expressed as

$$g(x,y) = f(x,y) - h(x,y) \tag{2.1}$$

is obtained by computing the difference between all pairs of corresponding pixels for f and h [39].

Many applications can benefit from this straight-forward operation including PCB inspection in order to locate the existence of defects, with condition of the alignment of the images are similar. For PCB inspection, the extracted differences indicate that the inspected PCB has possible defects. This detection gives an information on location and size of the defect. The quality of defect recognition depends on the kind and quality of features extracted from the image subtraction operation. Examples of work on PCB inspection that utilise image subtraction are presented in [21, 50].

2.6 Noise filtering

Noise filtering is the process of removing unwanted noise from an image and is often a preprocessing stage in image analysis and a filter is required to preserve any image structure such as edges and texture [51]. Sources of noise are explained in [52] and for most typical applications, image noise can be modelled with either a Gaussian, uniform or impulsive distribution. In this work, the impulsive noise is generated with the existence of pixels with gray level values not consistent with their local neighbourhood. Therefore, an optimal impulsive noise filter must smooth dissimilarities of pixels in homogeneous regions, preserve edge information and not alter natural information.

The median filter produced sharp outputs because it tends to alter rather than blur image structure. The weighted median filter has better structure preserving properties, but at the expense of not being able to clean smoother areas as effectively [51]. An improved median filter to eliminate recognised noise has been applied in [8]. The median filter is highly efficient when considering a small neighbourhood and has proved to be very effective in removing noise of an impulsive nature despite its simple definition [52].

2.7 Types of physical PCB defects

It is difficult to develop a system that has the ability to inspect all types of defects on inspected PCBs. A report from PCB manufacturers has been reviewed in [31], which reported that the PCB component defects can be classified into the following four categories: 1) component misplacement, which is

Defect Name	Brief Description of Defect
No Solder	No solder at all on joint
Cold Solder	Solder not sufficiently heated to form joint
Disturbed Solder	Solder joint disturbed during solidification
Grainy Solder	Contaminants in solder cause graininess
Excess Solder	Too much solder for joint inspectability
Insufficient Solder	Not enough solder for good joint structure
Dewetted Pad	Solder retracts from solder pad surface
Dewetted Lead	Solder retracts from component lead surface
Non-wet Pad	Solder wets lead but not pad
Non-wet Lead	Solder wets pad but not lead
Icicling	Solder forms sharp peaks on joints
Webbing	Solder strands sticks to surrounding insulation
Pinholes	Small holes form in joint fillet surface
Blowholes	Large holes form in joint fillet surface
Solder Pits	Hole or depression in solder where bottom is visible
Oil Entrapment	Oil droplets trapped with solder joint
Solder Bridging	Solder makes unwanted connections with other leads
Rosin Joint	Rosin flux surrounds lead rather than solder
Solder Balls	Solder adheres to balls (not at joints)
Spatter	Spattered solder adheres to board (not at joints)
Internal Voids	Open pocket within joint with no external signs
Bubbles	Open pocket within joint causing bulge in fillet
Outgassed Joint	Severe explosion disrupts joint surface
Grit and Dirt	Surface of joint dirty limiting inspectability
Flux Residue	Residual flux remains on PCB causing problems
Bad Leads	Component leads are too short, to long, bent over

Table 2.1: *Solder joint defects*

about 10%; 2) component with wrong polarity, which is about 25%; 3) component absent, which is about 20%; 4) solder joint defect, which is about 55%. Considering that solder joint defect represents the largest percentage of PCB defects, Table 2.1 describes the types of solder joint defects based on [4] and Figure 2.2 depicts the magnified vision of circuit patterns and typical defects based on [53].

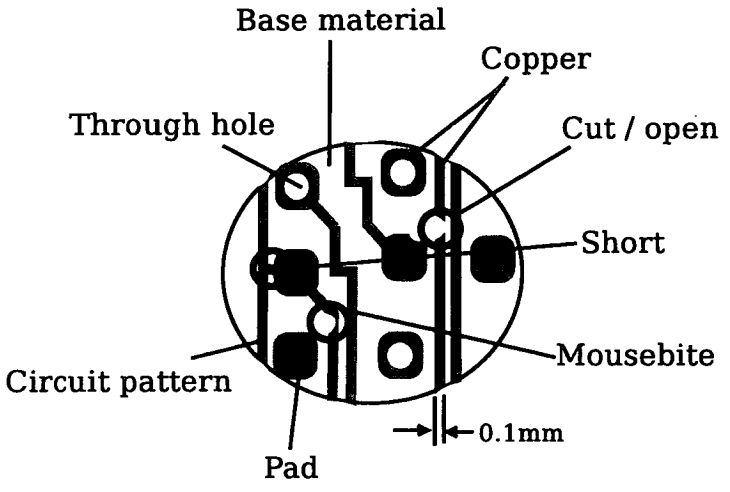

Figure 2.2: *Magnified image of PCB pattern and defects*

2.8 Image Registration

Image registration is the process of determining the transformation which best matches, according to some similarity measure, two images of the same scene taken at different times or from different view points or from different sensors [54, 55]. Image registration is one of the most important tasks in image processing and classified into two categories: the feature-based matching and intensity-based matching [56]. Each of them has its strength and weakness and hybrid implementation of both approaches has been investigated in [56].

The feature-based matching approach [54, 57] requires reliable feature extraction as well as robust feature correspondence to overcome missing feature and outlier problem due to partial occlusion and multiple motion. Its main advantage is the relative robustness against illumination change. It is also easy to adapt to handle non-rigid scene. However, its accuracy is up to certain amount of precision, and more importantly, the algorithm is more sensitive to the error of feature extraction and matching, for only a small portion of available image intensity information is used.

On the other hand, the intensity based matching approach [58] makes direct and complete use of all available image intensity information, thereby increasing accuracy and robustness of estimation. However, this approach suffers from a number of limitations. First of all, it is more sensitive to

illumination changes than the feature-based approach. Secondly, it tends to converge to the local minima, in particular when the initial value of the model are inaccurate.

Other optimisation methods for image registration include heuristic search [59], cross-correlation [60, 61], circular fiducial [62] and Levenberg-Marquardt [58].

2.9 Concept of Genetic Algorithm

GAs are search algorithms based on the mechanics of natural selection and natural genetics [63]. This search technique is for finding solutions to complex problems. In this work, the problem is to estimate the correct transformation parameters of the whole inspected PCBs. Solving the problem with incremental change is more likely to lead to better solution than trying a completely new random guess. The GA also combines approximate solutions to find better solutions. The recombination is profoundly important because the result of simultaneous searches can be used to accelerate the search for best results.

Figure 2.3 shows the flow of important operations in GA to optimise a problem. To formulate the conventional GA, all parameters are represented with binary strings or so called artificial genes. A chromosome is formed by concatenating genes representing different parameters of the evaluation function. An evaluation function that plays the role of the environment is required to rate the solutions in terms of their "fitness". The collection of the possible solutions (chromosomes) forms a population, which produce another generation through search process. A population is formed by a set of chromosomes representing the same parameter set. In the search, most of the fittest chromosomes will be selected to exchange the information (crossover) and alter the information (mutation) randomly in the existing generation to produce new generation. The fittest chromosomes can be computed as the chromosomes which give most accurate solutions. These chromosomes are randomised according to their historical information to speculate on new search point with expected improved performance.

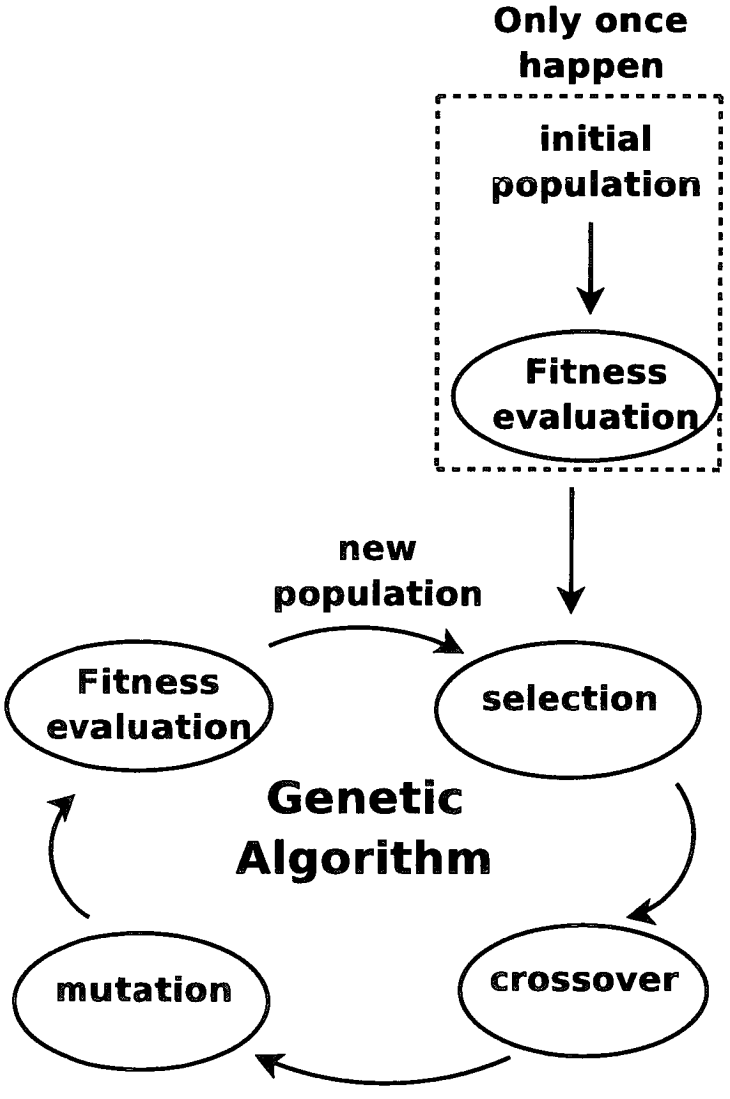

Figure 2.3: *Flow of Genetic Algorithm*

A new population evolves in each generation encouraging incorporation of new information and exchange in all direction of the multidimensional problem space. In every generation, GA tries to get rid of inferior members and encourages reproduction and exchange between superior members. Genetic operations direct evolution of the population in an optimal way towards the optimum solution.

Since in most interesting problems there is not sufficient time to search through all possible solutions, the best way is vary often a variation on an existing partial solution. The genetic operators which are responsible for achieving the optimum result based on [63] are described below.

Selection is the process of selecting chromosomes from the current population to create a new population. The selection is performed depending on the fitness value of chromosomes, which indicate the closeness of chromosomes to the optimal solution. This procedure makes chromosomes with higher fitness values to have a better chance and more copies to appear in the next generation. Selection methods include tournament, Roulette-wheel, and ranking mechanism. Tournament selection method selects some number of individuals and selects the best one from this set of individuals for the next generation. Roulette-wheel selection method chooses the individuals for the next generation with respect to the probability distribution based on fitness values. Higher fitness value gives higher probability to an individual to be selected. In ranking selection, the individuals are selected based on the rank of their fitness values.

Crossover occurs in chromosomes selected with a probability of p_C from the current population. Pairs of chromosomes are randomly or based on selection method selected from the selected group and the bit patterns beyond a randomly selected bit position of the two chromosomes are interchanged as shown in Figure 2.4.

Mutation introduces new information to the current population at bit level. Every bit in the population is selected with a probability p_m for mutation and if selected, reverses its value as shown in Figure 2.5.

There are an infinite number of variations on the GA that can be used for optimisation. Each variation gives more or less emphasis to the steps in the process. Within these variations the GA encompasses

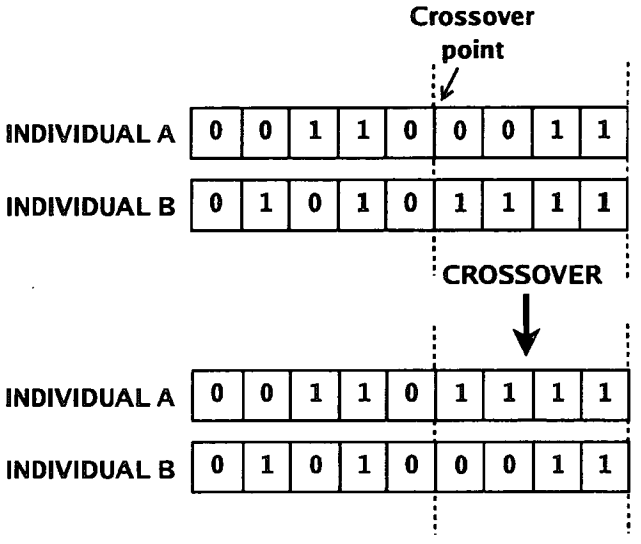

Figure 2.4: *Crossover operation.*

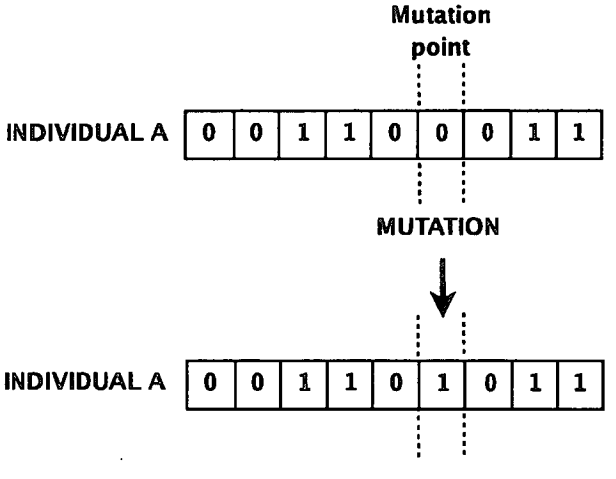

Figure 2.5: *Mutation operation.*

Algorithm 1 Genetic Algorithm.

```
Begin
Generate an initial population of binary coded solutions
Derive a fitness measure for each solution
Loop until convergence
  Loop for new population
    Select two parents according to their fitness
    Mate parents in order to create two offsprings (Crossover)
    Mutation
    Use offspring to create a new population
  Derive a fitness measure for each solution
End
```

an enormous variety of more specialised technique, but no variation of the algorithm is best for all situations. Reducing or removing recombination, for example, leads to an algorithm like simulated annealing which accepts or rejects random changes based on how much they improve the current solution. Increasing mutation leads to a Monte Carlo search which attempts new random solutions and tends to disregard older solutions under the assumption that they are not helpful. For any problem, the more that is known about potential solutions the more the search technique can be specialised. This gives us a robust technique which adapts itself to use those search operators which are best suited for the problem.

The main advantage of the GA approach for an image registration is that pre-alignment between views is not necessary to guarantee a good result. However, GA is a stochastic method and generally time-consuming. Besides their intrinsic parallelism, GAs are simple and efficient techniques for optimisation and search. The details of GA operations are described in Algorithm 1 to give a better idea of GA in a program.

2.9.1 Image Registration using Genetic Algorithm

GA has been used in many applications in image registration such as matching of two numerical surfaces through an elastic 3-D transformation [64], functional Magnetic Resonant Imaging (MRI)

[65], fingerprint registration [66], multi-resolution image registration [19] and medical image registration [67, 68]. In [69], GA is used to optimise automatic registration of successive images in a sequence of Digital Subtraction Angiographies (DSA). An image registration program which used a GA as the function optimiser was designed in [70] and the settings of the program were automatically tuned with a second GA.

Most of the applications are meant to detect changes from previous or reference image, for example image registration in medical which GA is used to diagnose cancer cell. However, there are applications to compute the transformation of image according to misalignment during image caption, this include implementation of GA in fingerprint registration. The reference image of fingerprint is transformed randomly and the transformed reference image is compared with the captured image. Then, the results of comparison are used in GA search in order to figure out the transformation mechanism that match the captured image. This process is repeated until the exact match is found. More examples of image registration using GA are presented in [69–74].

2.10 Conclusions

The advantages and disadvantages of the existing AOI systems have been studied in detail in this chapter. The comparisons of these reviewed systems and this work are presented in the table below.

The literature reviews on common image processing operations are discussed and the systems that employed these operations are also given. The types of normal physical PCB defects are described in this chapter for better idea of problems in PCB inspection.

Then, the concept of GA is given in detail for better understanding of this work. Finally, the proposed work of applying GA to optimise image registration in different fields are described and these work have proven the potential of GA in optimising image registration process.

System	Inspection method	Advantages	Disadvantages
Park et al [14]	Highlight separation and dual channel processing	- Detail information are provided. - Able to detect component missing, tilted, not properly seated components. - No CAD data is required.	- Manual registration. - Fixed thresholding. - Complicated processing.
S. Tominaga et al [26]	Based on spectral reflectance characteristics of 5 elements.	- Free from precise alignment. - All elements are detected.	- Expensive hardware. - Locations of defects are not provided.
M. R. Driels et al [7], P. J. Besl et al [4], P. Mengel [27], S. L. Bartlett et al [5], Q. Z. Ye et al [28], E. R. V. Dop et al [29]	Hough curve detection and minimum distance classification, Characteristics of intensity surfaces, Supplementary processing of 3D and gray level images, Statistical pattern recognition and expert system, Connectivity preserving shrinking, Multi-sensor recognition.	- Detect most types of solder joint defects. - Free from precise alignment.	- High complexity algorithms. - Expensive hardware. - Require updated CAD data assistance.
M. Moganti et al [10], C. Han et al [2]	Neural network and fuzzy logic, Artificial neural network.	- Able to detect many types of defects. - Free from precise alignment.	- Require rich information environment in learning stage. - Longer preprocessing time.
D. W. Capson net al [6], Y. Matsuyama [8]	A tiered-color illumination, Optical 3D image detection.	- Provide better information of inspected board by employing better lighting condition and several sensors.	- Expensive hardware. - Complicated process.
J. R. Evans [25]	Using GA to detect misalignment of individual ICs.	- Embedded on SOC. - Require the image of reference board.	- Only detect misalignment of large ICs. - Complicated setup. - Require large memory which is expensive.

This work	Using GA to register whole PCBs automatically.	- Detect and locate missing components in any shape and size. - Software based and run on PC.	- Variant lighting condition may affect the system performance. - The defect detection results are dependent on precise alignment. - No classification technique for detected defects.

Chapter 3

Genetic Algorithm based Image Registration

3.1 Introduction

In general, there are four main groups of image registration applications; different viewpoints (multiview analysis), different times (multitemporal analysis), different sensors (multimodal analysis) and scene to model registration [55, 75]. Image registration of a PCB placed arbitrarily on a conveyor belt during inspection is one of the examples of scene to model registration category.

Performing efficient registration of two images is a complicated task due to the large dimension of the search space and as previously mentioned, a GA is an ideal optimisation technique for a large search space. Therefore, this chapter presents an image registration of a PCB placed arbitrarily on a conveyor belt during inspection using a specially-tailored GA. For automating the inspection process, other techniques for accurately positioning the PCB under inspection include mechanical jig [14], automatic X-Y table [16, 76–78] and manual registration [5]. In industrial environment, the success of a system to produce high-quality inspection may be degraded due to jitters and irregular alignments of the conveyor belt.

Accurate placement of a whole completed PCB on a conveyor belt under the camera is a delicate task during physical defect inspection. Any misorientation of boards placement may lead to wrong analysis especially for reference-based method [21]. For this reason, [79] employed a GA to optimise the search of the rotation angle and displacement values of the whole inspected board based on the image captured, while detecting any physical defects.

Previously, [80] has used GA to find misorientation parameter values of individual IC on board to determine the ICs are positioned correctly on PCBs and the researcher has implemented the technique

on a System-On-Chip (SOC) platform. [81] also used a GA to estimate surface displacements and strains for autonomous inspection of structures. GA and distance transform has been combined in object recognition in a complex noisy environment in [82]. This research shows that the combination has produced fast and accurate matching and has scaling and rotation consistency.

Ideal parameter tuning of GA and good adaptation of GA operations plays an important role in boosting the capability of this technique in order to perform effectively in a specific application. Therefore, GA parameters are chosen carefully and GA operations are performed in a way that is most applicable to this work. Appropriate coding and operators and appropriate parameter settings are two important topics before applying a GA in an application to gain maximum power of GA as a search technique [83]. However, [84] suggested that good values in parameter tuning is an inappropriate way to increase the potential of GA compared to efficient parameter tuning.

This chapter is presented as follows: in Section 3.2, specially tailored GA operations such as individual representation, fitness function, crossover and mutation are presented, Section 3.3 presents an ideal settings of GA parameters and PCB images that are used in this work, Section 3.4 yields the findings on best solution found and convergence in generation run from the GA search technique applied on the test images and finally, Section 3.5 draws some conclusions from this work.

3.2 Algorithm implementation

The whole procedure in GA based image registration is described in Figure 3.1. The proposed technique uses a perfect (golden) board to act as a reference image and an inspected board as the test image. In this procedure, a specially-tailored GA is used to derive the transformation between test and reference images based on the simple GA as presented in [63] in order to provide high quality registered images for physical defect inspection process.

Fixed multi-thresholding operation is applied to a stored reference image and a test image to enhance

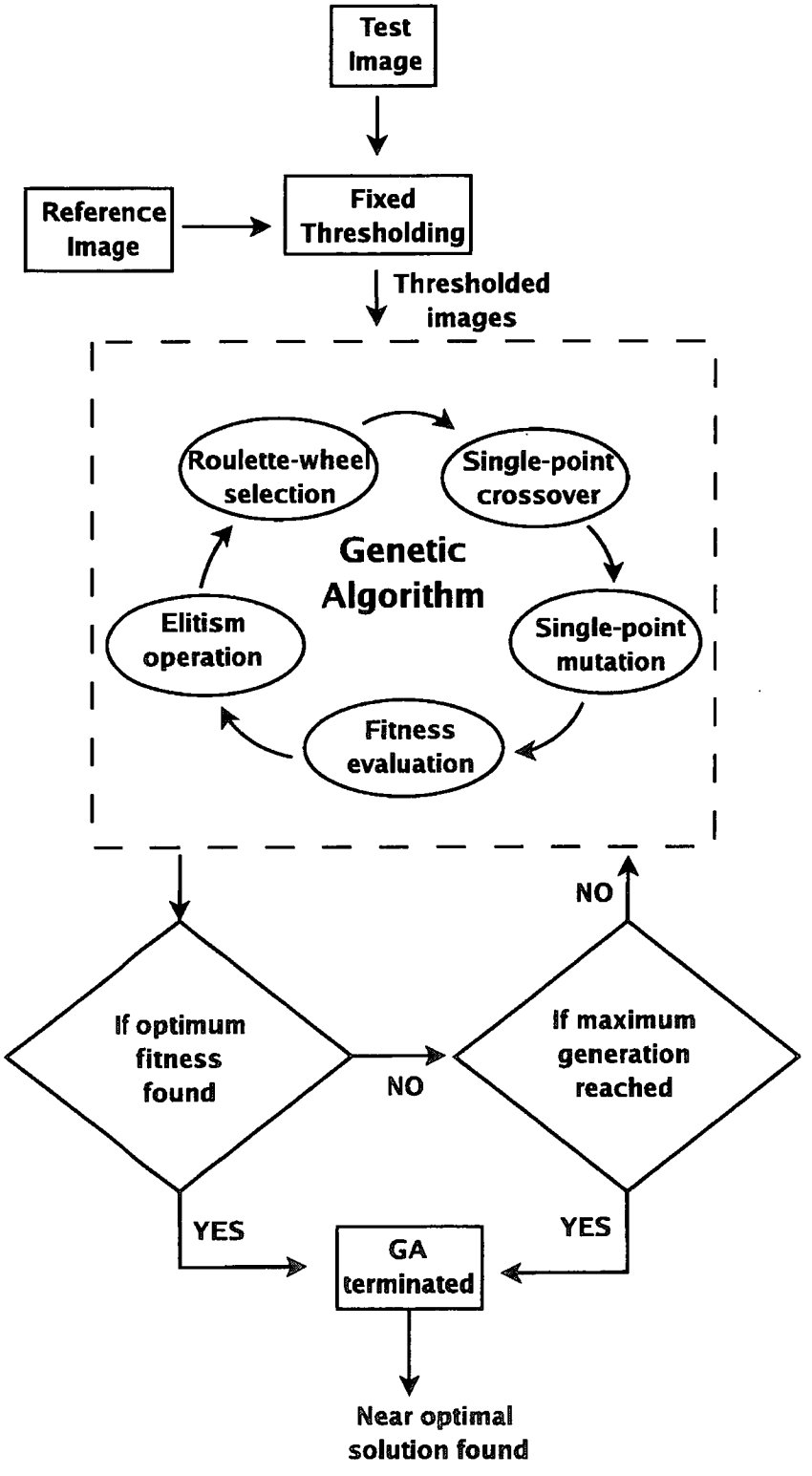

Figure 3.1: *Program flow-chart.*

the images and to highlight the details before performing image registration. The thresholding operation is also essential to deal with variations in intensity of components on PCB images. The thresholded images will be delivered to GA module for further GA operations in order to obtain the most accurate transformation parameters of test image.

In order for a GA to work, the important properties which are responsible for achieving the optimum result need to be defined as discussed in details as follows:

3.2.1 Fitness function

The fitness function is defined to evaluate an individual. The fitness function in this work is calculated from total similarities values in each pixels between test image and reference image, divided by total pixels in reference image assuming that both images are the same size. The fitness value is defined as follows:

$$\text{if } f(x_a, y_a) == g(x_b, y_b), \text{ counter ++}$$

$$\therefore fitness = counter/(W \times H)$$

where $f(x_a, y_a)$ is the pixel intensity of reference image, $g(x_b, y_b)$ is the pixel intensity of test image, in condition of $x_a = x_b$, $y_a = y_b$ where x and y are pixel location at x-axis and y-axis. W is width of the reference image and H is height of the reference image. The fitness may range from 0 to 1, which is when the ideal transformation parameters are found.

3.2.2 Coding for genes

It is essential to determine the type of encoding which will affect the performance of GA to optimise the search of transformation parameters in this application. Many encoding schemes have been proposed, for example, integer coding and gray coding. There is no standard way to choose these schemes and the choice really depends on the nature expression of the problems. In this prototype,

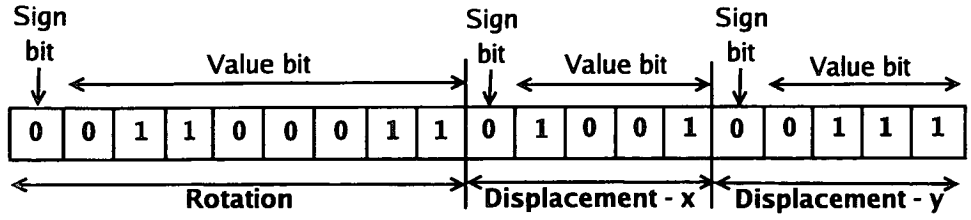

Figure 3.2: *The allocation of parameter in bit string for every individual.*

binary coding has been chosen as in conventional GA [63]. Figure 3.2 illustrates the coding for genes used in this work. 19 bits are allocated for a single individual which is 9 bits for rotation for value from 0 to ± 180 degrees, 5 bits for displacement of x-axis for value between -10 to 10 pixels and another 5 for displacement of y-axis for value between -10 to 10 pixels.

3.2.3 Selection operators

In this implementation, Roulette-wheel selection has been selected to choose individuals for mutation and crossover operations. This selection mechanism works on a probability directly dependent on the individual fitness. The GA operations on finely selected individuals are aimed to produce fitter individuals for better image registration.

Generational replacement produced very slow convergence. The elitist concept yields improved convergence times without loss of population diversity. Considering this advantage, elitism is also implemented in this specially-tailored GA to preserve high potential individuals in every generation. This strategy will always include the best search point from the last iteration to the current iteration to prevent early convergence. In this work, 100% elitism has been implemented where fittest individuals from the previous and current generation are selected based on rank to generate a new population for next generation.

3.2.4 A method for crossover and mutation

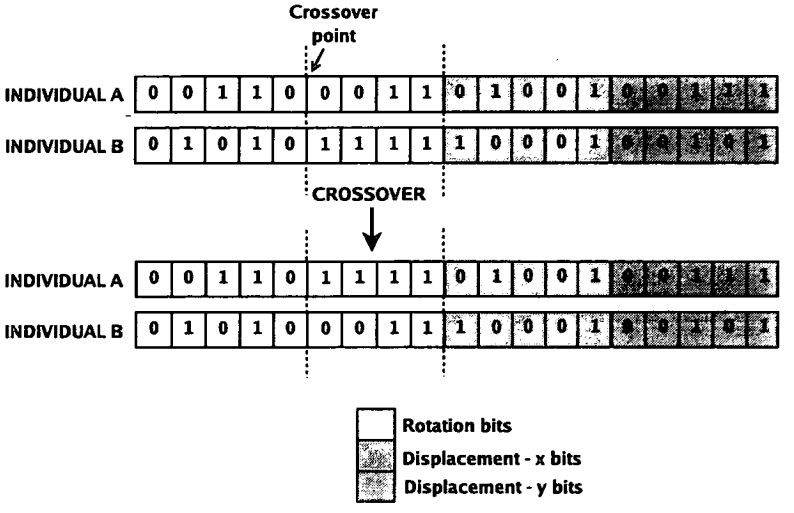

Figure 3.3: *The crossover operation.*

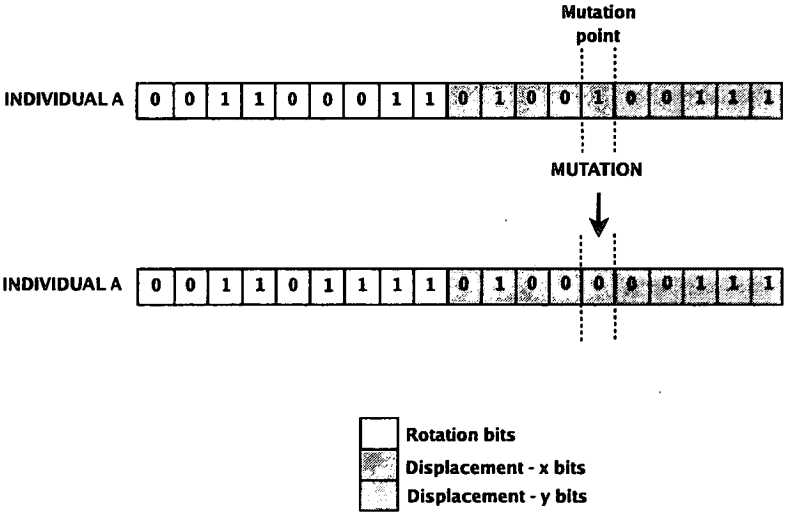

Figure 3.4: *The mutation operation.*

Crossover and mutation operations are some of the main advantages of GA and they are usually tuned to different values for different problems. Our purpose is to see the effectiveness of GA-guided parameter optimisation. Therefore, the crossover and mutation operations are modified to suit this application where only one type of transformation parameters will be affected when these operations happen (as shown in Figure 3.3 and Figure 3.4 respectively). Both operations are performed at a single point when the probability value is satisfied.

Crossover proceeds in two steps: First chosen individuals are mated based on Roulette-wheel selection, and then crossover between the two individuals occurs at an integer position along the string of randomly selected transformation parameter, known as crossover point. This position is also selected at random. For example if we have two individuals A and B as shown in Figure 3.3. After crossover occurs, both individuals will have new partial of information resulting from the exchange at a selected transformation parameter. The new information gives new value to the parameter and may improve fitness value of the individual.

The crossover probability, p_C controls the rate at which solutions are subjected to crossover. The higher the value of p_C, more frequent crossover will happen and the new solutions are introduced into the population quicker. Solutions can be disrupted faster than selection can exploit them when p_C increases. In many applications, typical values of p_C are between 0.5 and 1.0 [85].

Mutation is the occasional (with very small probability) random alteration of the value of a string position at randomly chosen transformation parameter in an individual. For example, the state of individual A before and after mutation as shown in Figure 3.4. New value of transformation parameter is introduced when a mutation happen to a chosen individual. This alteration will diversify the population even more every time the mutation happen.

Mutation is only a secondary operator to restore genetic material. Nevertheless the choice of p_m is critical to GA performance for better individual reproduction. Large values of p_m transform the GA into a purely random search, while some mutations required to prevent the premature convergence of GA to suboptimal solutions. Typically, p_m is chosen in the range of 0.005 to 0.05 [85].

3.2.5 Population of individuals

For this application, every individual represents the combination of transformation parameters and the agreement between the transformed reference image and the test image is measured as a fitness value. Initial population of GA is constructed by transforming the reference image with random rotation and displacement values. The transformation function is defined as:

$$x' = t_x + xcos\theta - ysin\theta$$
$$y' = t_y + xsin\theta + ycos\theta$$

where θ is the rotation angle while t_x and t_y are the displacement at x-axis and y-axis respectively while x' and y' represent the new locations of the processed pixel in the image.

Iteratively, the whole population for the next generation is formed by wisely selected individuals from the current and previous generations. These individuals are ranked based on their fitness performance and the top fittest are selected. A new population evolves in each generation encouraging incorporation of new information and exchange in all directions of the geometric values considered. In every generation, GA tries to get rid of inferior members and encourages reproduction and exchange between superior members. Genetic operations direct evolution of the population in an optimal way towards the optimum solution.

3.2.6 Termination criterion

The population will perform GA activities such as selection, mutation and crossover in every generation with expected improved solution until the termination criterion are fulfilled. This criterion determine how far the GA should evolve the population considering time to consume and an acceptable solution. The GA termination criterion defined for this work is when an individual with an ideal solution which is fitness of 1 is found or maximum generation is reached. If the maximum generation is reached, the global fittest solution found throughout the GA search will be the near optimum estimation for this image registration.

3.3 Environment and parameters

Performance study of GA-based PCB inspection is conducted on a Linux-based PC and the images of PCB are captured by a black and white CCD camera. The basic image processing functions such as single global thresholding [39] and transformation are built using Vision Group's image library [86]. For this work, few assumptions have been made: 1) Both test and reference images are the same size and 2) Camera position and focus of the camera is constant across the samples.

Image segmentation is one of the most important tasks in image processing, having a wide range of applications in image visualisation, image coding, image synthesis, pattern recognition, rendering, displacement estimation etc [87]. Hence, the thresholding is applied on every pixel by setting the value of object point, T equals to 100 based on visual observation. A thresholded image defined as:

$$g(x,y) = \begin{cases} 0 & f(x,y) \leq T \\ 255 & f(x,y) > T \end{cases}$$

where *f(x,y)* is the gray level of point *(x,y)* in the image and *g(x,y)* is the pixel intensity for the corresponding location in target image.

The effectiveness of thresholding operation on PCB images before GA search is studied on a few samples of PCB images. Figure 3.5 shows samples of reference image and test image of a real PCB while the output images after thresholding performed on both images as shown in Figure 3.6. The fitness function of GA is evaluated between the transformed reference image and test image with and without thresholding operation. As predicted, GA search on thresholded images outperformed the GA on non-thresholded images significantly. The highest fitness obtained in fitness evaluation without thresholding is average of 0.17 while average fitness value of 0.49 is successfully found in fitness

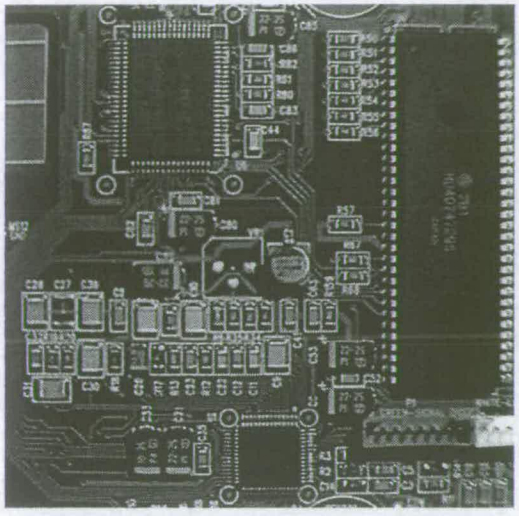

(a) Reference image

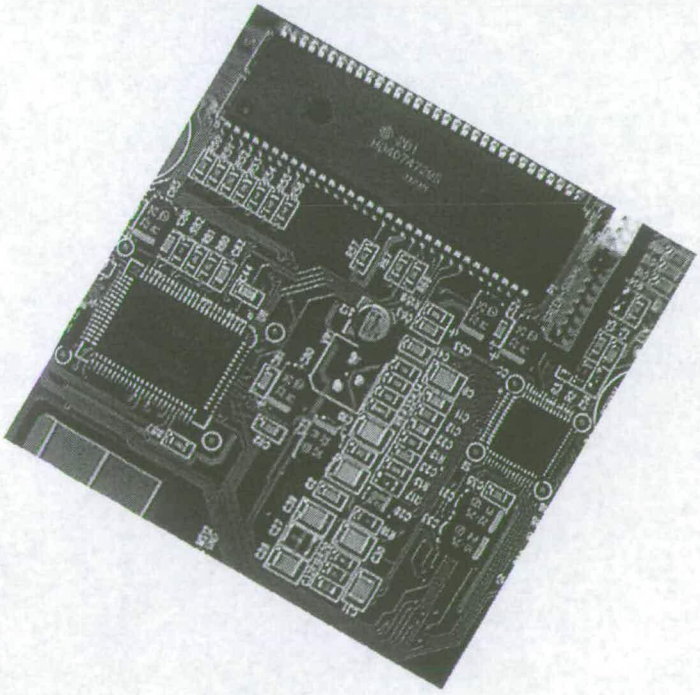

(b) Test image

Figure 3.5: *Samples of original image*

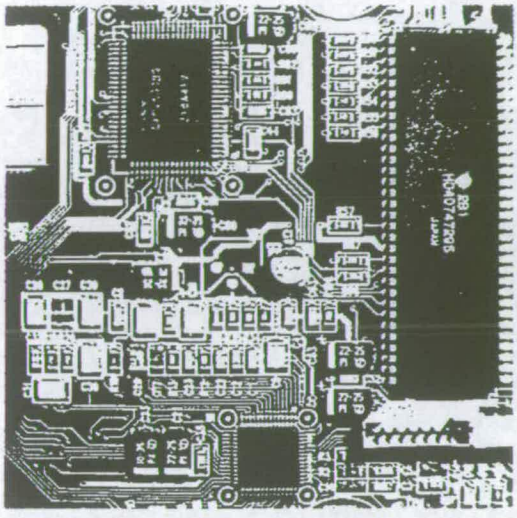

(a) Thresholded reference image

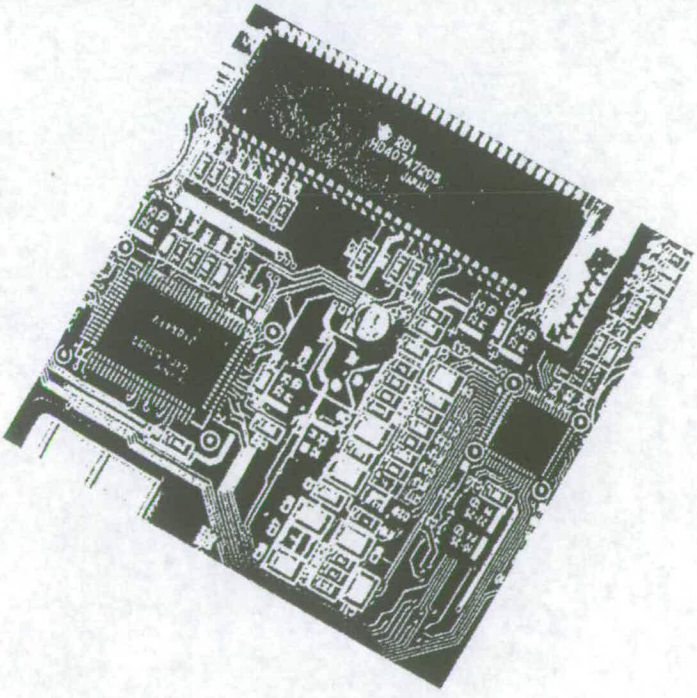

(b) Thresholded test image

Figure 3.6: *Samples of thresholded image with T=100*

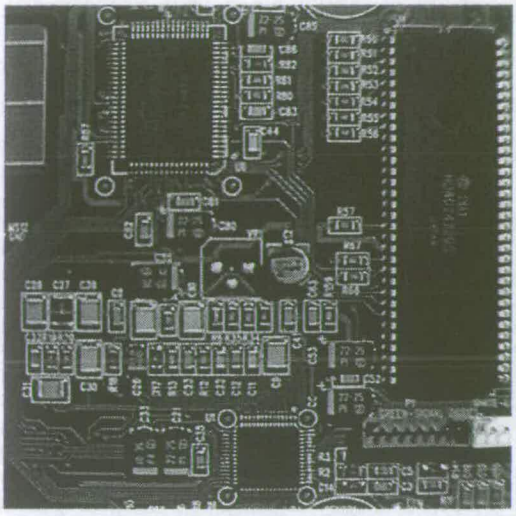

Figure 3.7: *Image of the reference board (804 x 804 pixels)*

evaluation with thresholding. Better fitness values gives higher accuracy in values of transformation parameters. From these fitness findings, it is crucial to perform the thresholding operation before GA search in order to increase the efficiency of GA for high precision image registration.

In this simulation, full image matching is performed in order to compute fitness value of each individual. The fitness value is derived by comparing every pixel's value in both images (transformed reference and test) and divided by total pixel. The reference image is displayed in Figure 3.7 and the misorientated test images with known values are shown in Figure 3.8 and Figure 3.9. Both test images are artificially transformed from the reference image, however an artificial defect of one IC missing is added to the test image in Figure 3.9 to create a faulty board.

To maximise the performance of GA, parameters are tuned using various typical values found in the

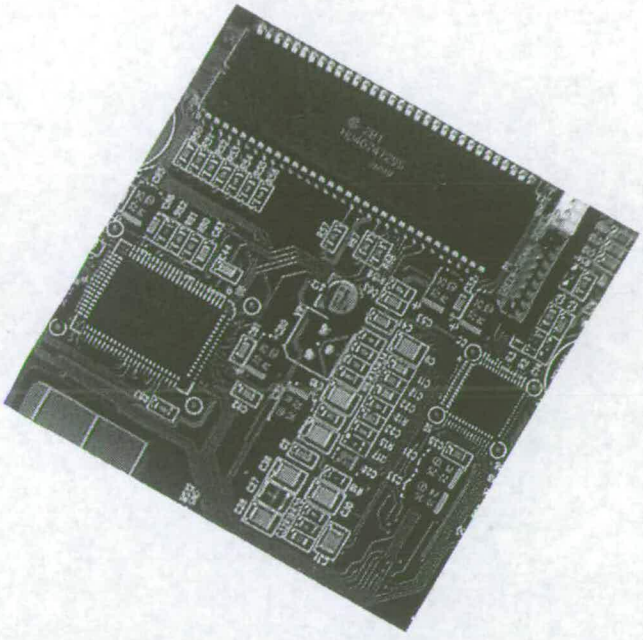

Figure 3.8: *Image of the test board (fault-free board).*

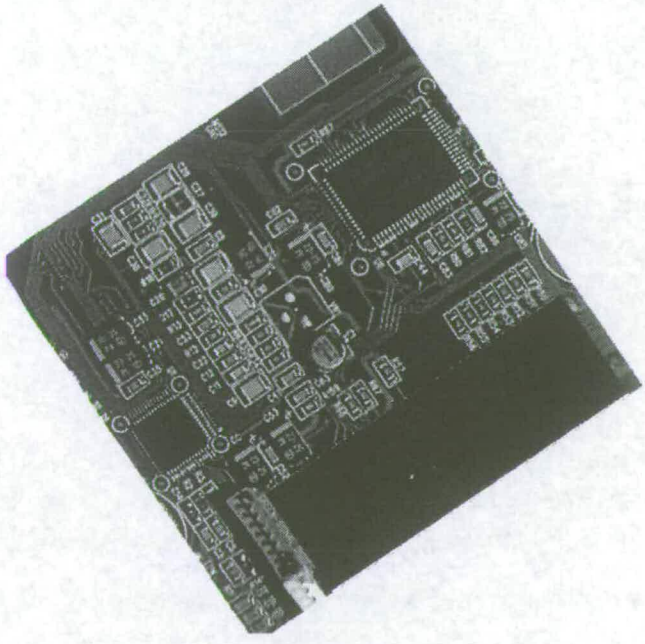

Figure 3.9: *Image of test board (faulty board).*

literature. Every parameter are evaluated in sequence of importance based on maximum fitness obtain and number of generations for a search to converge. The parameters which are analysed with various parameter settings are maximum generation, probability of crossover (p_C), probability of mutation (p_M) and size of population. Every experiment of parameter tuning is performed on test images as shown in Figure 3.8 which are transformed to 30 different images with known values.

First of all, the performance of variant maximum generation ranges from 50 to 300 are studied with value of p_C equals to 0.6, p_M equals to 0.005 and population size is 48. In Figure 3.10(a) and 3.10(b), maximum generation of 200 yields the highest average fitness value in a reasonable generation time compared to other values. This indicates that 200 generations provide enough time for GA to search in high dimension search space of geometric transformations and able to produce high fitness value for higher accuracy results. Shorter period of generation may stop the evolution prematurely while more generations consume too much time which is a critical issue in current PCB manufacturing with a comparable results.

Tuning the p_C is a crucial task since exchanging information involved in this operation and it gives a big influence on overall performance of GA. Figure 3.11 shows the results of experiment on p_C ranging from 0.1 to 0.9. The probability of 0.5 and 0.8 give the highest average fitness but the probability of 0.5 converges much faster. This proves that GA is performed well in this application using a moderate p_C of 0.5. As expected, higher probability requires longer time but does not necessarily produces individual with highest strength.

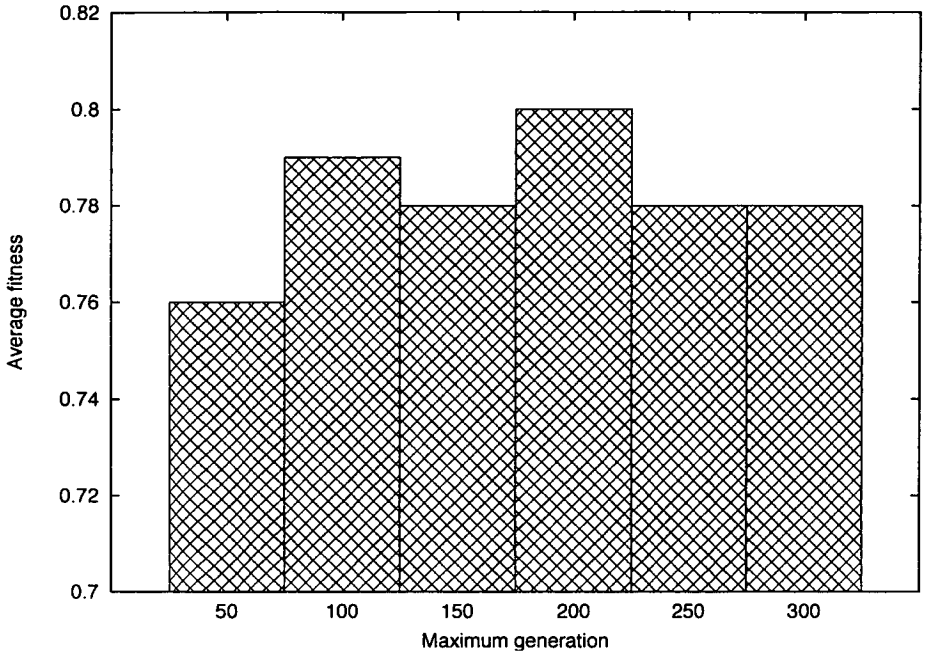

(a) Maximum generation vs average fitness

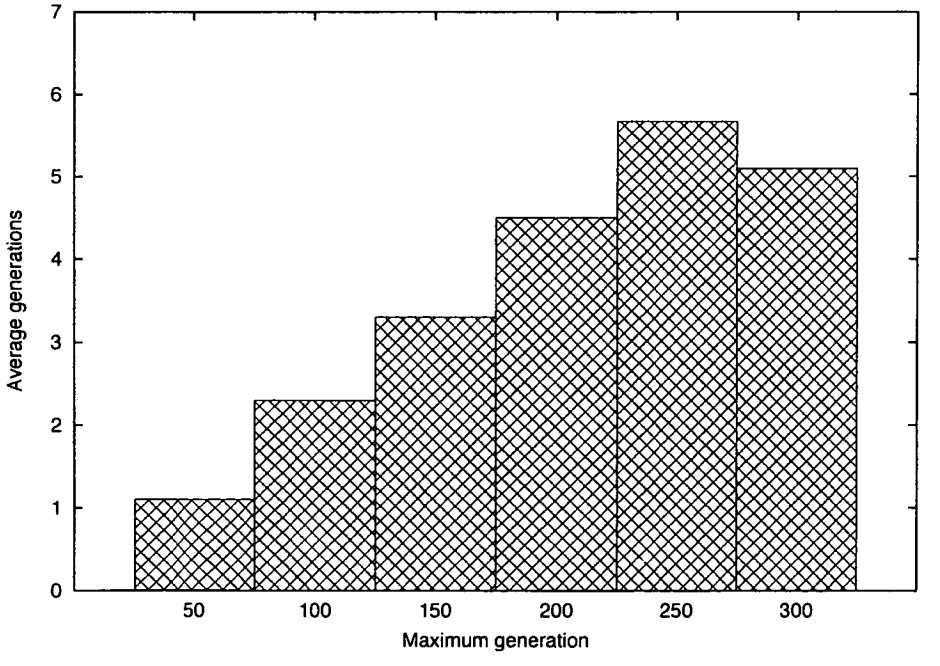

(b) Maximum generation vs average generations

Figure 3.10: *Maximum generation parameter tuning*

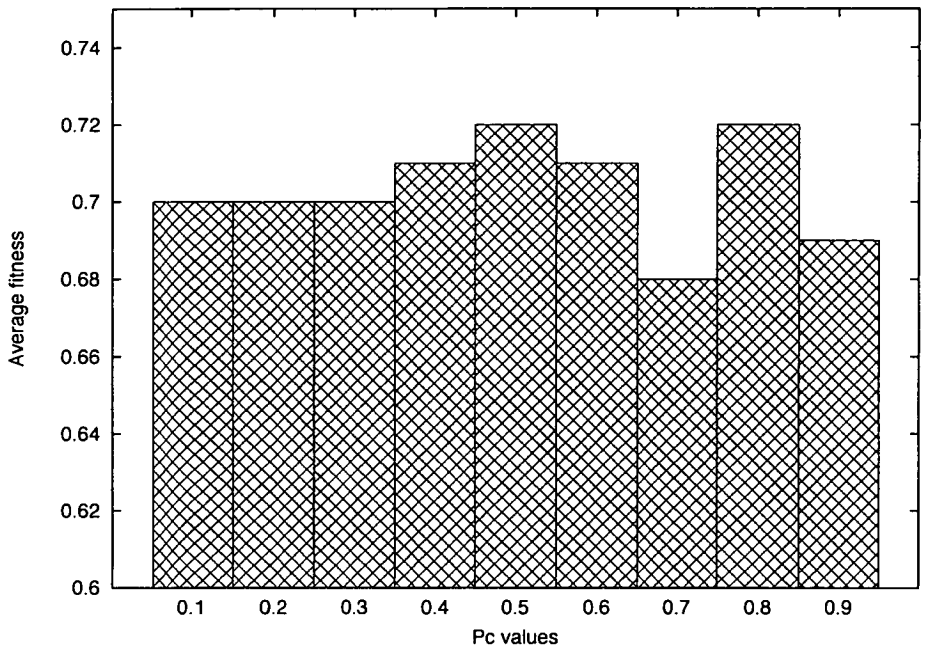

(a) Pc values vs average fitness

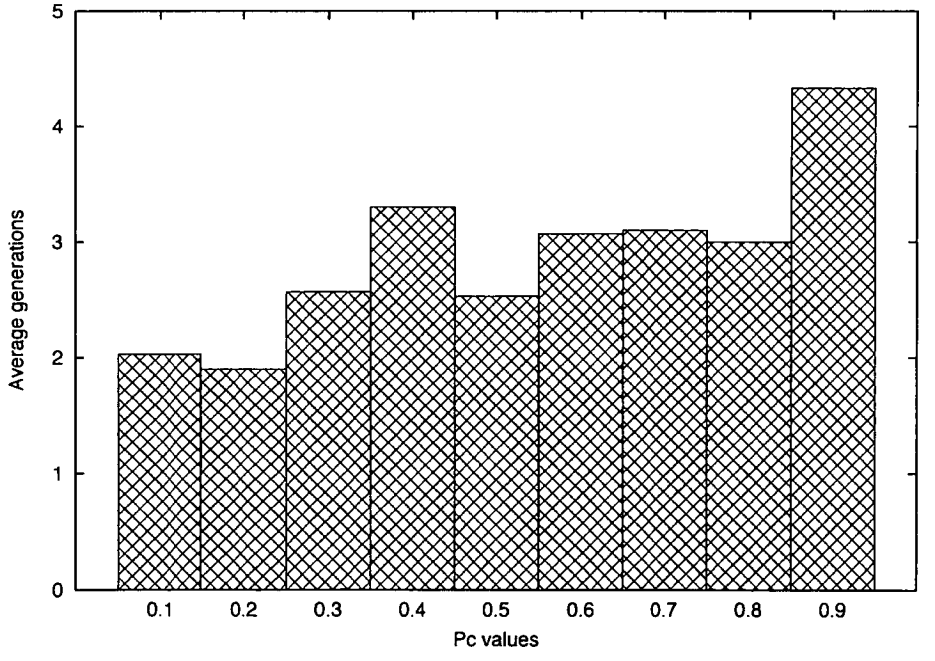

(b) Pc values vs average generations

Figure 3.11: *Probability of crossover, p_C parameter tuning*

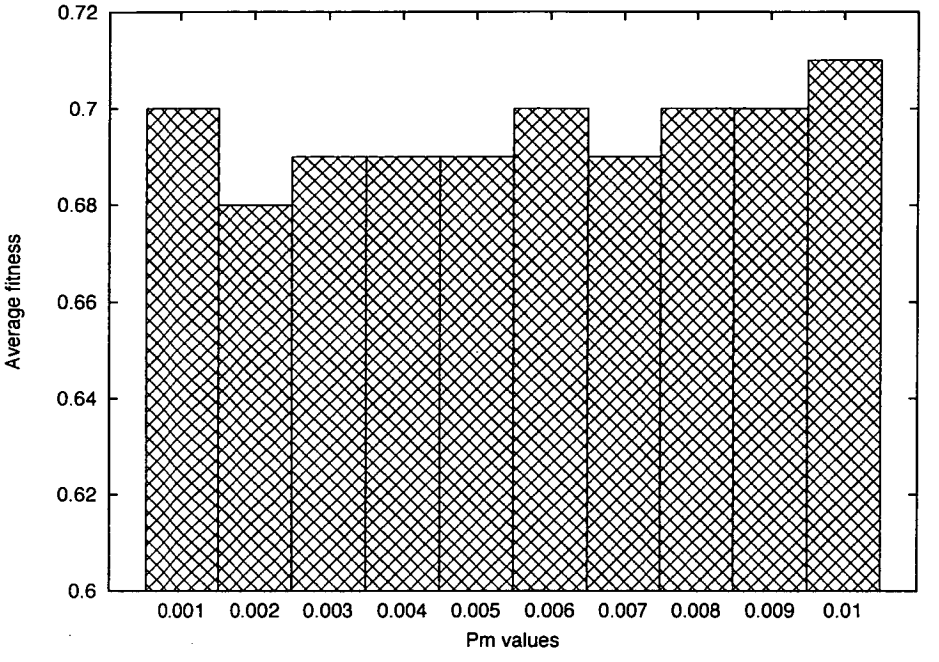

(a) Pm values vs average fitness

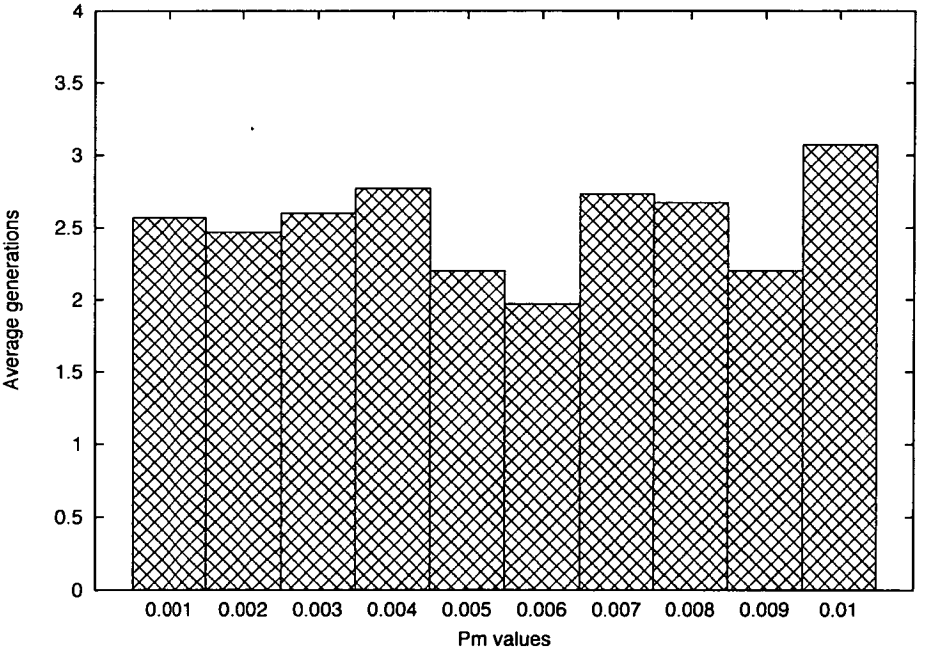

(b) Pm values vs average generations

Figure 3.12: *Probability of mutation, p_m parameter tuning*

As discussed before, mutation is a rare process and tuning it ideally is important to prevent GA from transforming to a random search. Therefore, various p_m are performed in this experiment ranges from 0.001 to 0.01. Figure 3.12 depicts the performance of these probability values in terms of average fitness value and average generation evaluation. The probability of 0.01 gives significantly high fitness value but requires the longest generation time to converge. This convergence time is still reasonable considering this process is very seldom to occur.

Previous experiments have discovered the ideal settings for maximum generation, probabilities of crossover and mutation for this application. Population size ranging between 16 to 104 are evaluated using values obtained from the previous GA experiments as the results are shown in Figure 3.13. Population of 72 individuals yields the highest strength of individual found in adequate number of generations. This size of population provides enough individuals to diversify the population for the GA search to produce high degree of accuracy in registering transformed PCB images.

Parameters	Setting Values
Generation	200
Population size	72
Probability of crossover, p_c	0.5
Probability of mutation , p_m	0.01
Best fitness found	0.8

Table 3.1: *Values of parameters in GA*

The GA parameters used throughout this work is shown in Table 3.1 based on parameter tuning test that has been carried out in the previous section. Different value setting gives different results in terms of maximum fitness and generation time of convergence. To produce high accuracy and efficient image registration, this work prefers value setting that gives maximum fitness in short generation and low computational time which is suitable for implementation in a real-time image registration.

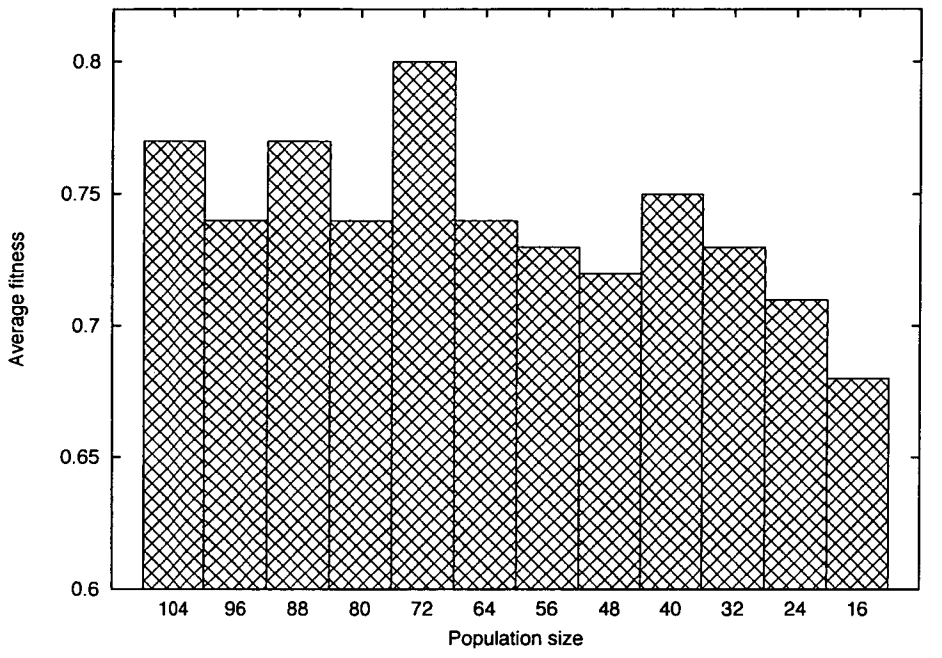

(a) Population size vs average fitness

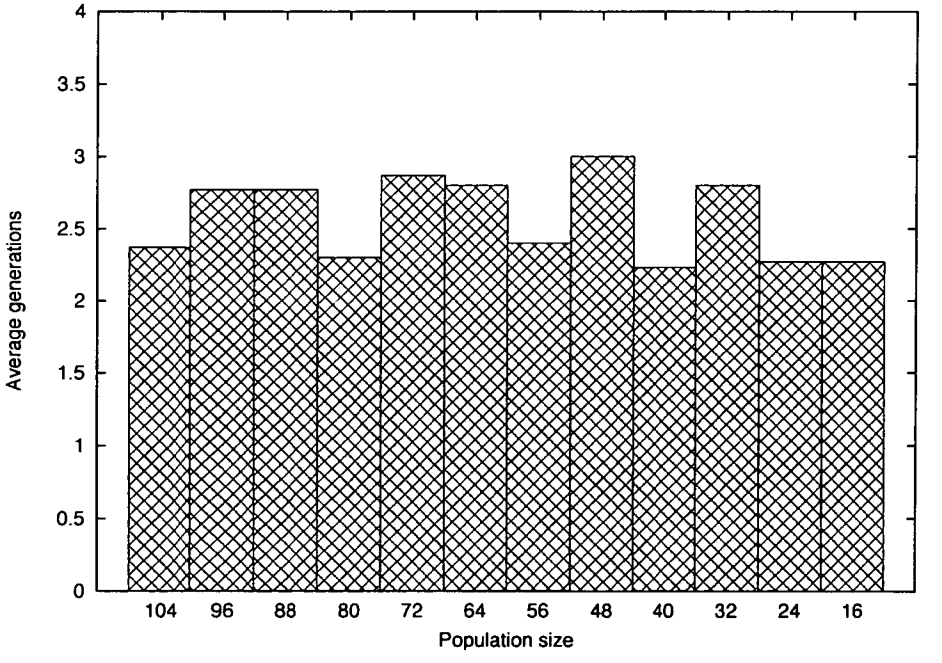

(b) Population size vs average generations

Figure 3.13: *Population size parameter tuning*

3.4 Performance analysis

We implemented this framework on a Linux-based Personal Computer (PC) and perform the analysis on two misorientated test images. One of them is a fault-free board and another one is a faulty board (has one IC missing). The analysis is repeated six times to evaluate the consistency of the results. As GAs are stochastic methods, conclusions based on a few trials could be misleading. This analysis was also used for measuring the randomness of the random function that is used to initialise the first population and in the GA operations of crossover and mutation.

In this simulation, average performance of GA, best fitness values obtained and number of generation required for the search to converge are studied. The maximum fitness value measures the accuracy of transformation parameters of the test image and therefore will determine the precision of registration. Convergence time determine the efficiency of GA and may vary among the trials due to dependent on random initial population created and random GA operations.

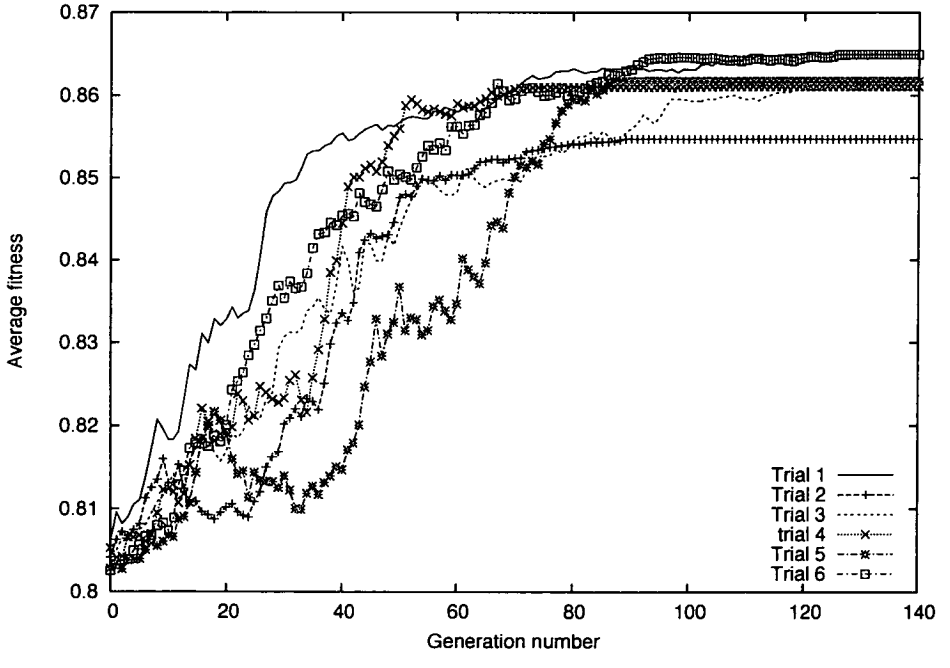

Figure 3.14: *Average fitness values vs generation number for fault-free board for six trials*

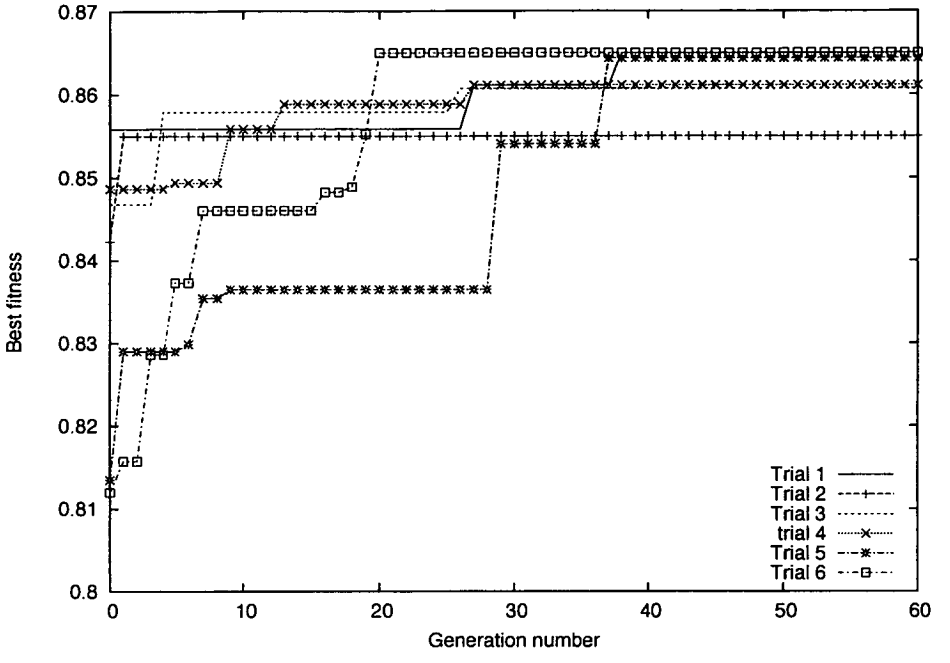

Figure 3.15: *Best fitness values vs generation number for fault-free board for six trials*

From Figures 3.14 and 3.15, the GA performance on the fault-free board are consistent and the fitness values increases in every generation for all trials. The average of best fitness values obtained from the trials are high which is 0.86 and the runs converged after generation of 120 in general. The average values are computed in each generation caused statistical increase and decrease of the average fitness. Sometimes the decrease in average fitness occurs when the chosen pairs are not fit enough to produce fitter offsprings as expected. Individuals with low fitness also give a lower average. The best individual found so far is appointed as the global fittest individual until better individual is found.

Low fitness values in all trials are related to the loss of pixels information due to pixel interpolation during rotation operation. The loss of pixels information leads to less matching pixels and directly decrease the fitness values. This problem caused the rotation values produced inaccuracy of ± 2 degrees and displacement values in both axis have inaccuracy of ± 4 pixels. These results implies that the quality of image has a big impact on the accuracy of the results since this work is a reference-based method.

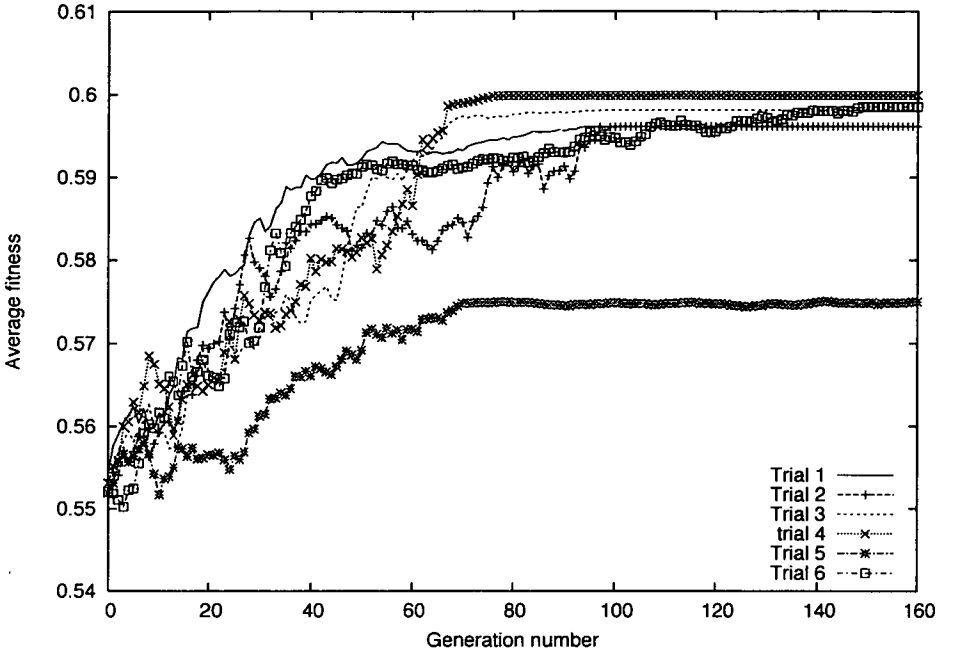

Figure 3.16: *Average fitness values vs generation number for faulty board for six trials*

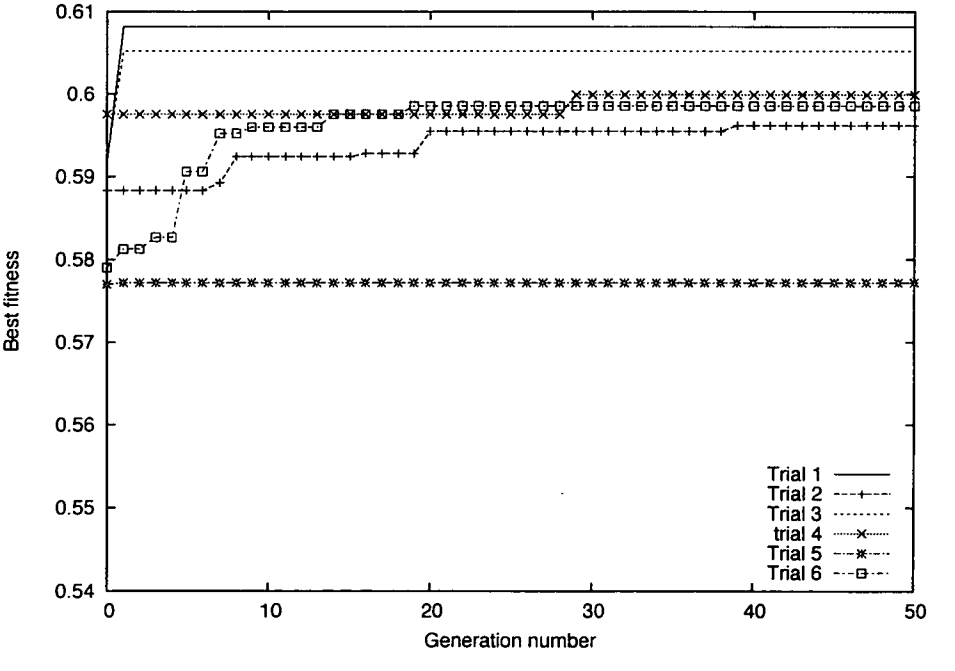

Figure 3.17: *Best fitness values vs generation number for faulty board for six trials*

The consistency of the results in six runs continues during testing the faulty board as shown in the plotted results in Figure 3.16 and Figure 3.17. The maximum fitness value that can be found is about 0.6 and the search converged around generation number of 150. As explained before, inaccuracy happens prior to rotational operation. Therefore, the inaccuracy of transformation parameters produced in this experiment is about ± 2 degrees in rotation and ± 5 pixels in displacement at both axis. The values are obtained at the end of the simulation resulting to the best fitness value found when the GA is completed.

As shown in both figures on results of faulty board, trial 5 has converged prematurely compared to other trials may be due to lack of diversity in the population and caused the GA lost ability to evolve. Dependency on random functions without study of relation distance among the parameters may also be one of the reason for this irregular finding.

The convergence of GA failed to yield nearly ideal fitness value in all trials prior to the production of identical individuals in later generations. These identical individuals are recognised as high potential individuals in early stage and they are preserved throughout the generations by elitism process. The superior of their fitness leads the GA to evolve slowly and only able to end the search with theirs fitness value. This phenomenon will contribute to inefficiency in GA search which then may affect the whole inspection process. To achieve better performance, elitism must be performed in a better way which preserves potential individual that has the quality to evolve while maintaining the diversity of population.

The best fitness values gained in both test boards show the vast difference in value which is about 0.26 with regard to the existence of defect. This work that is based on full image matching performed unsatisfactorily caused by the existence of physical defect, though GA converges in a reasonable period of generation. In this implementation, defect detection process may be effected by misleading transformation estimation given by these fitness values.

New mechanism to perform rotation operation is also needed to minimise the loss of pixels information. Original value of pixels intensity is not only important for GA operation but also important for future defect detection algorithm which is operating in pixel domain. Based on these

findings, more strategies are required to optimise this GA-based framework in order to produce high degree of accuracy in the registration stage and at the end producing high quality of inspection output in shorter time.

3.5 Conclusions

This chapter introduced an image registration of PCB placed on a conveyor belt using a specially-modified conventional GA. The coding representation of possible solutions of geometric transformations using binary code and a special fitness function based on full reference image matching have been described in detail in this chapter. Elite individuals are selected based on their rankings for the next generations and Roulette-wheel selection is implemented in this GA framework.

Few independent experiments are performed in order to find optimum setting for every parameter of GA such as maximum generation, probability of crossover, probability of mutation and size of population. Modifications on GA operators and efficient parameter settings presented here are essential in order to prove the robustness of GA in this application. The efficiency of thresholding implementation before GA search starts is also studied to produce better findings.

The results show the performance by GA on misorientated fault-free and faulty PCB images are consistent where the solutions are found in 120 to 150 generations. However, maximum fitness found in the faulty PCB image is low compared to the fault-free one due to the existence of defect. This gives motivation in using other method other than full image search to improve the performance of this image registration. An early convergence in GA search that happened in simulation presented in this chapter is an important issue that has to be tackled using local search technique such as hill-climbing.

Simulation results also have shown the potential of GA in finding near-correct values of transformation parameters. However, there are more improvement to be done on the GA to provide the highest accuracy registration in a low computational time and good quality registered image for defect detection procedure as will presented in the next chapters.

Chapter 4

Tailoring the GA and Image Registration Algorithm

4.1 Introduction

Accuracy, speed and reliability are the main considerations in producing a robust image registration system. Therefore more improvements are required for the previous framework of image registration in order to achieve the objectives of the developed inspection system.

Despite their effectiveness, GAs are generally expensive to compute and have many parameters to adjust [88]. GAs can reach a solution close to the global optimum in a reasonable time. However, a great deal of time is required to improve the solution significantly beyond this point and this means a cooperation with a local search agent such as hill-climbing is needed in order to mitigate this problem. Local search methods are designed to climb from a given starting point in the search space and locate the local optimum of the corresponding attraction basin [89].

Elitism (E) is also a good solution to be implemented in the GA to ensure that at least one copy of the best individual in the population is always passed onto the next generation. The main advantage is that convergence is guaranteed (i.e., if the global maximum is discovered, the GA converges to that maximum). However, there is a risk of the search is being trapped in a local maximum. The concept of selection intensity to be a quantitative measure that can be used for elitist and steady-state mechanisms in order to guide the selection to better direction has been proposed by [90]. It is important to explore the solution space very carefully before becoming too committed to any subset of solutions that appears to be promising by not focus too much energy on only the most fit individuals [91]. Hence, the less fit individuals must be kept in the population in case new directions of exploration need to be initialised when the search is stuck in a local optimum.

Appropriate coding and operations and appropriate parameter settings are two categories of decisions that a user must make before applying a GA [83]. Computational time is also a big issue that has to be solved with regard to the performance in the previous chapter. Using a centre block of image in fitness evaluation is one way to reduce the computational time of GA search. Further accuracy improvement can be achieved by implementing a more efficient rotational operation.

When the complexity or the size of the problem grows, it becomes important to tune the GA parameters in order to obtain an acceptable performance . A GA with advanced features, such as sharing and hybrid operators can be a powerful optimisation tool, but there is a need for careful tuning of its parameters to behave effectively [92]. For each enhancement in this chapter, some preliminary experiments are conducted to establish reasonable settings for these variables.

The rest of this chapter is organised as follows: Section 4.2 describes the performance between binary and Gray coded mutation, fitness evaluation using centre block matching is presented in Section 4.3, Section 4.4 presents the study of elitist selection schemes, rotation by shear is more effective rotational operation as discussed in Section 4.5, Section 4.6 describes the conversion from binary to real integer coding, study on hybrid methods is explained in Section 4.7 and Section 4.8 concludes the chapter.

4.2 Binary vs Gray coded mutation

A drawback of encoding variables in a binary string is the presence of Hamming cliffs which large Hamming distances between the binary codes of the adjacent integers [93]. Gray codes alleviate this problem by ensuring that the codes for adjacent integers always have a Hamming distance of 1. As mentioned previously, 19 bits (nine for the rotation and five each for the displacements) are used in a binary string to represent each combination of transformation function.

The results in [94] indicate that while there is little difference between the two for all possible functions. Gray coding does not necessarily improve performance for functions which have fewer local optima in the Gray representation than in binary. Gray coding is also used in [92]. For that, a set of experiments are performed to evaluate if there is any improvement in performance using Gray coded mutation. Mutation operation is done as presented in previous chapter by randomly selecting

any individual with a prespecified probability. For Gray coded mutation, the binary string will be converted to Gray value before mutation occurs. Then, the mutated string is converted back to binary coding as a new individual.

4.2.1 Experiments

Four test images, as shown in Figure 4.1, are used in comparison experiments between binary and Gray coded mutation. The experiments are performed using GA parameters decided in previous chapter (as shown in Table 3.1) and the reference image used as shown in Figure 3.7. The simulation on each test image is repeated twice and the results are shown in Figure 4.2.

Both techniques typically converged after 20 generations with best fitness values ranged between 0.67 to 0.98 in all test images except in Test image 4. Early convergence occurred in simulations using Test image 4, which are terminated before 10th generation. As shown in Figure 4.2(b), Gray coded technique is stucked at local optima with fitness about 0.67 for both trials in simulations on Test image 2.

From these findings, there is no significant difference in performance for this application between these two mutation techniques. In Test image 1 and 4, these techniques give almost similar performances in finding the maximum fitness and converged approximately at the same time. The binary coded mutation performs better in Test image 2 but Gray coded mutation outperformed the binary in Test image 3. This implies that any of these techniques are suitable for this application. Therefore, Gray coded mutation is chosen to be used in the next experiments.

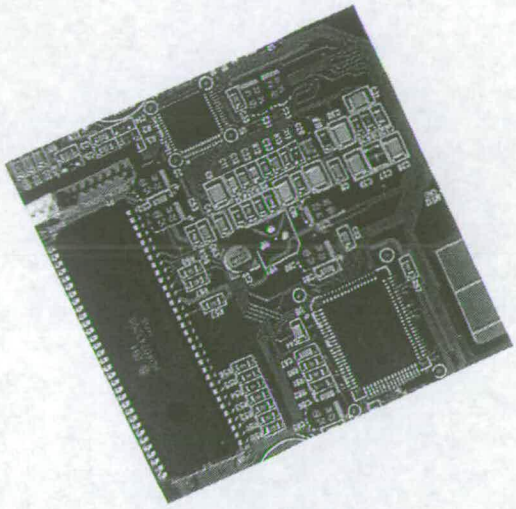

(a) Test image 1

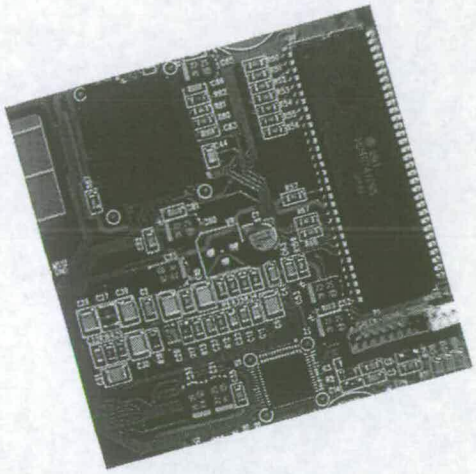

(b) Test image 2

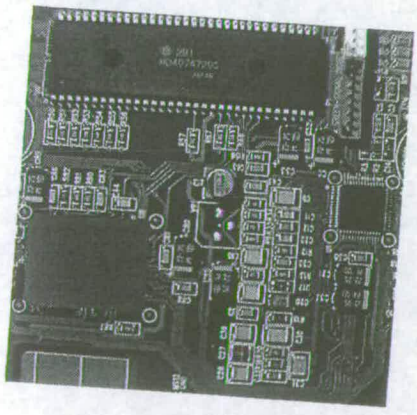

(c) Test image 3

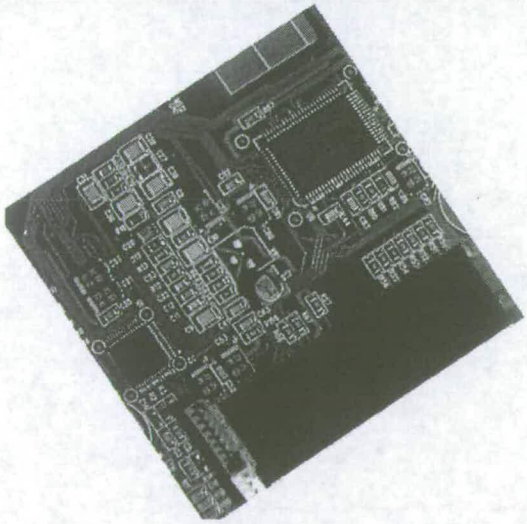

(d) Test image 4

Figure 4.1: *Test images for binary and Gray-coded mutation experiments*

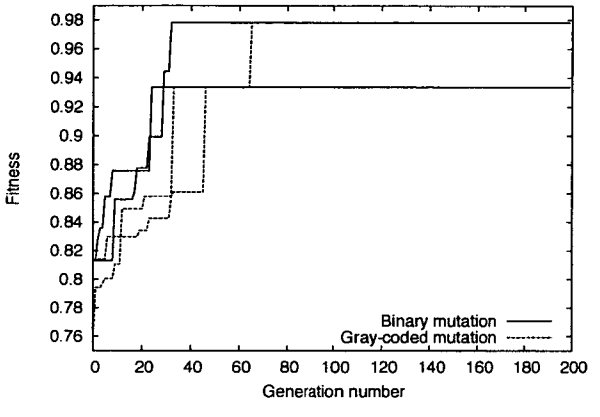

(a) Test image 1

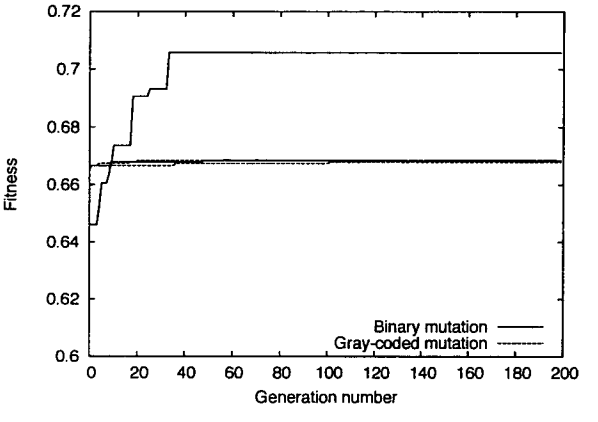

(b) Test image 2

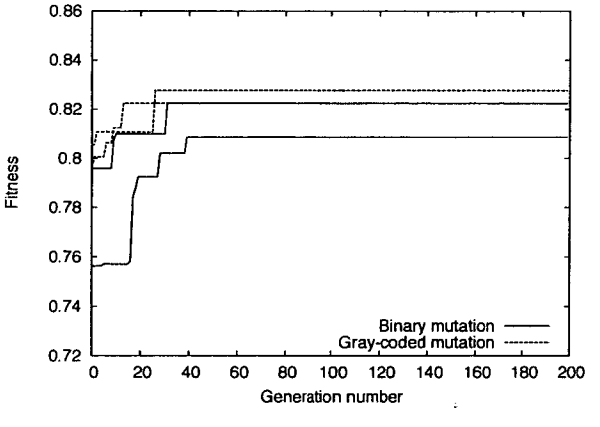

(c) Test image 3

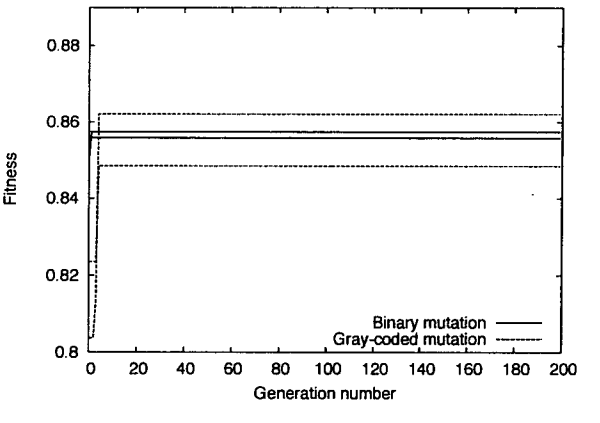

(d) Test image 4

Figure 4.2: *Performance of GA using binary and Gray-coded mutation on test images*

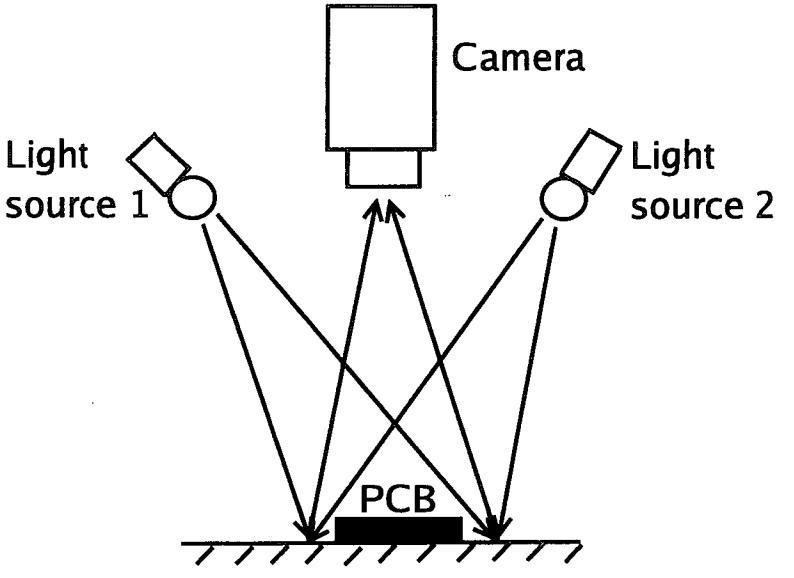

Figure 4.3: *Bidirectional lighting based on [23]*

4.3 Fitness evaluation using centre block matching

Previously, the whole image matching has been used to evaluate the fitness value for estimating the transformation of a test image. The results are accurate but the time consumption is not suitable for a real-time application as each GA search requires 10 minutes to converge and found the solutions. Therefore, a block matching method is investigated and applied on the algorithm to speed up the processing time. However, the accuracy of this technique has to be studied before it is fully implemented. The selection of block in an image plays an important role to ensure that the block matching gives enough information to the GA for finding the correct transformation function.

Each pixels intensity in the image is very important when reference-based method is used. However, the shading will affect the quality of image captured and may give wrong analysis. Poor quality of image will give less information in every individual of the population in GA operations. Therefore, a solution for the shading problem is highly required. A shading correction algorithm is needed or

better lighting condition has to be created during image capture to enhance the performance of the system. Both of these solutions have been implemented in many inspection system work and produce good results [1, 6].

Due to the above-mentioned issues, a centre block of image is chosen to be implemented in the fitness evaluation in GA. The centre block is the safest spot from shading since the system utilises bidirectional lighting and the camera is normally focussed to the centre of PCB, as shown in Figure 4.3. 40 $\times$40 pixels of centre block size is used to reduce computational time in pixel processing which has significant computation time reduction especially on large size images. The next experiments will employ this setting in order to speed up the GA processing time and also to improve the findings of transformation functions.

4.4 Study of elitist selection schemes

Elitist selection scheme is a technique to choose the offsprings that have to compete with their parents to gain admission for the next generation of the GA. The outstanding advantage of this environment is it always preserve the best solutions in every generation. Discussions on exploitation and exploration trade-off by [90] has initiated the idea to investigate tournament and Roulette-wheel schemes other than deterministic in E environment. The researcher has used tournament in this discussion and [25] used Roulette-wheel successfully in his evolvable hardware system for AOI.

This study investigates the GA performance by implementing elitist selection scheme for a low-cost PCB inspection system. This strategy aims to explore the possibilities of tournament and Roulette-wheel in improving the existing system which has used deterministic selection method. Deterministic, tournament and Roulette-wheel selection scheme have been compared in terms of maximum fitness, rate of accuracy and computation time.

4.4.1 Implementation

In E environment of this work, deterministic, tournament and Roulette-wheel selection methods are implemented. Additionally, centre block matching of size 40 x 40 pixels is used in this work to reduce the number of pixels compared and directly decrease computational time requirement. Four artificially transformed and defected images have been tested using these selection methods to evaluate the performance in terms of maximum fitness, accuracy and computation time. These investigations aim to develop a better understanding of their capabilities to improve the strength of existing GA framework in finding optimum solutions.

In this simulation, all individuals from previous and current generation are considered for these survival selections. Deterministic selection depends on the rank of the individuals, which is based on their fitness values. Only the top ranked individuals will survive for the next generation. For tournament selection, two individuals are selected randomly and they will compete with each other in terms of fitness value. The winner will be included as one of the next generations population. A tournament size of 2 is commonly used in practice as this often provides sufficient selection intensity on the most fit individuals [91]. The Roulette-wheel selection depends on the weight of each individual, defined as their fitness value over the total fitness of all individuals. Higher weight gives larger opportunity to be selected in a random pick for the next generation.

These three selection schemes will be compared under three different categories:

- Maximum fitness: this is the maximum value of fitness found at the end of the search; the ideal value is 1.
- Accuracy: this is calculated using this formula, $error = \sqrt{\frac{\sum_{m=1}^{n}(x_i - x_m)^2}{n}}$ where x_i is the ideal value of transformation parameter, x_m is the transformation value gained from the maximum fitness and n is the total experiments for each sample.
- Computation time: this is assessed by the number of generation evaluations to reach the maximum fitness.

The following assumptions have been made in this simulation as listed below:

1. Both test and reference image have the same size.

2. Camera position and focus of the camera is constant across the samples.

4.4.2 Experiments

Performance study is performed using previous configurations as described in Section 3.3. The thresholding is applied for every pixel by setting the value of object point, T equals to 100 as implemented in the existing framework.

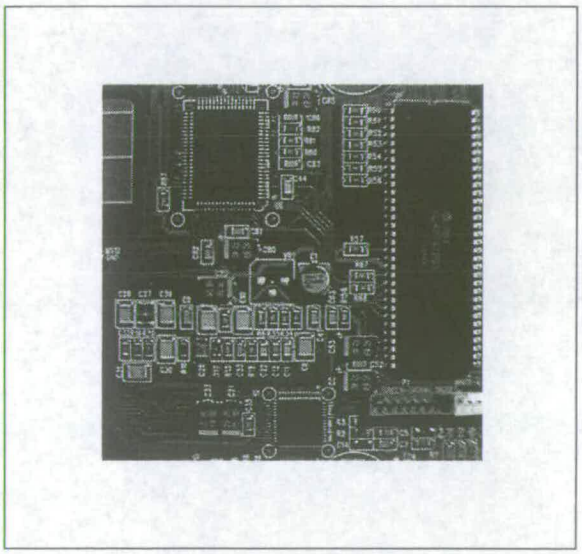

Figure 4.4: *Image of reference board*

Fitness value is derived by comparing every pixel value in 40 x 40 pixels centre block of both images (reference and test) and divided by the total pixel of block, in this case is 1600 pixels. The reference image is displayed in Figure 4.4 and the test images are shown in Figure 4.5. Parameters for all methods are configured according to the previous GA framework [79] where maximum generation is 200, selection is based on Roulette-wheel method, crossover probability is 0.5 and mutation probability is 0.01 while population size is 18.

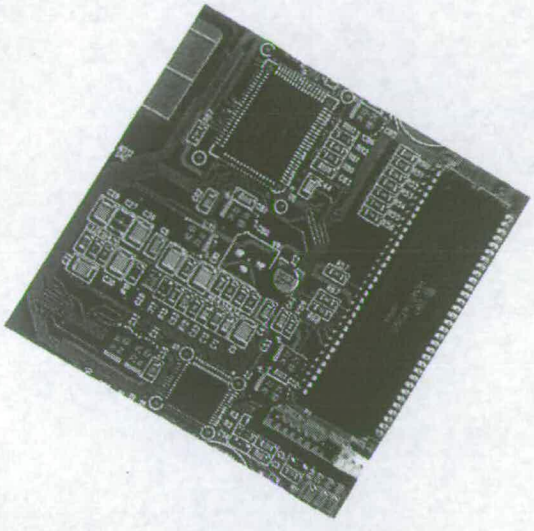

(a) Test image 1 (T1)

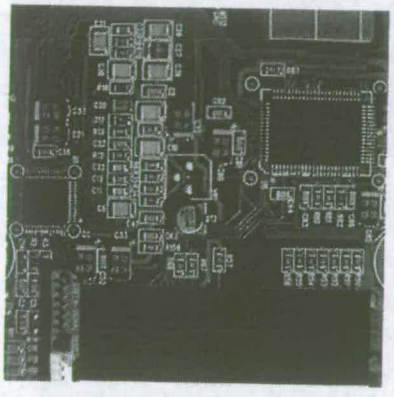

(b) Test image 2 (T2)

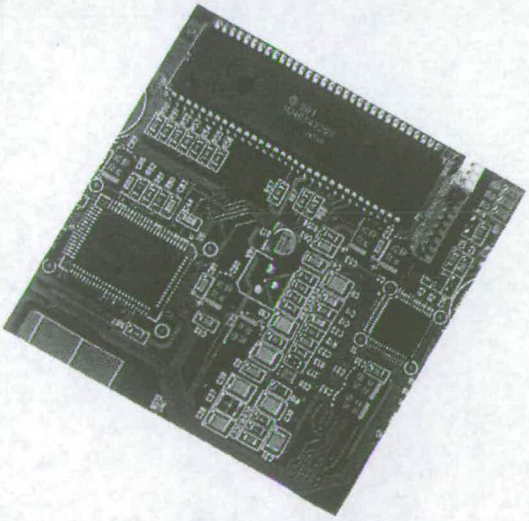

(c) Test image 3 (T3)

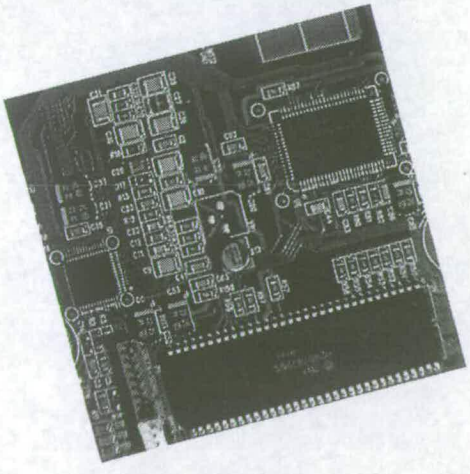

(d) Test image 4 (T4)

Figure 4.5: *Test images transformed using different rotation and displacement values*

Gray-coded mutation is also added in this implementation to produce more variant individuals. The variance leads to better estimation of transformation values. Another modification is a smaller population size compared to [79]. The main reason is the previous population size has redundant individuals which only increases the computational time. The new population size has reduced time consumption with the same performance as the previous setting and is proved to be viable for this 'soft' real-time system.

4.4.3 Experimental results and discussion

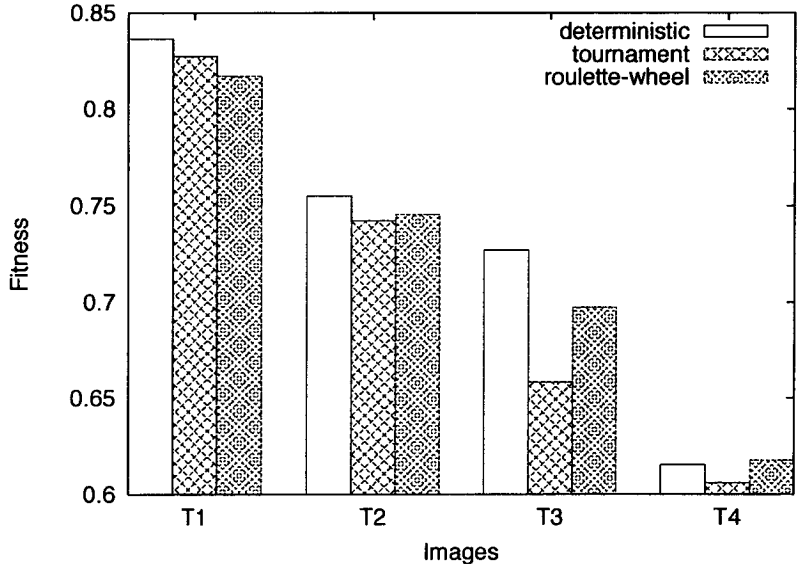

Figure 4.6: *The schemes are compared in terms of maximum fitness*

The random nature of GAs makes it difficult to predict their performance on a given problem for each run. As a result, performance measurements are generally taken as averages over sets of runs [95]. For each scheme and sample, 10 experiments are performed with initial transformation values taken at random. The values given in the results are average values, computed over these 10 experiments.

Deterministic selection has the ability to reach the highest maximum fitness, followed by Roulette-wheel and tournament for all test images as shown in Figure 4.6. Preserving strong

individuals in deterministic method has effectively increases the maximum fitness values, resulting in nearly accurate transformation values of inspected images. Roulette-wheel and tournament concept that provide chances for weak individuals to be selected prove to be ineffective method for this work.

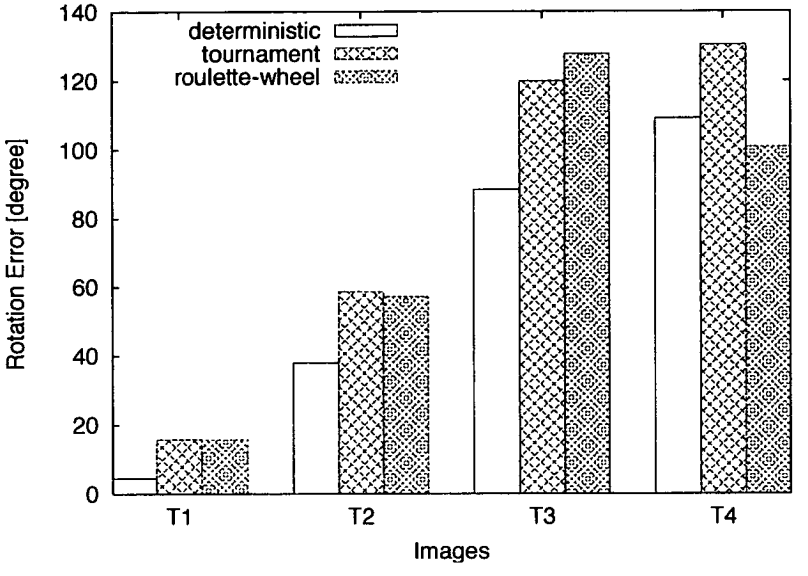

Figure 4.7: *The schemes are compared in terms of accuracy of rotation value*

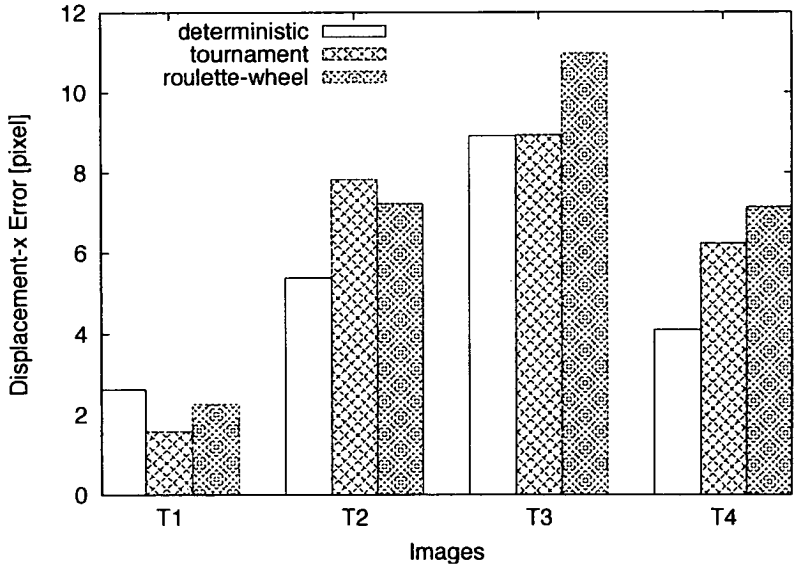

Figure 4.8: *The schemes are compared in terms of accuracy of displacement-x value*

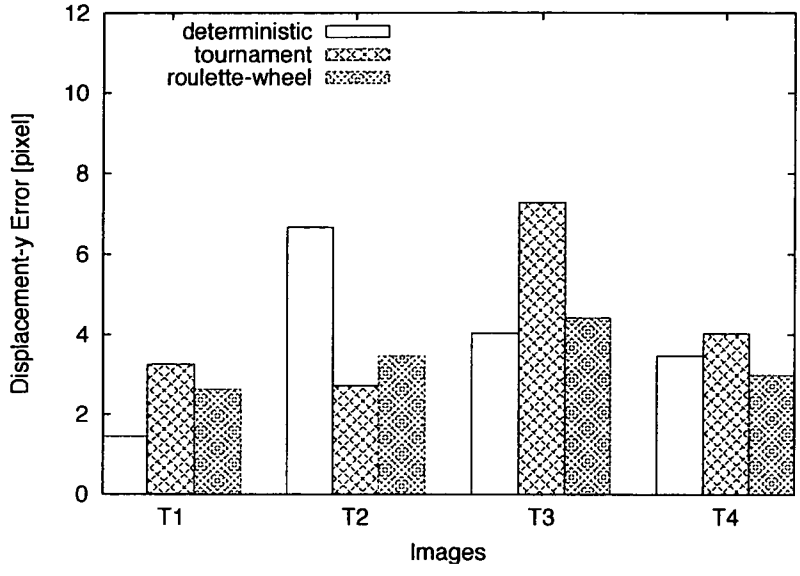

Figure 4.9: *The schemes are compared in terms of accuracy of displacement-y value*

Deterministic scheme also produced least errors in estimating rotation, x-axis displacement and y-axis displacement parameters as shown in Figure 4.7 to Figure 4.9. Roulette-wheel outperformed tournament in most cases and is slightly favourable as deterministic in this category. Although Roulette-wheel permit selection of weak individuals for the next generation, probability of strong individuals are still dominant.

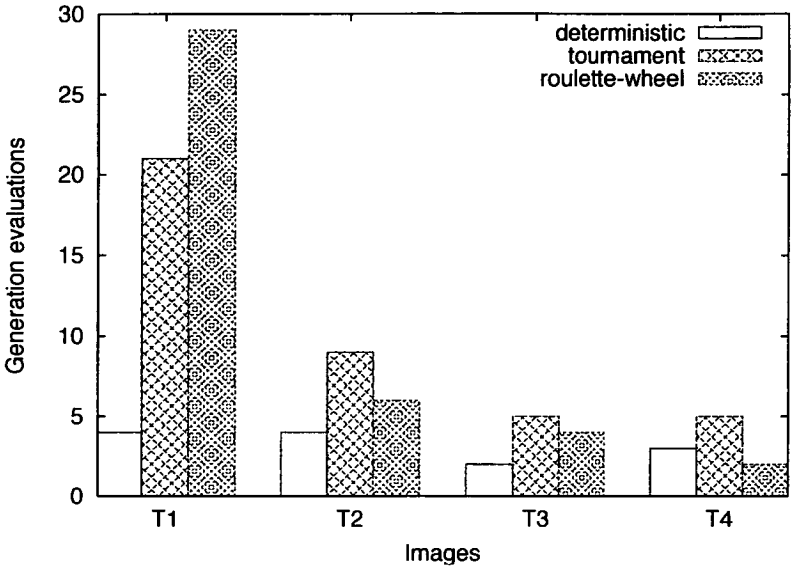

Figure 4.10: *The schemes are compared in terms of generation evaluation*

Deterministic scheme converges fast to reach maximum fitness compared to other two methods as illustrated in Figure 4.10. This inspection system indirectly benefited from the early convergence characteristic of deterministic scheme and low computational time will be produced. The small population size and block matching algorithm improvement also contribute to the overall computational time. Tournament scheme has the worst overall performance while Roulette-wheel is only a fraction slower than deterministic method considering generation evaluations. It is worth noting that all the schemes produced best maximum fitness and high accuracy of transformation parameters considering only rotated test image (T1). However deterministic scheme still prove to be an excellent option if computational time is an essential requirement.

Symbol	Description
•	represents significant exists, significant level, p<=0.05
≈	represents slightly significant exists
=	represents no significant exists

Table 4.1: *Description of symbols in Wilcoxon test analysis*

Test images	Deterministic vs Tournament	Deterministic vs Roulette-wheel	Tournament vs Roulette-wheel
Image 1	=	=	=
Image 2	=	=	=
Image 3	●	≈	=
Image 4	=	=	=

Table 4.2: *Wilcoxon test analysis on maximum fitness*

Test images	Deterministic vs Tournament	Deterministic vs Roulette-wheel	Tournament vs Roulette-wheel
Image 1	=	=	=
Image 2	●	=	≈
Image 3	=	=	=
Image 4	=	●	●

Table 4.3: *Wilcoxon test analysis on generation evaluation*

Test images	Deterministic vs Tournament	Deterministic vs Roulette-wheel	Tournament vs Roulette-wheel
Image 1	●	●	●
Image 2	●	●	●
Image 3	●	●	●
Image 4	●	●	●

Table 4.4: *Wilcoxon test analysis on rotation accuracy*

Test images	Deterministic vs Tournament	Deterministic vs Roulette-wheel	Tournament vs Roulette-wheel
Image 1	=	=	=
Image 2	●	●	●
Image 3	=	=	●
Image 4	○	●	●

Table 4.5: *Wilcoxon test analysis on displacement-x accuracy*

Test images	Deterministic vs Tournament	Deterministic vs Roulette-wheel	Tournament vs Roulette-wheel
Image 1	=	=	=
Image 2	•	•	•
Image 3	=	=	=
Image 4	•	•	•

Table 4.6: *Wilcoxon test analysis on displacement-y accuracy*

Table 4.2 to 4.6 shows the results of Wilcoxon test on the performance of these three elitist selection schemes in terms of maximum fitness found, generation evaluation and accuracy of every transformation parameter. Table 4.1 describes the symbols used in the analysis. Wilcoxon test is used in this analysis due to the distribution of every performance by the schemes are not normally distributed. The test is performed using R-language which is a language and environment for statistical computing and graphics [96]. Based on the test results, the schemes give nearly identical performance especially in generation evaluation and accuracy of all transformation parameters. In Table 4.2, only one test image produces significant difference between deterministic and tournament scheme. Based on both statistical analysis as presented in this section, deterministic scheme slightly outperformed tournament and Roulette-wheel schemes in term of maximum fitness, accuracy and computational time. Consequently, it has been established as an ideal selection method in E for this work.

4.5 Rotation by shear

Previously, rotation function in University of Edinburgh Vision's group library [86] is used in image transformation in GA search. It is discovered that the GA is not able to find high maximum fitness due to loss of pixel information during rotational operation and this may give big implication on the performance of image registration. Due to this limitation, rotation by shear is studied and cause almost no pixel information loss.

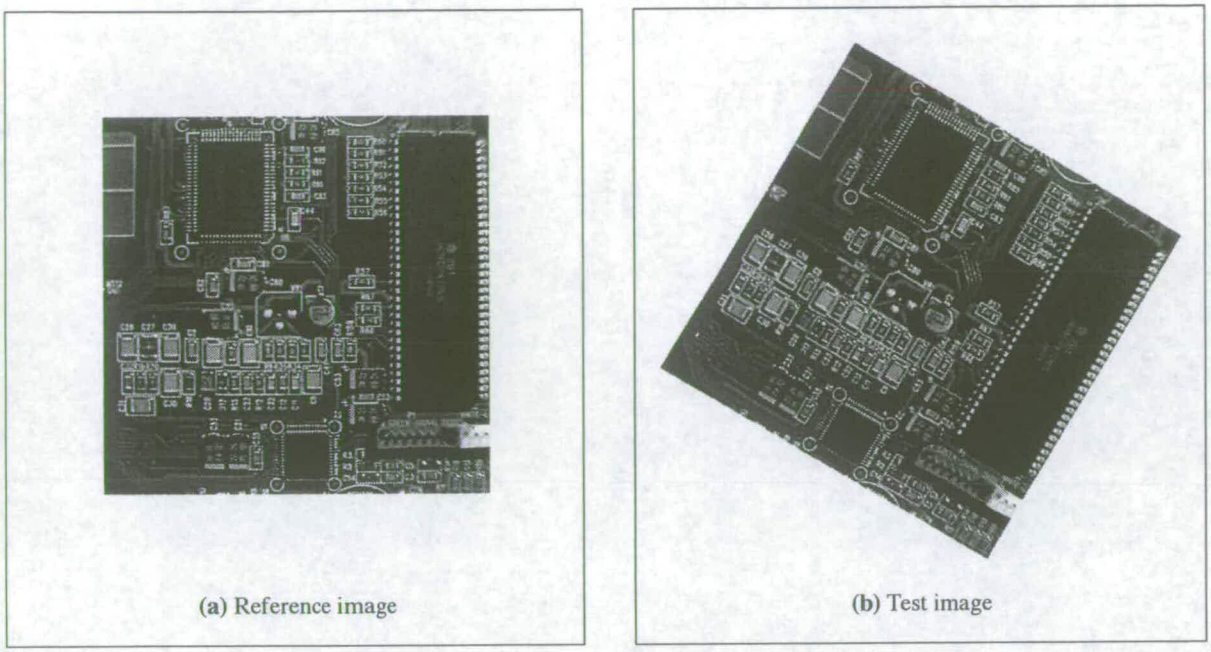

(a) Reference image

(b) Test image

Figure 4.11: *PCB images*

Rotation by shear or Paeth rotation [97] involves rotating an image by using 3 independent shear transformations. Each shear operates on a single image axis allows for anti-aliasing to be implemented very simply. The end result is very high quality image rotation. The C-Language implementation is based on [98] and has been experimentally evaluated. The test image in Figure 4.11(b) is aligned to correct position as the reference board shown in Figure 4.11(a) using both techniques. From the experiments, the rotation by shear successfully preserved nearly all original information of the image pixels by producing maximum fitness of 0.99 compared to Vision library rotation technique which only able to give maximum fitness of 0.86. However, both of the techniques execute the operation in very short time which are less than 1 second. As a result, the rotation by shear is selected as rotation function in the optimised version of GA based image registration since less loss of image transformation is produced.

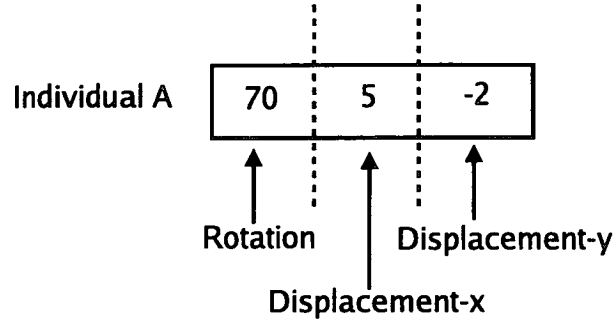

Figure 4.12: *Real number coding*

4.6 Binary to real integer coding

Choosing a good encoding of a chromosome is vital for solving any GA search problem [99]. In [100], a discussion on used coding schemes such as binary, gray and floating-point is presented and compared with the proposed method using fuzzy coding. In [101], a real-coded GA is proposed capable of simultaneously optimising the structure of a system and tuning the parameters that define the fuzzy system.

The standard GA codes the genes as binary strings similar to how DNA codes information in living organisms and it works fine in searching parameters that are really binary. Complications happen when the parameters are real numbers and the original distances are destroyed in the transformation. As a consequence, the standard GA does not search the parameter space as efficiently as it might and it has more potential to get stuck in local optima.

Previously, binary coding is implemented in GA based image registration framework and it has few drawbacks when range of solution is set according to the scope of consideration. It generates bigger search space than the space needed for range of consideration which contributes to poor performance of GA. It also must adapt the parameter values in the considered ranges since it is likely the parameters are over or below valued due to the GA operations.

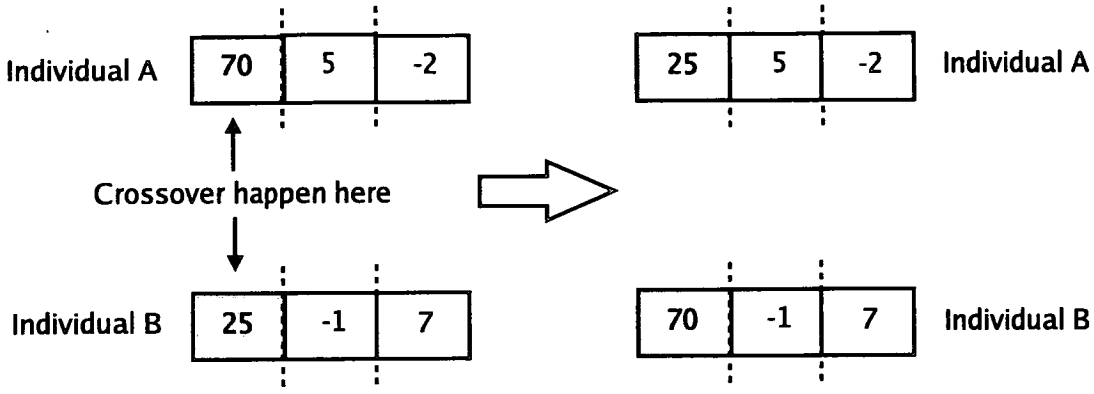

Figure 4.13: *Crossover operation on real number coded individuals*

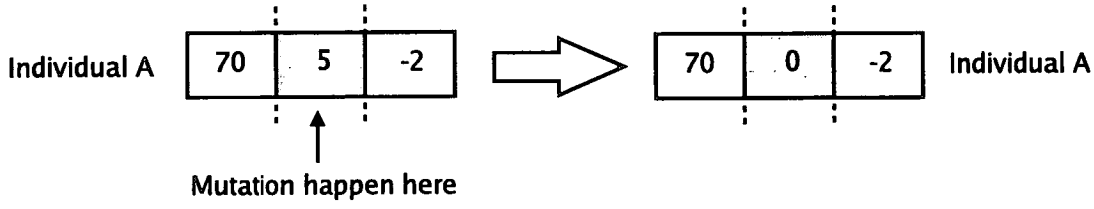

Figure 4.14: *Mutation operation on real number coded individuals*

Hence, the improved GA is coded in real numbers shown in Figure 4.12 and new ways to perform crossover and mutation operations are developed, as depicted by Figure 4.13 and Figure 4.14 respectively. As is normal practise, the probability values of these operations are set initially. If random generated numbers fall below the probability values, the crossover and mutation will happen. Then, a type of transformation parameter that will experience the GA operations is selected randomly. For crossover operation, two selected individuals will exchange the value of chosen parameter while the selected parameter for mutation is randomly altered within the considered range, where in this application the rotation value ranges from 0 to 359 degrees and displacement value at both axis are considered from -10 to 10 pixels.

4.7 Study on hybrid methods

Hybridisation of GA and HC has been done on range image registration in [88] by exploring 3 novel approaches: a hybrid algorithm that combines a GA with hillclimbing heuristics (GH), a parallel

migration GA (MGA), and a MGA using hillclimbing (MGH). They have proved that HC provides fast convergence and good performance in finding correct registrations compared to GA alone. Two strategies of hybridising GA with HC and E methods for global optimisation has been presented in [102].

It is very unlikely that GA alone will outperform a specialised scheme tailored to a problem. Most successful applications of GAs have been hybrids [103]. Combination of HC and E usually performs better than either one alone. This happens because there is a possibility of incorporating domain knowledge, which gives it an advantage over a pure blind searcher (i.e a standard GA).

In this section, hybridisation of HC and E with a specially tailored GA for image registration of whole PCBs placed arbitrarily on a conveyor belt during inspection is proposed to maximise the robustness of the existing framework. These hybrid methods are investigated individually and in combination for accuracy, reliability and performance.

Based on the performance of the first prototype with GA alone [79] and motivated by previous reviews, the hybrid method cooperating GA with HC and E is studied to maximise the robustness of the search technique in order to provide better quality and more reliable performance in registration of whole inspected PCBs during inspection process.

4.7.1 Implementation

The proposed technique uses a perfect board as the reference image and the inspected board as the test image. In this work, GA is used to derive the transformation between test and reference images based on a simple GA strategy as presented in [63] during registration stage.

For this work, real number coding has been implemented for this problem considering the range of transformation value that we are going to find. The rotation value ranged from 0 to 359 degrees while the displacement of x-axis and y-axis value is considered between -10 to 10 pixels. The domain of search for these parameters is large ($360 \times 21 \times 21 = 158760$) which is suitable for GA to explore.

Fixed global multi-thresholding operation is applied to both images to enhance the images and

highlight the details before performing GA search. It is also essential to deal with variations in intensity of components on PCB images. For this application, the threshold value for the thresholding operation is chosen based on visual observations. The reference image will be transformed using random rotation and displacement values to create the initial population for GA. Every transformed reference image is compared with the test image to evaluate the fitness value and individuals with solution of rotation and x-y translations information are created.

Iteratively, the whole population for the next generation is formed by selected individuals from the parents and offsprings in current generation. These individuals are ranked based on their fitness performance and the top fittest only are selected for a new population. The population will perform GA activities such as selection, mutation and crossover in every generation until the termination requirements are fulfilled. The GA search will be terminated if an individual with an acceptable approximate solution is found or maximum generation is reached.

At each iteration, the best 5% individuals of the previous generation are preserved. The remaining 95% are from the top ranked individuals after all the GA operations are performed. The preservation of the best 5% individuals are required in case there is no better individual found in the next generation.

The concept of hill climbing algorithms is individual parameter values are modified in such a way that the overall fitness will be maximised. Hill climbing algorithms are typically very efficient at locating local maxima although this leads to their major deficiency; they tend to get stuck at local maxima rather than continuing to the proper global maxima.

In this implementation, a limit for the generation, l is set for every set of GA search. This limit is the number of times the same individual is recognised as the fittest individual. HC will be performed if the limit is reached. The fittest individual of the current generation will be selected for this process where every transformation values (rotation, x and y displacement) will be incremented and decremented by a single unit sequentially. The modifications will be evaluated to examine the fitness value which may replace the current solution. The GA search will be terminated with the current solution unless a

Algorithm 2 The implementation of HC.

```
If generation less than maximum generation
 If limit of generation, l is reached
  current_fitness equals to old_fitness
  current_fitness equals to highest_fitness
  Loop for current_rot-1 to current_rot+1
   Loop for current_disx-1 to current_disx+1
    Loop for current_disy-1 to current_disy+1
     Calculate fitness with current transformation values
     If current_fitness more than highest_fitness
      Then highest_fitness equals to current_fitness
  If old_fitness more than highest_fitness
   GA search is terminated with old_fitness
  Else
   GA search is continued with highest_fitness
```

better individual is found during HC. If the search is continued, the HC process will be repeated when the limit is reached again. The HC implementation is described by Algorithm 2.

4.7.2 Experiments

Performance study is performed using previous configurations as described in Section 3.3 but the basic image processing functions such as global multi thresholding [39] and transformation including rotation by shear function are written in C-language using NetPBM image library [104].

First, the hybrid methods are investigated individually by combining GA with E (GA+E) and combining GA with HC (GA+HC). Finally, GA is combined with HC and E (GA+HC+E) and few adjustments have been done on few parameters in GA+HC+E known as hybrid GA (HGA).

Parameters for all methods are configured according to the previous GA framework [105] where maximum generation is 200, selection is using Roulette-wheel method, crossover probability is 0.5 and mutation probability is 0.01. The first three methods (GA+E, GA+HC and GA+HC+E) have a population size of 18 while hybrid GA (HGA) has a population size of 50. The limit of generation, l is set to 20 for GA+HC and GA+HC+E cases while HGA has a limit of generation of 10. These settings and adjustments are made on observation of all methods performance which aims to improve the robustness of the HGA.

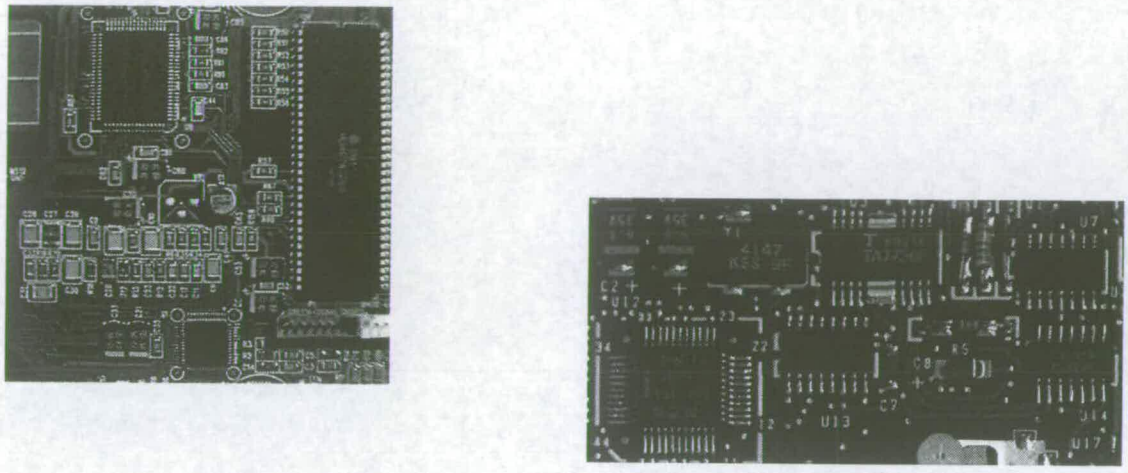

(a) (b)

Figure 4.15: *(a) - (b) Reference images*

Two reference images shown in Figure 4.15(a) - 4.15(b) and four test images shown in Figure 4.16(a) - 4.16(d) are used in the experiment. Test image 1 (T1) and 2 (T2) are artificially transformed images of the reference image shown in Figure 4.15(a) while test image 3 (T3) and 4 (T4) are artificially transformed images of reference image shown in Figure 4.15(b). Estimation of transformation parameters using each search method is repeated 20 times for every test image.

4.7.3 Experimental results and discussion

4.7.3.1 Fitness and generation evaluation

Three types of hybrid methods have been simulated and the performance of each method has been compared with a standard GA search. The comparison is made based on the percentage of simulation that successfully gain a maximum fitness of more than 0.85 and the number of generations to converge. Higher maximum fitness gives better accuracy in estimating the transformation value. It is worth

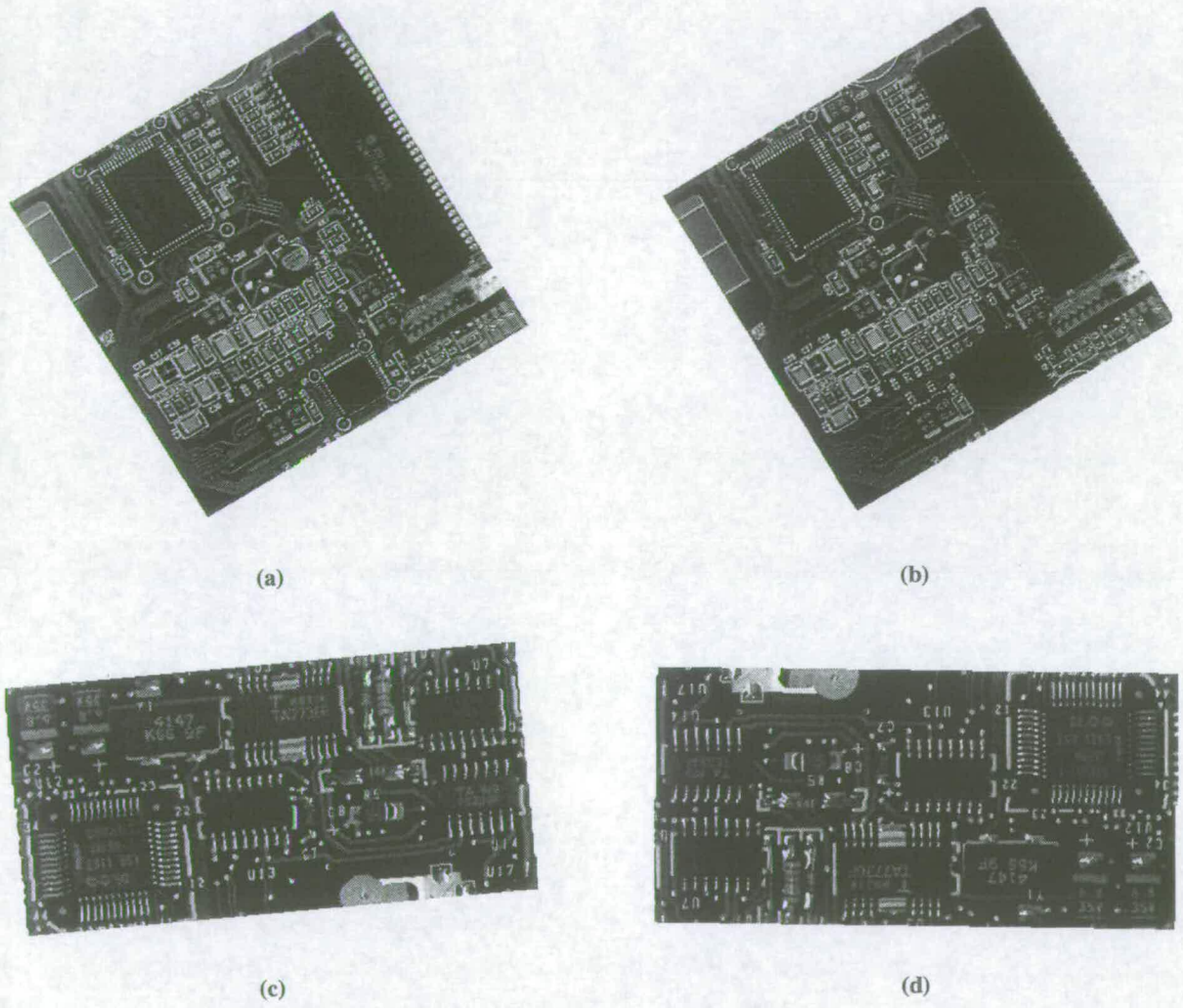

(a) (b)

(c) (d)

Figure 4.16: *Test image: (a) T1, (b) T2 with artificial defects (multi components missing), (c) T3 and (d) T4. All test images are transformed with known values.*

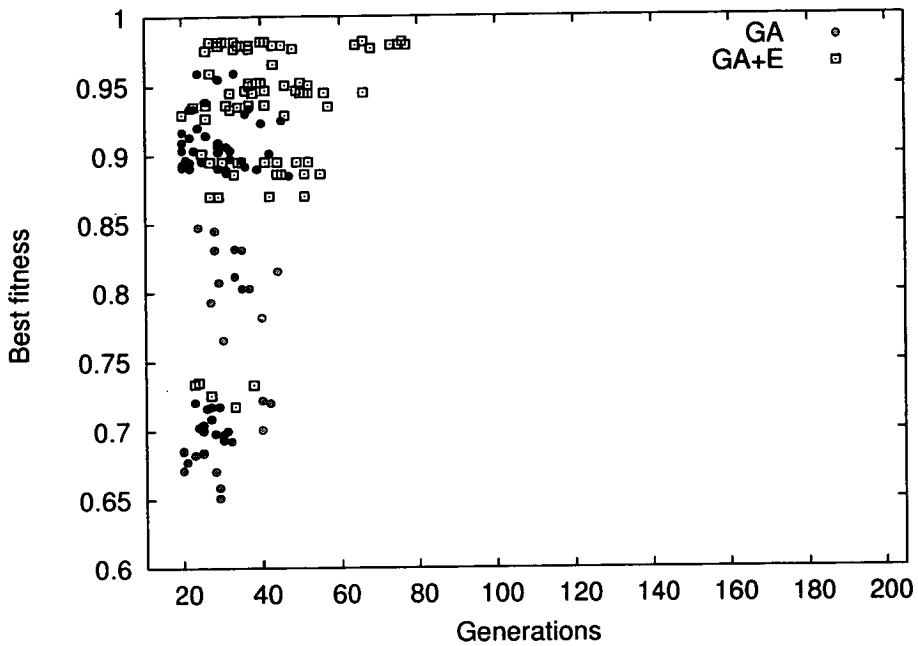

Figure 4.17: *Generations vs optimum fitness for GA and GA+E for all test images.*

noting that all scatter plots are purposely represented by two symbols to highlight the performance of each method, rather than considering the results from different test images.

Figure 4.17 shows that GA+E has outperformed GA considering only best fitness. About 93% of the total number of runs using GA+E has produced best fitness of more than 0.85, while GA was able to produce the same best fitness range in only 50% of the total simulation. However, GA+E requires more generations than GA to converge for these solutions. GA requires between 20 to 45 generations to converge while GA+E requires between 20 to 78 generations to yield a near correct estimation.

This "elitist" concept yielded improved convergence times without loss of population diversity. Preservation of 5% of already known potential individuals for the next population with new creations, provides new variants of individuals for next GA operations such as selection, mutation and crossover. These characteristics complement each other and make the GA search more robust. The variations of population have activated exploration activity for fitter individual which may become the final

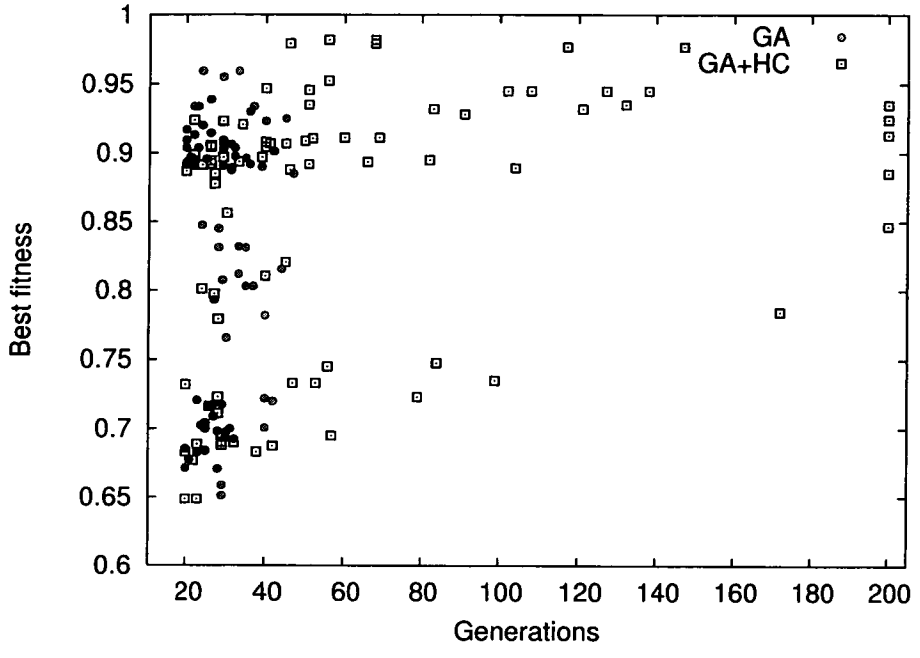

Figure 4.18: *Generations vs optimum fitness for GA and GA+HC for all test images.*

solution. However, there are few evaluations that require more generations to converge and this may be caused by the small size of population which is not enough to contribute for population diversity in the GA search.

The results from implementation of HC on GA (GA+HC) are slightly improved compared to GA as shown in Figure 4.18 when 63% of the total number of runs achieved maximum fitness of more than 0.85. The spread of termination for GA+HC is also longer compared to GA ranging from 20 to 200 generations.

By hybridising with HC, the GA search has the advantage of exploiting the local maxima to extract more information at local level. This exploitation may lead to the fittest individual that possibly has the near exact transformation values. However, the possibilities of the search getting stuck in local maxima is still high when considering another 37% of the evaluations failed to yield maximum fitness of more than 0.85. With regard to the number of generations, the method lacks in generation

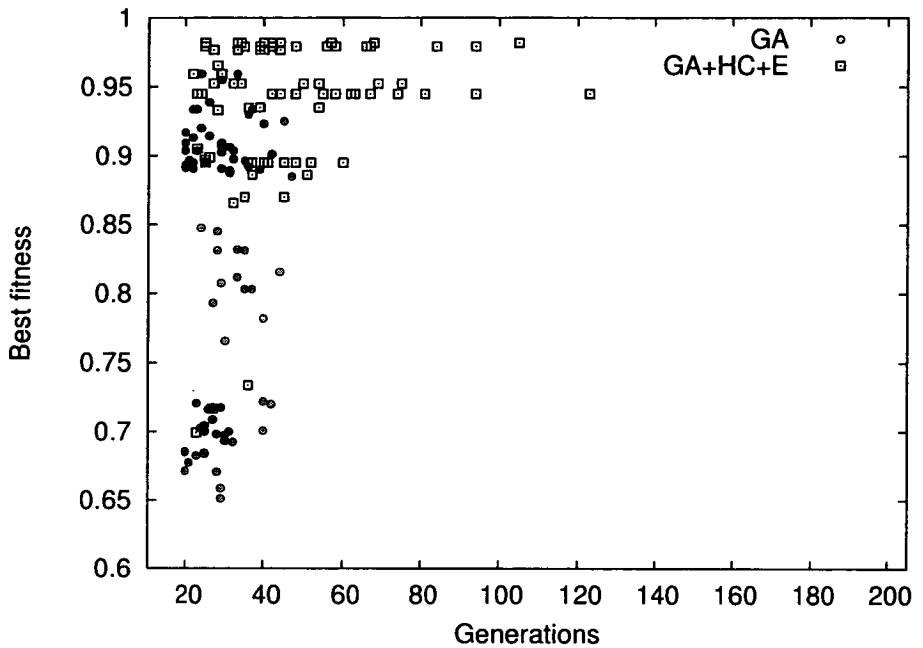

Figure 4.19: *Generations vs optimum fitness for GA and GA+HC+E for all test images.*

efficiency due to generation limit, l of 20 and small population size of 18. The expected reward of the GA will be greater at the beginning of the simulation and at some point when the population has almost converged, the expected reward of the HC will be greater.

GA+HC+E enhanced the GA's robustness when this method outperformed GA significantly as shown in Figure 4.19 because the method benefited from both specialities of HC and E when it successfully achieved excellent results. GA+HC+E needs 22 to 120 generations to estimate the most accurate transformation values of all test images.

GA+HC+E has produced best fitness of more than 0.85 in 96% of the total number of runs. However about 4% of the simulation failed to reach more than 0.85 of maximum fitness that raise an issue with regard to reliability. This issue has been investigated and small population size is identified as one of the reasons. The population size is set to 18 based on the experiments in the previous chapter. If the population size is too small, the GA search may not explore enough of the solution space to

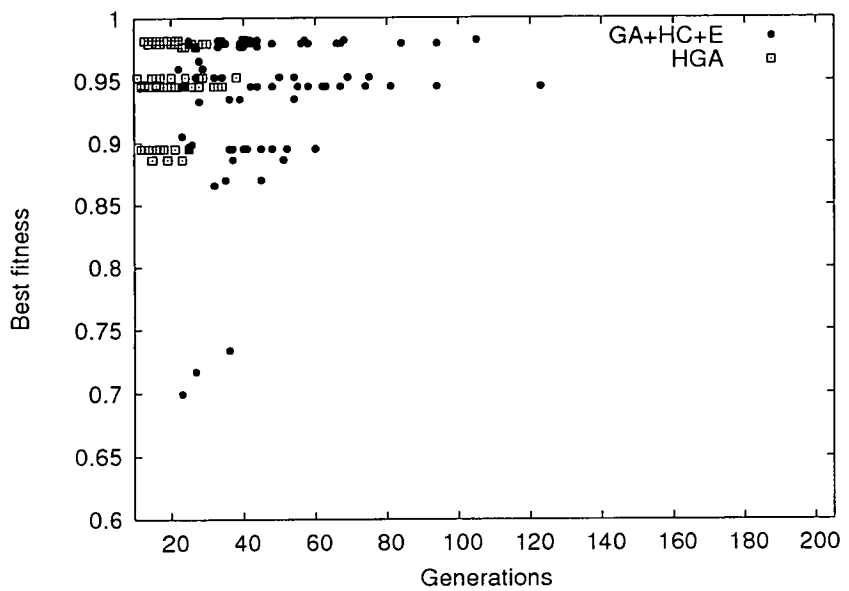

Figure 4.20: *Generations vs optimum fitness for GA+HC+E and HGA for all test images.*

consistently find good solutions. Longer period of generation is caused by longer generation limit, l of 20. To overcome these issues, the parameters of GA+HC+E are tuned optimally to obtain more reliable results.

The enhanced GA+HC+E with population size of 50, known as HGA, is more reliable than GA+HC+E. HGA is able to find individual with fitness of more than 0.85 in all 20 trials of each test image (as shown in Figure 4.20). It managed to converge with these excellent results efficiently in 10 to 38 generations. Based on this plot, it is obvious that the increment of population size and decrement of generation limit, l to 10 have boosted the robustness of HGA.

The best fitness found by these methods are not normally distributed. Hence, a Wilcoxon test has been performed on the methods pair by pair and all p-values from the test are less than 0.01 except

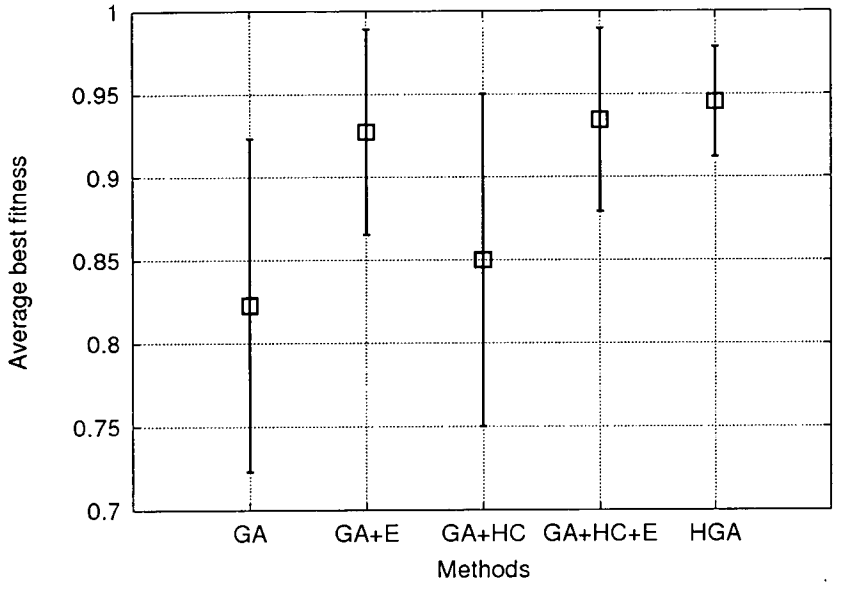

Figure 4.21: *Average best fitness obtained from median value while error-bar shows the standard deviation of each method.*

pair of GA and GA+HC. The p-values smaller than 0.01 indicate there are significant differences in performance among the methods but GA and GA+HC produced nearly similar performance.

Figure 4.21 depicts the average best fitness found by every method using the median value and the standard deviations of best fitness found are shown by the error-bars. As discussed before, HGA outperformed other methods with highest average best fitness and smallest standard deviation, followed by GA+HC+E, GA+E, GA+HC and GA. These statistical findings support that the HGA is the most robust method to register PCB images in this inspection framework.

From the presented findings, it is almost impossible to obtain a maximum fitness of 1.0 due to loss of pixel's information during image rotational operation. This deficiency may affect the accuracy of the results since this work is a reference-based method.

4.7.3.2 Computational efficiency

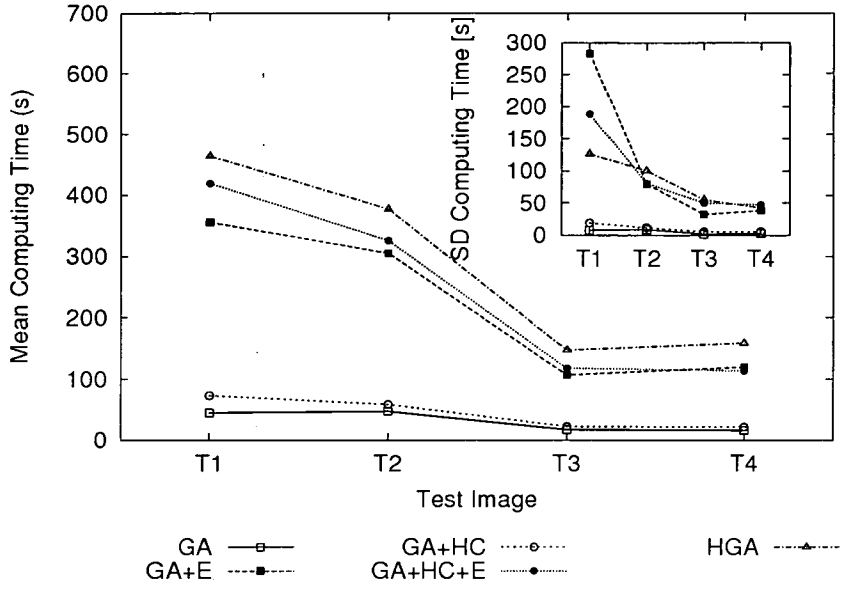

Figure 4.22: *Mean of computing time for every test image and standard deviation of computing time for every test image (sub-figure).*

Each investigated hybrid methods has outperformed GA in maximum fitness findings, however these methods generally require more generation to find those results. Figure 4.22 shows that GA computes the maximum fitness in the least mean time followed by GA+HC and GA+E. As predicted, GA+HC+E and HGA require the most computing time to find the finest estimations. However, HGA needs slightly more time than GA+HC+E in all test images due to the use of larger population size. It also shows that implementation of E costs more computational time due to individual sorting based on fitness value and selection of the fittest individuals that will be preserved.

As we can see in Figure 4.22, on average, each method needs more time to compute the first and second test image (T1 and T2) and reduced drastically in third and forth test image (T3 and T4). This is caused by the different size of T1 and T2 compared to T3 and T4.

Referring to the inset of Figure 4.22, the standard deviation of computing time for GA and GA+HC is negligible compared to GA+E, GA+HC+E and HGA. In general, the performance of GA+E, GA+HC+E and HGA depend on the complexity of the image transformation and the size of the images. Image T1 has the worst standard deviation of computing time compared to T2, T3 and T4 for

Image	Known [degree]	Mean [degree]	RMS [degree]
T1	329	329.0	0.00
T2	329	329.2	0.41
T3	354	356.1	2.79
T4	180	182.0	1.12

Table 4.7: *Rotation accuracy of HGA on all test images.*

Image	Known [pixel]	Mean [pixel]	RMS [pixel]
T1	0	2.0	0.00
T2	-6	-5.2	0.41
T3	5	3.0	0.00
T4	0	0.2	1.86

Table 4.8: *Displacement at x-axis accuracy of HGA on all test images.*

GA+E, GA+HC+E and HGA cases.

4.7.3.3 Registration accuracy

For the inspection system to be reliable, it must reduce 'escape rates' (i.e. non-accepted cases reported as accepted) and 'false alarms' (i.e. accepted cases reported as non-accepted) as much as possible [17]. For that reason, HGA has been selected as the best hybrid method considering its consistency in finding the target maximum fitness.

Based on Table 4.7 - 4.9, the accuracy of each transformation parameters for all test images are

Image	Known [pixel]	Mean [pixel]	RMS [pixel]
T1	0	3.0	0.00
T2	4	2.8	0.41
T3	5	2.0	0.00
T4	0	0.0	0.00

Table 4.9: *Displacement at y-axis accuracy of HGA on all test images.*

presented. The first column denotes the known value of corresponding parameter, second column is the mean value estimated by the HGA for 20 evaluations and the last column is the root mean squared (RMS) error between truth and every estimation value from the simulation.

The inaccuracy of transformation parameters are about ± 2 degrees in rotation and ± 2 pixels in displacement at x-axis while displacement at y-axis may varies up to ± 3 pixels .

Generally, RMS error values are reasonable, ranging from 0 to 2.79. As we can see, the rotational parameter has slightly high errors especially in T3 when compared to other images. This may be caused by loss of pixels information from rotation operation compared to displacement operation.

Experimental results highlight the potential of the hybrid GA (HGA) that consists of all methods in combination because of the most accurate findings and significantly more reliable than GA alone. However, there is a compensation on performance, though it converges efficiently in terms of number of generations. A specially-tailored GA combined with all methods, HGA also has outperformed individual hybrid methods (GA+E and GA+HC) in terms of reliability and accuracy.

4.7.4 Quantitative analysis on Hybrid GA

In this experiment, three types of PCB image as shown in Figure 4.23 are used and they are randomly transformed to 1000 different orientation images. The developed HGA from previous section is executed once for every image to search for the correct transformation function that has been applied to each image. This experiment aims to evaluate the reliability and robustness of the HGA based image registration in more number of trials using more types of PCB. The results are shown in histograms and the values of mean and median in each case are calculated. Mean and median are needed to describe the overall distribution of the results which are not normally distributed.

Figure 4.24 depicts the distribution of HGA performance in term of maximum fitness found. The mean value is about 0.93 and median is about 0.94. Approximately 5% of the results fail to find fitness more than 0.85 and the lowest fitness the HGA found is 0.66. The highest peak of the histogram is at fitness

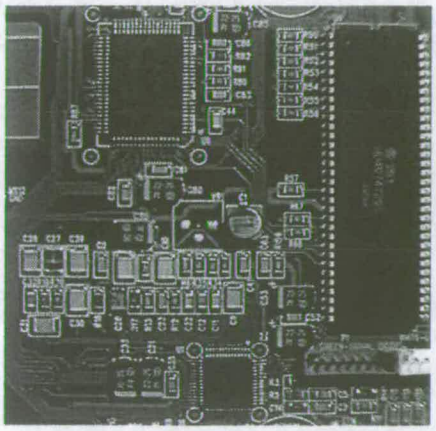

(a) Type 1

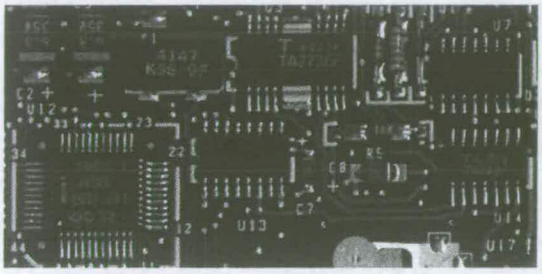

(b) Type 2

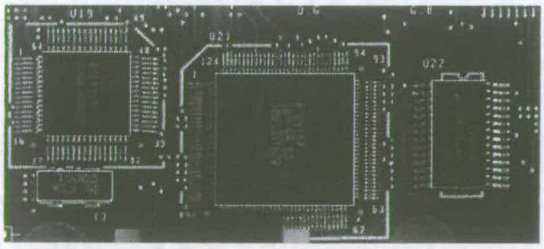

(c) Type 3

Figure 4.23: *Images of different types of PCB*

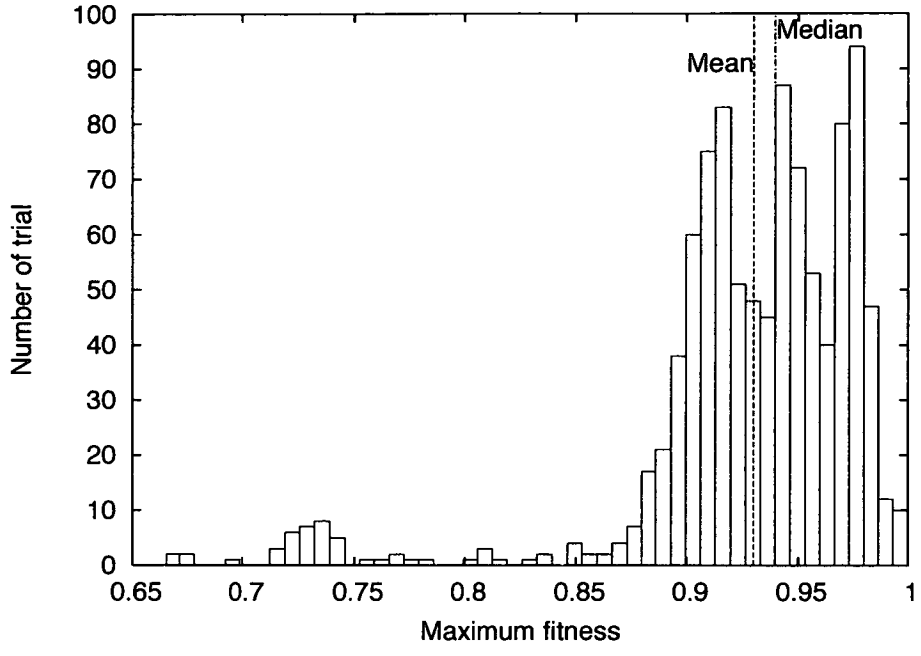

Figure 4.24: *HGA fitness performance on 1000 trials*

value of 0.985 which is a very good value of maximum fitness and 1% of the results obtained the ideal value of fitness which is 1.0. This implies that most of the transformation functions found are high in accuracy.

The distribution of results on HGA generation is shown in Figure 4.25 which gives mean and median value of 19 and 18 respectively. The HGA found the maximum solution as fast as in fifth generation and the slowest is in 46th generation. The maximum fitness found by HGA is most frequently happen at 14th generation.

The computing time performance is plotted as shown in Figure 4.26 and about 30% of the results are computed less than one minute. The mean computing time is around 80 seconds and the median falls in 75 seconds. The quickest time is 15 seconds and the longest time is about 240 seconds. Most of the fitness found in 55 seconds.

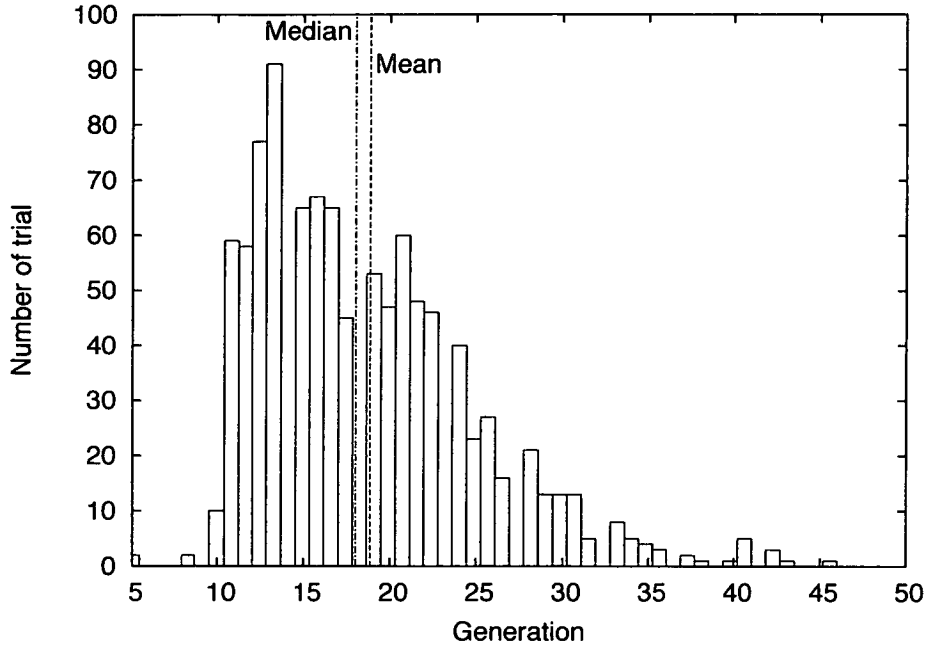

Figure 4.25: *HGA generation performance on 1000 trials*

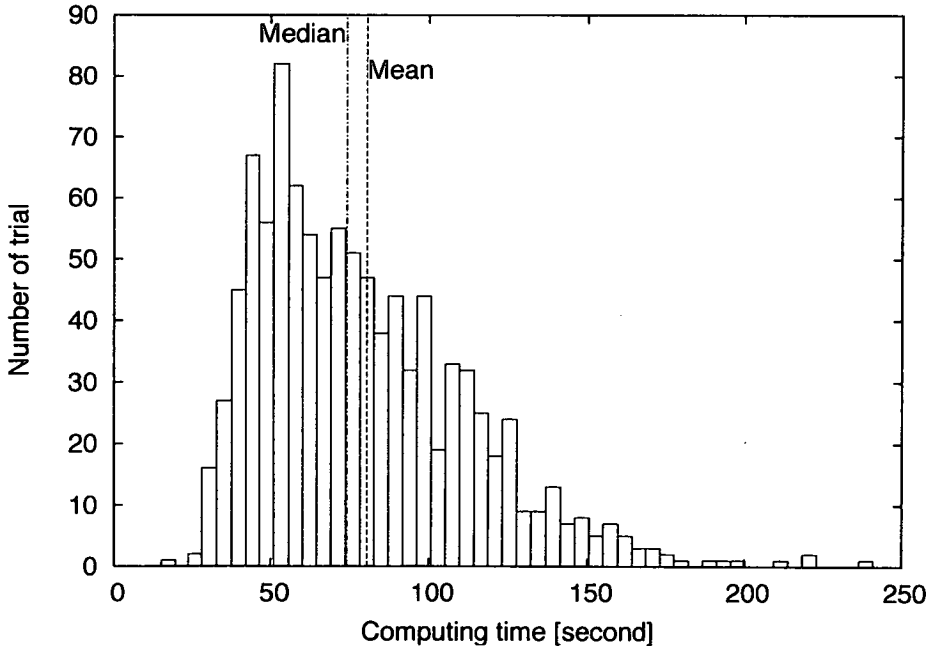

Figure 4.26: *HGA computing time performance on 1000 trials*

In this last case, the compensation mechanism allows a better balance between the exploitation and exploration capabilities of the search procedure, and the global optimum is approached much closer. The basic idea underlying the introduction of the hybridisation in the GA has improved the reliability and time computation characteristics of the evolutionary optimisation process.

4.8 Conclusions

In this chapter, enhancement works are done on the existing framework of GA based image registration especially in GA optimisation to improve the performance in terms of quality of registration and computing time.

From the experiments on the two types of mutation techniques, there is no significant difference in performance for this application between these techniques and proves that any of them is suitable for this application. Computing time is mainly improved by using centre block matching in fitness evaluation. Rotation by shear solves the problem of pixel information loss due to rotational operation.

The implementation of E is very effective and deterministic selection in E scheme is the most suitable for this work. The compensation mechanism between GA and E allows a better balance between the exploitation and exploration capabilities of the search procedure, and the global optimum is approached much closer.

Conversion from binary to real integer coding also improves the efficiency of the GA in searching for the correct transformation function by providing the accurate size of specified search space. The last enhancement is the hybridisation of GA with E and HC and the most ideal setting of GA for this application is produced. The improved version of the developed image registration has been tested and it successfully yields the expected performance.

Chapter 5
Defect Detection Procedures for the GA

5.1 Introduction

Industrial applications of 2D object recognition such as quality control often demand robustness, highest accuracy and real-time computation from the object recognition approach. Some approaches do not simultaneously meet the high industrial demands such as robustness to occlusions, clutter, arbitrary illumination changes and sensor noise, as well as high recognition accuracy and real-time computation. Hence, many ongoing works on visual inspection employ various techniques of object recognition to detect defects on products and sometimes the techniques are incorporated in order to attain an optimal performance of the inspection.

Research on defect detection of PCB inspection has been previously done using Wavelet Transforms in [106, 107]. Morphological image processing has also been implemented in automatic PCB inspection which enable the detection of pin defects while binarisation and twist angle estimation are used to recognise component twist [108]. Hough transform and Susan edge-detection are used to recognise individual IC on completed PCBs during inspection as presented in [43] which performed successfully. [109] employed model-based vision that capable of rapidly locating the modelled structures in noisy, cluttered images even if they are partially occluded using a training set which is based on Active Shape Models (ASMs). This research has been implemented on PCB images as an example to demonstrate the robustness of the technique.

Many researchers try to avoid processing the image pixel by pixel regarding misinterpretations due to misaligned image. It also may suffer from the increase of inspection time and too many false alarms such as discussed in[110]. In [111], a research has been carried out on auto-alignment for image registration. The researchers have developed a searching algorithm that combines a modified tree search and a dynamical search together. The work also implemented a stereo matching technique

which is very effective when the images are well aligned (rotated and translated) and applied on inspection on Circuit Card Assemblies / Printed Circuit Boards (CCA / PCB).

The procedure presented in this chapter is a pixel-based processing techniques which has low complexity and requires low computational time with satisfactory results which is suitable for this specific system. The main disadvantages of pixel-based processing are many possibilities of false alarms due to variation on PCBs and correct alignment by precise board positioning mechanism is essential for this method to work successfully [16]. Good segmentation technique and effective noise filter may solve the problem of false alarms. In previous chapters, a specially-tailored GA has promise to register image in high accuracy which enable this procedure to work successively in detecting the existence of possible physical defects.

In PCB inspection process, common requirements of an inspection system include checking to see if components are present, measuring the positions of components and determining whether surfaces are finished properly [112]. Typical component defects on PCBs are missing components which comprises 20 percent of faults and 55 percent are solder joint defects compared to other types of defects [31]. Therefore, this procedure focuses on detection of missing components and open solder joint in any shape and size.

This chapter describes an image processing module for defect detection of an existing GA based PCB inspection system. The first stage of the defect detection procedure is segmentation operation and the whole operation of few segmentation methods applied in this inspection are explained in Section 5.2. Section 5.3 explains the defect localisation operation using image subtraction technique. Image difference is computed between segmented image of defect-free board (reference image) and segmented image of inspected board (test image). Image noise filtering techniques have been used to eliminate noise resulting from invariance of image intensity which has been extracted during defect localisation operation. The objective of this operation is to avoid the occurrence of false alarms and the details of this operation is described in Section 5.4 while the simulation environment is described in Section 5.5. There are four types of approaches have been tried which are adaptive bi-level thresholding approach, edge-detection approach, hybrid method of bi-level thresholding and edge-detection and composition approach with multi-thresholding and edge-detection. The

Algorithm 3 Multi-thresholding program

```
For x from zero and less than input image width
  For y from zero and less than input image height
    If intensity of image, i(x, y) less than threshold 1
      set intensity image, t(x, y) to 0
    Elseif intensity of image, i(x, y) more than threshold 1 and less than threshold 2
      set intensity image, t(x, y) to 128
    Elseif intensity of image, i(x, y) more than threshold 2
      set intensity image, t(x, y) to 255
```

performance of every approach is featured and discussed in Section 5.6. Conclusion from all schemes are concluded in Section 5.7.

5.2 Segmentation of PCB image

PCBs are constructed from different materials and colours of components. Therefore, segmentation to multi-regions is necessary to separate these elements within the captured image of a PCB in order to detect the existence of physical defects. The existing automatic image segmentation methods can be classified into four approaches, namely, 1) thresholding, 2) boundary-based, 3) region-based, and 4) hybrid [40]. In this work, thresholding and boundary-based segmentation approach have been implemented using fixed global multi-thresholding, adaptive bi-level thresholding and Sobel edge detection method.

5.2.1 Fixed global multi-thresholding

Thresholding approach using multi-thresholding [113] of three gray-level regions is implemented using threshold values selected from grayscale value range from 0 to 255. These threshold values have been carefully selected to obtain the best outcomes in term of clear separation among objects and between objects and background. It is also important that all information printed on the inspected PCBs are retained for future reference.

In this operation, the captured image act as the input image, named as image *i*, while the resulting thresholded image from the operation is named as image *t*. Algorithm 3 shows multi-thresholding operation implementation.

During this segmentation operation, every pixel intensity of an input image is compared to the threshold values. A new image *t*, created as the result that has same size with image *i*. The operation is described in Equation (5.1).

$$t(x,y) = \begin{cases} 0 & i(x,y) < threshold1 \\ 128 & threshold1 \leq i(x,y) < threshold2 \\ 255 & i(x,y) \geq threshold2 \end{cases} \tag{5.1}$$

where *i*(*x*, *y*) is the input image intensity and *t*(*x*, *y*) is the pixel intensity of image *t* while *x* and *y* are pixel location in x-axis and y-axis.

Figure 5.1(a) depicts an original image of PCB captured using a black and white CCD camera. Images shown in Figure 5.1(b) - Figure 5.1(d) are obtained from multi-thresholding operation using three different sets of threshold values. Threshold values of 60/120 segmented the input image clearly as shown in Figure 5.1(b) while in Figure 5.1(c) and Figure 5.1(d), some component regions are computed as a background region after multi-thresholding process using threshold values of 80/120 and threshold values of 80/100 respectively. Based on visual observations, grayscale values of 60 and 120 are the best candidates for threshold values to produce best segmented image for further processing. Therefore, *threshold1* and *threshold2* values are 60 and 120 for this experiment.

5.2.2 Adaptive bi- level thresholding

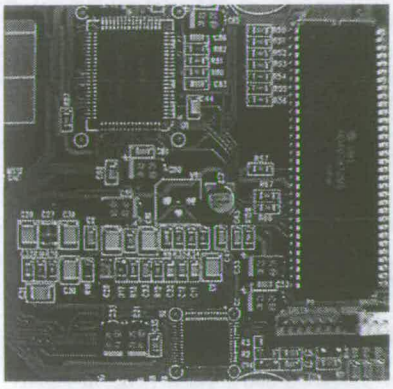

(a) Original PCB image

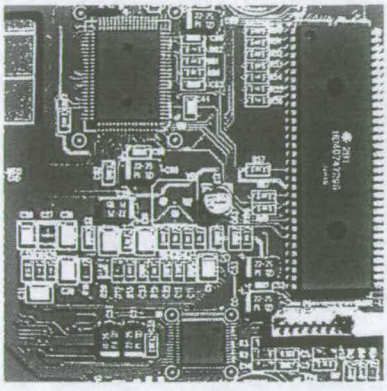

(b) PCB image with threshold 60 and 120

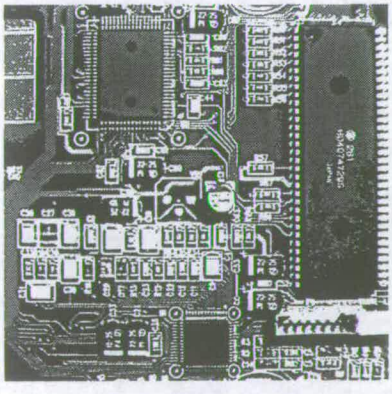

(c) PCB image with threshold 80 and 120

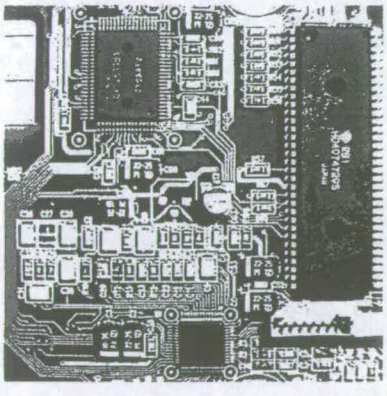

(d) PCB image with threshold 80 and 100

Figure 5.1: *Original PCB image and outcomes from multi-thresholding operation using different threshold values*

Algorithm 4 Adaptive bi- level thresholding program

For x from zero and less than input image width
  For y from zero and less than input image height
    Calculate mean value in $N \times N$ window
    If intensity of image, $i(x + ((N\text{-}1) / 2), y + ((N\text{-}1) / 2))$ more than 0 and less than (mean-C)
      set intensity image, $t(x + ((N\text{-}1) / 2), y + ((N\text{-}1) / 2))$ to 0
    Elseif intensity of image, $i(x + ((N\text{-}1) / 2), y + ((N\text{-}1) / 2))$ more than (mean-C) and less 255
      set intensity image, $t(x + ((N\text{-}1) / 2), y + ((N\text{-}1) / 2))$ to 128

Previous thresholding method has a disadvantage of using fixed threshold values which may not be practical in real inspection environment where the colour on PCBs varies and lighting conditions are different. Therefore, an adaptive bi-level thresholding based on local mean is implemented as in Algorithm 4 in order to adapt with uneven illumination and various types of inspected PCB. A mean value in $N \times N$ window is calculated to determine the threshold value for the window. The centre pixel of the window will be thresholded based on threshold value that has been determined considering the local neighbourhood of the centre pixel. On the margin, however, the mean of the local area is not suitable as a threshold, because the range of intensity values within a local neighbourhood is very small and their mean is close to value of the centre pixel . The situation can be improved if the threshold employed is not the mean, but (mean-C), where C is a constant. Therefore, a constant of C is set to -40 for this thresholding operation in creating a safe margin between the neighbouring pixels.

Figure 5.2 depicts the segmented images by adaptive bi-level thresholding without the constant, C. The image as shown in Figure 5.2(d) using neighbourhood size, N of 9 produced the most clear segmentation of the PCB compared to other N values. However, the separation of regions in crowded area are very hard to identify and details of components on the PCB are poorly highlighted. Opposite to that, the usage of constant (C = -40) yields much better segmentation outcomes as shown in Figure 5.3 where every component on the board are clearly recognised. As before, 9 × 9 pixels neighbourhood is the most effective value to segment the PCB image as depicted by Figure5.3(d) and this makes a reasonable setting for adaptive bi-level thresholding for defect detection implementation.

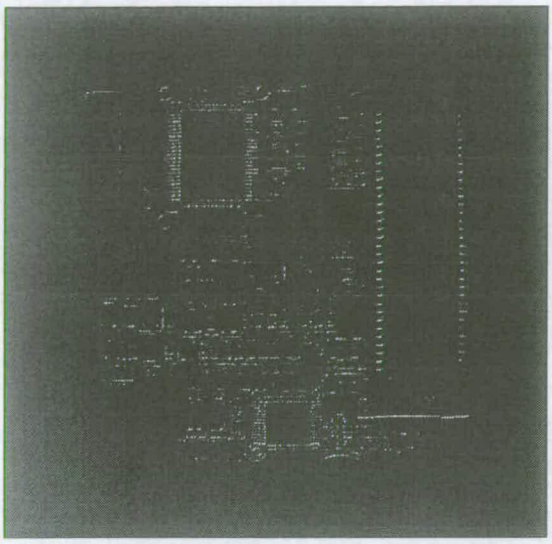

(a) $N = 3$

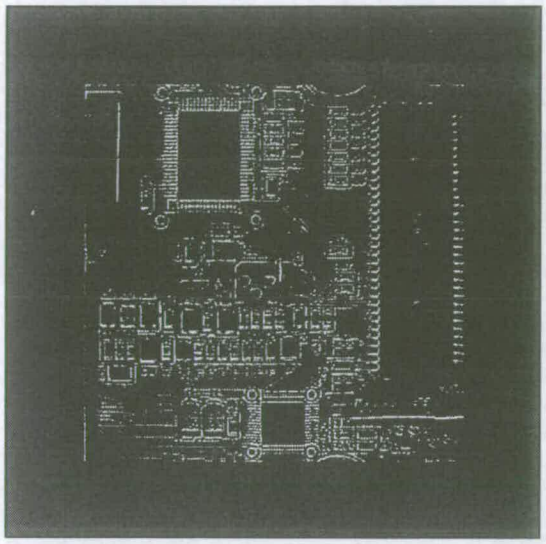

(b) $N = 5$

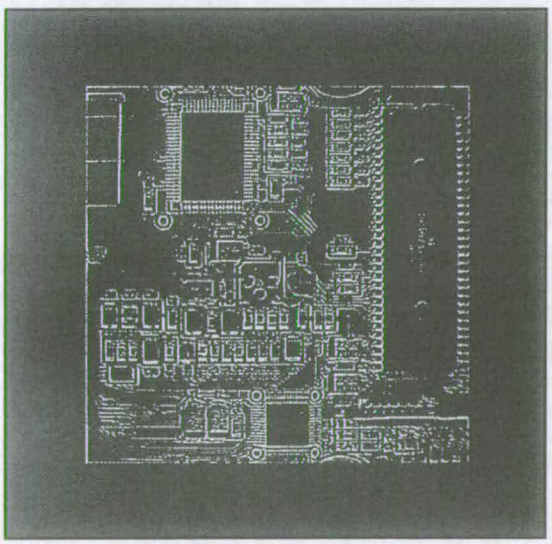

(c) $N = 7$

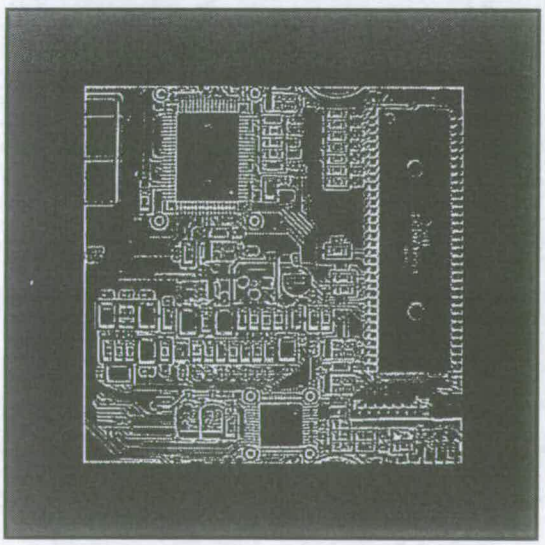

(d) $N = 9$

Figure 5.2: *PCB images after adaptive bi-level thresholding without constant, C using different size of neighbourhood, N*

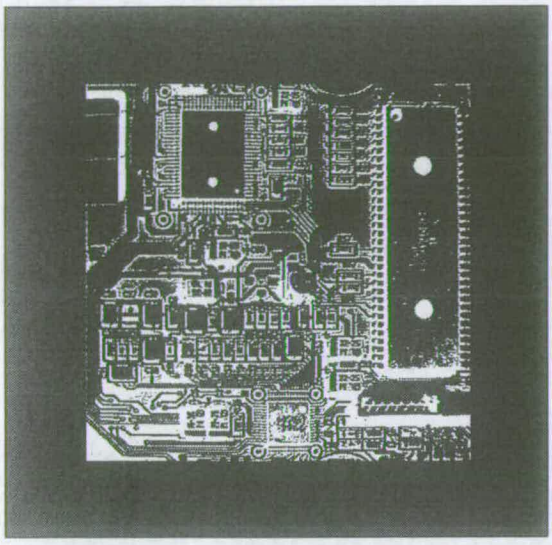

(a) $N = 3$

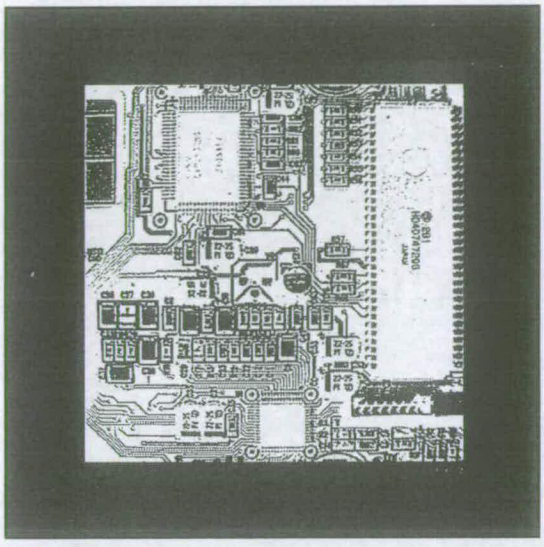

(b) $N = 5$

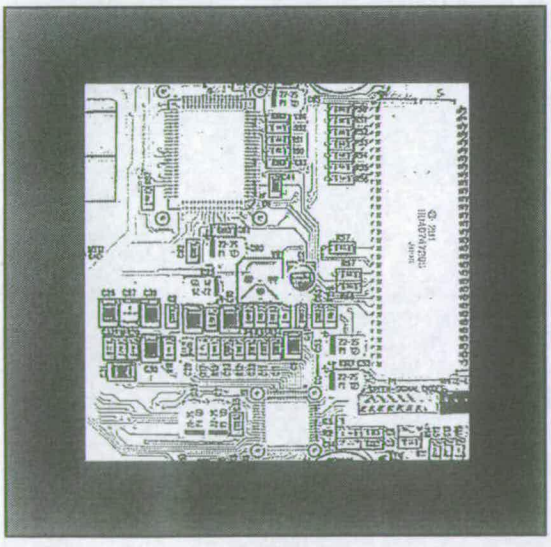

(c) $N = 7$

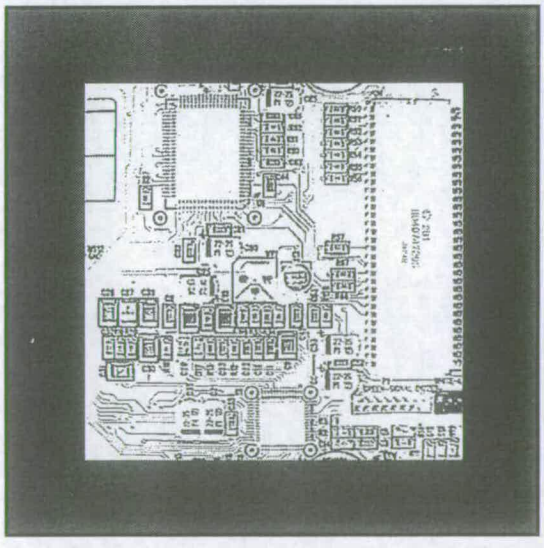

(d) $N = 9$

Figure 5.3: *PCB images after adaptive bi-level thresholding with constant, C= -40 using different size of neighbourhood, N*

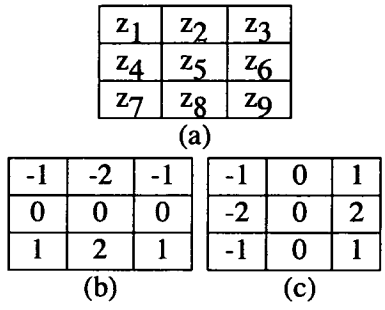

Figure 5.4: *(a) A 3x3 region of an image (the z's are grey-level values), (b) and (c) Sobel edge detector masks*

5.2.3 Sobel edge-detection

Boundary based segmentation method using gradient operator is used frequently in industrial inspection, either to aid humans in the detection of defects or as a preprocessing step in automated inspection [39]. The choice of an edge -detection algorithm depends mainly on signal to noise ratio (robustness), the localisation and the quality of the detection and the implementation efficiency [114]. The edge representation of an image drastically reduces the amount of data to be processed, yet it retains important information about the shapes of objects in the scene [115]. The ability to enhance small discontinuities in an otherwise flat gray fields is one of the important feature of gradient. Sobel edge-detection is one of the popular gradient operators because of its ability to detect edges accurately to create boundaries. The Sobel operator performs a 2-D spatial gradient measurement on an image and so emphasises regions of high spatial gradient that correspond to edges. Typically it is used to find the approximate absolute gradient magnitude at each point in an input grayscale image. The horizontal and vertical masks are shown in Figure 5.4 and using this mask the approximate magnitude at point z_5 is given by Equation (5.4).

$$G_H = (z_7 + 2z_8 + z_9) - (z_1 + 2z_2 + z_3) \tag{5.2}$$

Algorithm 5 Image subtraction program

For x from zero and less than reference image width
  For y from zero and less than reference image height
    If intensity of test image, $f(x, y)$ subtract intensity of reference image, $g(x, y)$ not equal to zero
      set intensity image, $d(x, y)$ to 255
    Else set intensity image, $d(x, y)$ to 0

$$G_V = (z_3 + 2z_6 + z_9) - (z_1 + 2z_4 + z_7) \tag{5.3}$$

$$\nabla f \approx R \times (|G_H| + |G_V|) \tag{5.4}$$

During this segmentation operation, a factor, R of 0.3 is implemented in Sobel edge-detection to reduce the blobs or noise. The effect of different values of factor in Sobel edge-detection is shown in Figure 5.5 where factor of 0.3 produced the most clear edges with very low noise.

5.3 Defect localisation

Defect localisation procedure is necessary to extract the difference between the reference image and the test image using image subtraction operation. The advantage of this method is that it is easy to implement with hardware, and therefore high processing rates are possible. Another advantage of this method is that large defects (i.e missing conductor wires etc.) can be detected whereas the non-reference method will not detect these [16]. The concept has been demonstrated by many researchers such as [3, 23, 50, 116] and prove this technique is very effective and accurate as long as the images are correctly aligned.

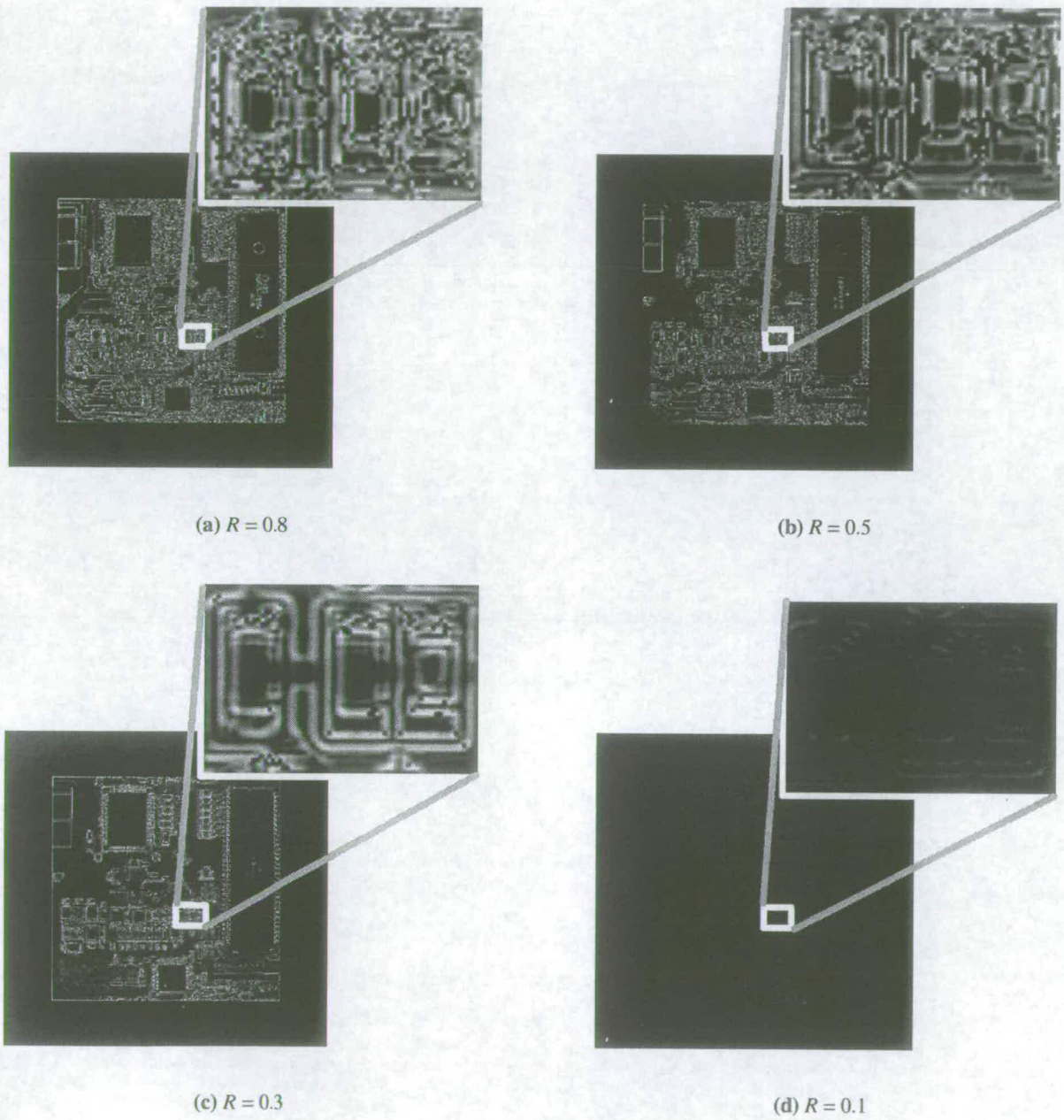

(a) $R = 0.8$ (b) $R = 0.5$

(c) $R = 0.3$ (d) $R = 0.1$

Figure 5.5: *Results of Sobel operation with different factors, R. Each sub-image is a zoomed image on highlighted PCB area.*

Algorithm 6 Window-filtering operation

For x from zero and less than input image width
 For y from zero and less than input image height
  For j from x to x + (M-1) and less than input image width
   For k from y to y + (N-1) and less than input image height
    count pixel with value of 0 in the window
     If count more than *window_threshold*
      set intensity image, $ne(j + ((M\text{-}1) / 2), k + ((N\text{-}1) / 2))$ to 255
     Else
      set intensity image, $ne(j + ((M\text{-}1) / 2), k + ((N\text{-}1) / 2))$ to 0

The image subtraction is performed between reference image and test image represented as image g and image f respectively. The differences of these images, referred to as image d, inherit the size of the input image. Image subtraction operation is described in Algorithm 5 and Equation (5.5).

$$d(x,y) = \begin{cases} 0 & f(x,y) - g(x,y) = 0 \\ 255 & f(x,y) - g(x,y) \neq 0 \end{cases} \tag{5.5}$$

where g(x,y) is the pixel intensity of image g, $f(x, y)$ is the pixel intensity of image f and $d(x, y)$ is the pixel intensity of image d. The pixel location is represented as x for x-axis and y for y-axis.

5.4 Image noise elimination

Noise elimination is a main concern in computer vision and image processing because any noise in the image can provide misleading information and cause serious errors. Noise can appear in images from a variety of sources: during the acquisition process, due to camera's quality and resolution, and also due to the acquisition conditions, such as the illumination level, calibration and positioning [52]. In this case, the occurrence of noise are mainly contributed by invariance of pixel intensity during image repositioning due to rotational operation. Loss of information from the inspected image may happen and also contribute to false alarm in inspection process.

To overcome this issue, noise elimination technique using window-filtering [106] has been used in this procedure. The window-filtering technique is also capable of highlighting identification information of component (eg: IC identification number). The output image from this operation is referred to as image *ne* while *M* and *N* are 3. The window-filtering process is implemented in the procedure as described in Algorithm 6.

This operation is done by moving a small window within an input image row by row. For every pixel that is covered by the window, the pixels with intensity value of 255 are counted. The counter value will be compared with value of *window_threshold* which is a threshold value of each size of window. In this work, threshold value of 6 is set for window size of 3x3 pixels. These threshold values for window-filtering determine the sensitivity in noise elimination within window. The higher the threshold values, less noise can be filtered. If the counter exceeds the window-threshold values, the pixel in image *ne* at same location of centre pixel of window in input image will be set to value of 255. Otherwise, value of 0 will be set for that corresponding pixel in image *ne*. This process will be repeated until all pixels in input image are filtered by the window.

Figure 5.6 shows the images obtained from window-filtering operation using three different window sizes and when the window-filtering is not used in defect detection procedure. Based on these figures, more noise components can be eliminated using bigger window size, in this case 7x7 pixels, as shown in Figure 5.6(d). However, component identification information cannot be extracted as shown in the inset of the figures. The output image without window-filtering shows much clearer recognition of component information, however noise is not filtered. In this case, complications may arise if PCBs are inspected in noisy environment. Smaller window size can highlight the component identification information clearly with acceptable noise as shown in Figure 5.6(b). For this reason, 3x3 pixels size window is an ideal selection for this work.

After window-filtering stage, the median filter which is best-known filter in nonlinear category is used to eliminate remaining noise and preserve the spatial details contained within the image. For

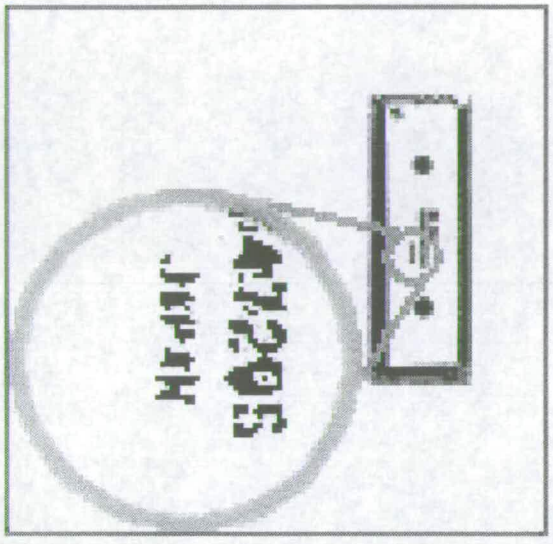

(a) With no window-filtering

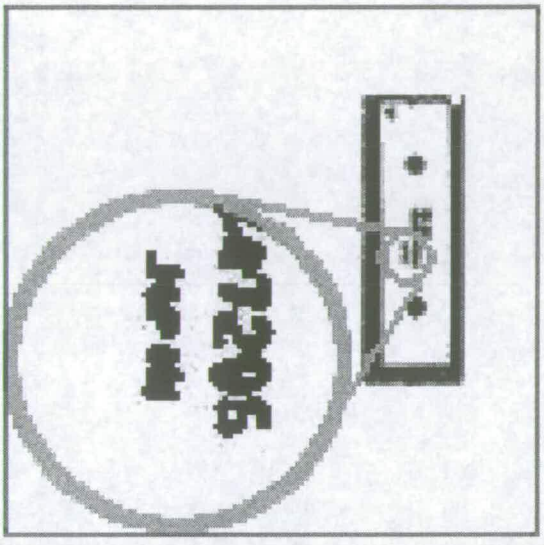

(b) Window-filtering with 3x3 window

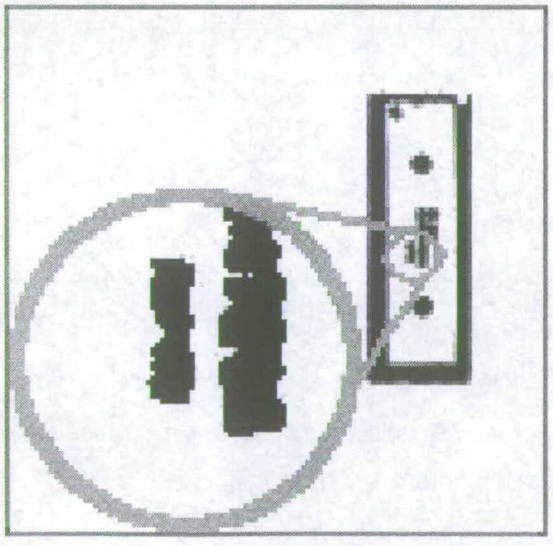

(c) Window-filtering with 5x5 window

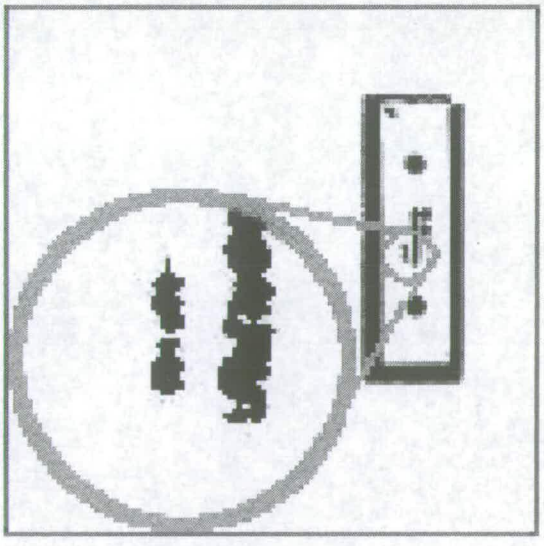

(d) Window-filtering with 7x7 window

Figure 5.6: *Noise eliminated images without and with different window sizes. The zoom view for the component ID is shown in the inset of the figures with window_threshold value of 6*

the median filter, the filter kernel size was set to 3×3 since its computational burden is less and in accordance with the researchers recommendation, where they considered a 3×3 kernel size to be convenient and sometimes optimum [117]. The filter will replace the value of a pixel by the median of the gray levels in the neighbourhood of that pixel (the original value of the pixel is included in the computation of the median) [39]. It is quite popular because of it is excellent in noise-reduction capabilities with less blurring in acceptable computation time compared to spatial filter such as Gaussian filter [118].

5.5 Simulation approach

The PCB defect detection image processing module has been implemented using four approaches that are based on image operations discussed previously. A sample of PCB with defects of various missing components are tested using these approaches. Each detection approach is performed on an artificial defected image with size of 804 × 804 pixels. The simulation has been simulated on a Linux-operating system based PC and the defect detection approaches are written in C-language using NetPBM image library [104].

Every approach is simulated using the same reference and test image. Figure 5.7(a) depicts the image of defect-free PCB captured using a black and white CCD camera which acts as a reference image. A test image from the same type of PCB with the reference image is in wrong alignment and has artificial missing components as shown in Figure 5.7(b). For further defect detection process, it is assumed the GA has found an ideal transformation estimations of the test image. Therefore, the test image is transformed to the correct position as the reference image before a defect detection approach starts.

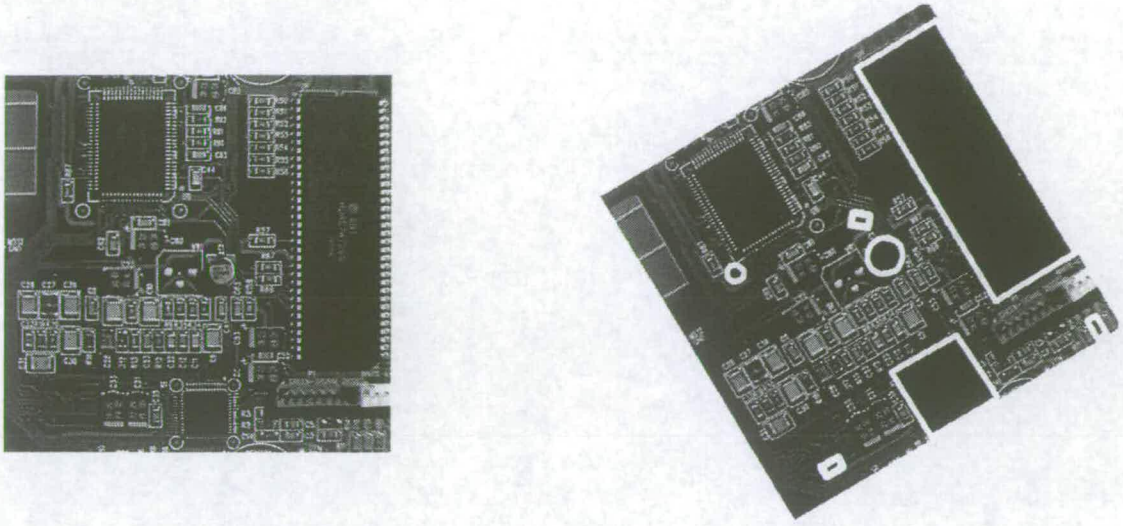

(a) (b)

Figure 5.7: *(a) Sample of reference image and (b) sample of test image with artificial defects are highlighted with white border*

5.6 Results and discussions

Every approach is evaluated based on the outcome of each operation used. An effective approach is the one that produces high accuracy of defect detected at the end of the approach with low noise and in short computational time. Absence of components and open solder joints on completed PCBs are the types of defects that are common in industrial production line. Therefore, the defect detection approaches studied in this research are focused on these types of defects. Based on the test image as shown before, there are three ICs with different sizes are missing and represent rectangular shape defects. A missing transistor and absence of a hole (known as a via) will represent defects in circular shape while two open solder joints are categorised as very small size of defects. These various types of defect are used as evaluation of the robustness of each approach in detecting missing components and open solder joints of varying shape and size.

5.6.1 Adaptive bi-level thresholding approach

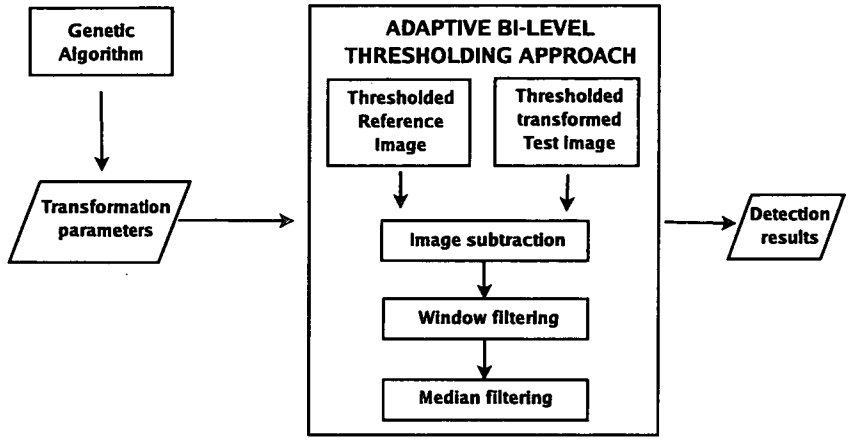

Figure 5.8: *Flow diagram of adaptive bi-level thresholding approach*

Adaptive bi-level approach is performed as in Figure 5.8 where both reference and test image are thresholded using previously mentioned adaptive bi-level thresholding operation. The thresholding operation is performed using 9×9 pixels window and a constant, C at -40. Both segmented images are passed to image subtraction module for defect localisation and the noise resulting from movement of pixel during rotational operation is eliminated by window-filtering and median filter.

A thresholded reference image is shown in Figure 5.9 while Figure 5.10(a) depicts thresholded test image. Clear segmentation between background and objects are successfully created by this adaptive thresholding operator. Therefore, image subtraction between these images managed to recognise the differences as depicts by Figure 5.10(b). However, there are other small objects that appear as unwanted noise. Based on Figure 5.10(c), more than half of noise components has been eliminated and the defects are much clearer at this stage. The identification information on the components also

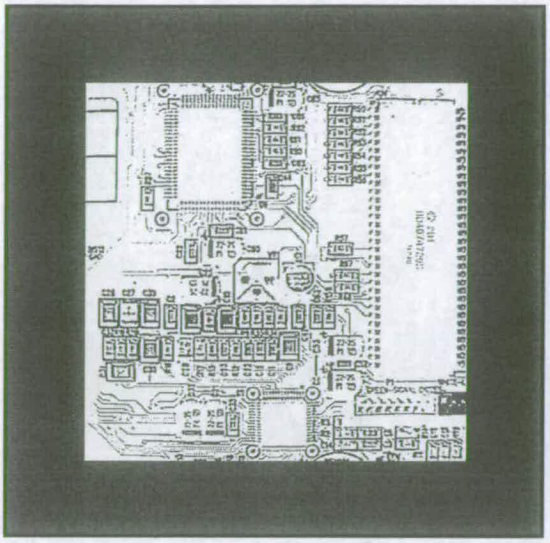

Figure 5.9: *Thresholded reference image using adaptive bi-level thresholding*

clearly recognised at this stage. However, the noise level is still not acceptable which may cause future complications and this make the approach requires median filter to reduce the noise as low as possible. Figure 5.10(d) shows high improvement in terms of noise reduction after median filtering is applied while more details of components are preserved. The approach is performed efficiently with acceptable results using less than 5 seconds processing time.

5.6.2 Edge-detection approach

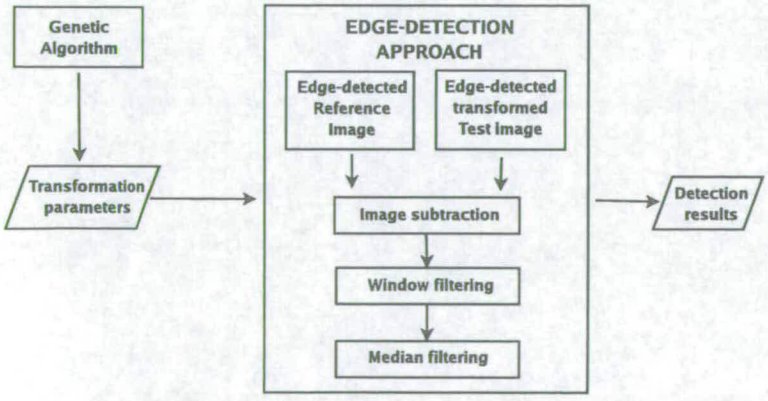

Figure 5.11: *Flow diagram of edge-detection approach*

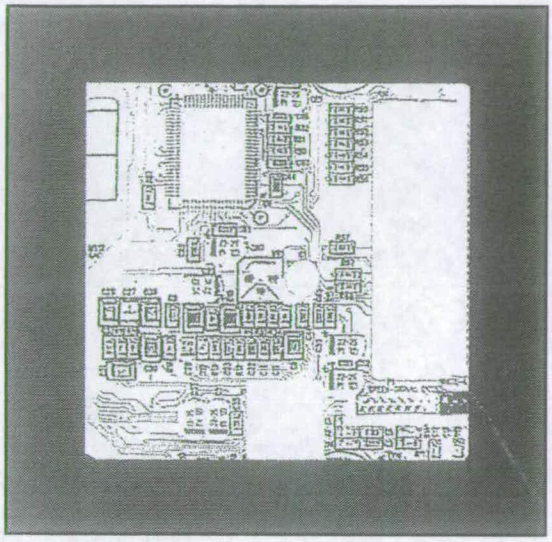

(a) After alignment correction and adaptive bi-level thresholding

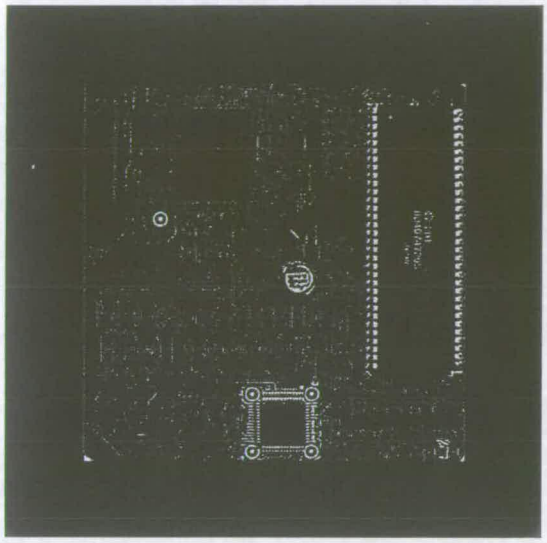

(b) After image subtraction

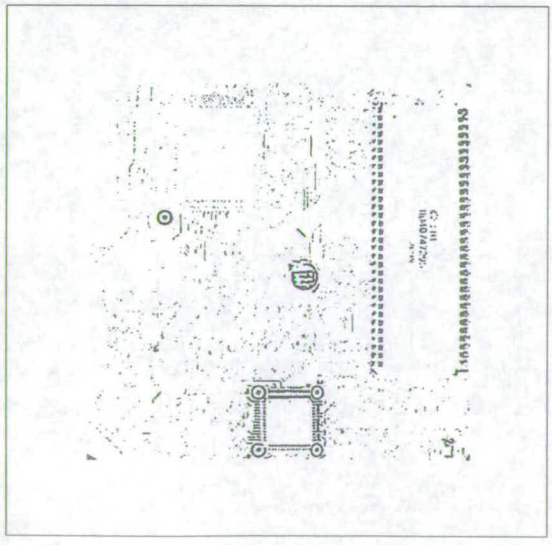

(c) After window-filtering

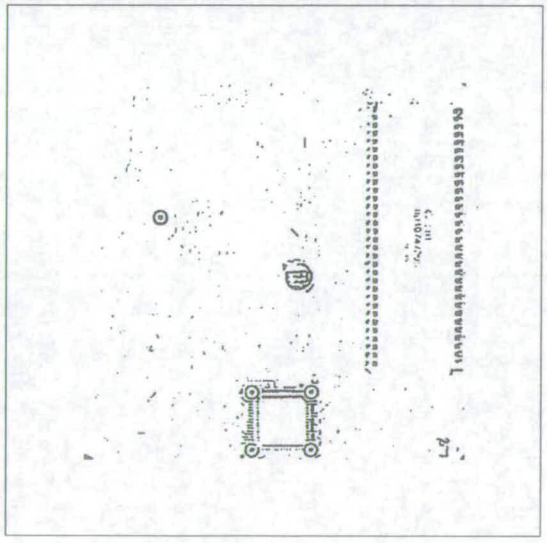

(d) After median filtering

Figure 5.10: *Images obtained from adaptive bi-level thresholding approach*

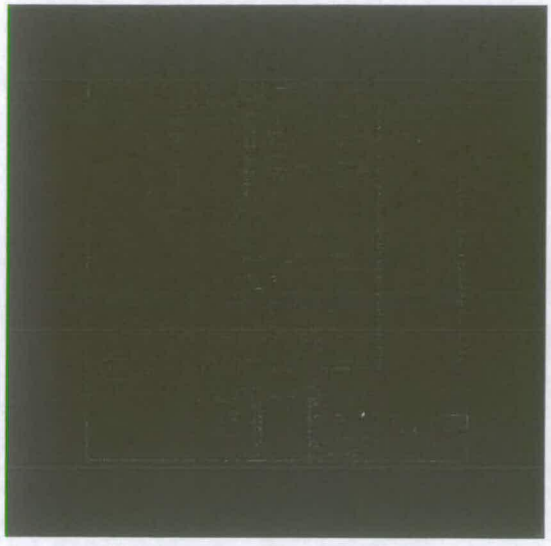

Figure 5.12: *Edge-detected reference image*

Figure 5.11 depicts the detail flow of the edge-detection approach where the Sobel edge-detection is applied with factor of 0.3 on the reference and the test image. Then, the edge-detected images will be subtracted between each other to locate the differences. The window-filtering eliminates the noise on image from subtraction while median filter is needed to remove the remaining noise.

The segmented reference image and segmented test image resulting from Sobel edge-detection operation are shown in Figure 5.12 and Figure 5.13(a) respectively. All important edges are visually detected and boundaries are accurately emphasised as can be seen in these images. After image subtraction, the pixel differences of these two images are coloured in white as shown in Figure 5.13(b). Some of the missing components are already recognisable although there are many more objects which can be mistakenly identified as defects. With respect to that output, the approach needs more processing to eliminate the noise and other unwanted objects. Both filters successfully reduce the small size of noise as shown in Figure 5.13(c) and 5.13(d). But the filters are not as conducive as in previous approach since the existence of unwanted objects are unavoidable. Based on these results, it is obvious that the approach is only able to locate few of the missing components but hard

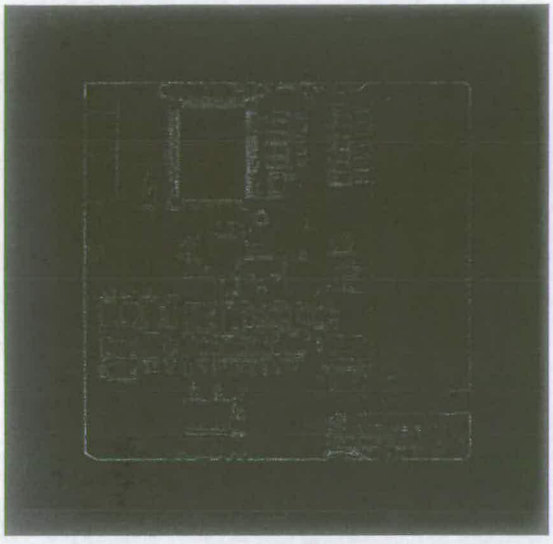

(a) After alignment correction and edge-detected

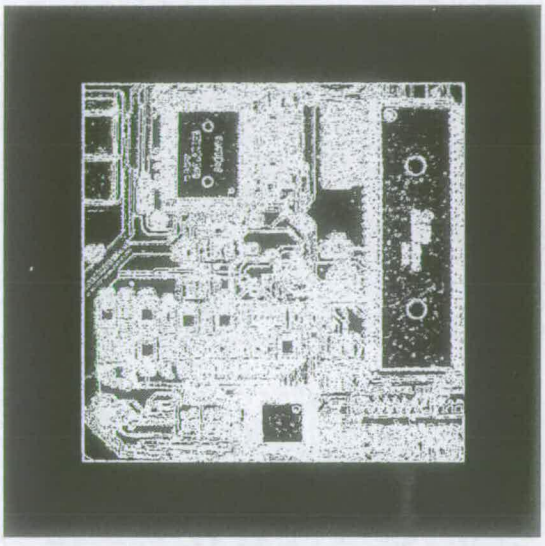

(b) After image subtraction

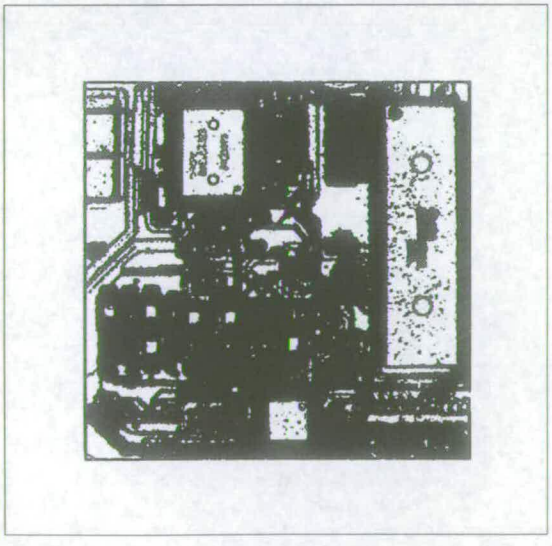

(c) After window filtering

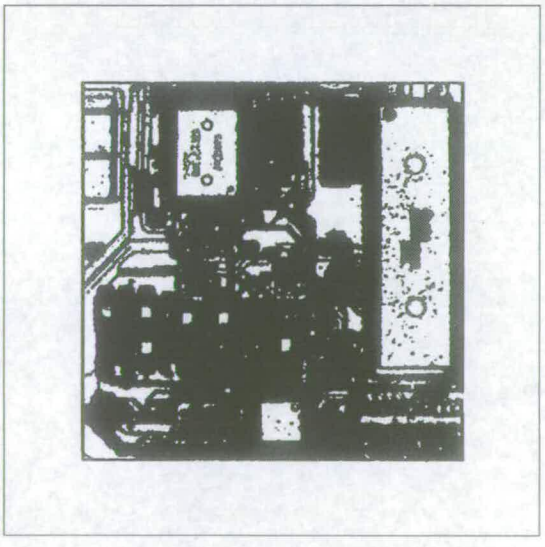

(d) After median filtering

Figure 5.13: *Images obtained from edge-detection approach*

Approach	Advantages	Disadvantages
Adaptive bi-level thresholding	• Noise in final output is less and smaller. • Details on component nearly able to be identified. • Adaptive threshold value solves the changes in lighting conditions and shading problem	• Edges of few defects are lost in final output.
Edge-detection	• The robustness of edge-detection is well-known in inspection process. • The defects highlighted much clearer.	• Noise may detected as defect considering the size. • Details on component cannot be identified in final output.

Table 5.1: *Advantages and disadvantages of individual approaches*

to recognise due to the appearance of other objects. The approach computes the whole operation in less than 5 seconds which is an acceptable duration for real-time inspection.

5.6.3 Hybrid approach

Nowadays, considering the state-of-the-art inspection system, the combined inspection methods are used. This hybrid type merged the advantages of the thresholding method and the edge-detection method to overcome the weakness of each methods. In this approach, defect detection has been performed with two different methods consisting of adaptive bi-level thresholding approach and edge-detection approach as discussed before.

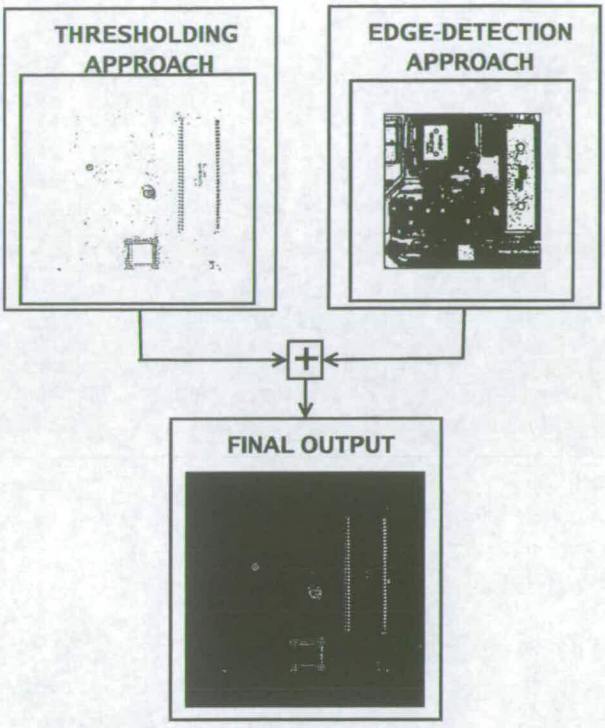

Figure 5.14: *Flow of hybrid approach*

The major shortcoming of previous two individual approaches is related to the noise problem where it is important for the inspection process to avoid anything that leads to major errors. Both approaches have advantages and disadvantages as listed in Table 5.1. To complement both approaches abilities, the end results of these two approaches are logically AND-ed together as illustrated in Figure 5.16. It is worth mentioning that the composition stage must be implemented after both approaches have been completed in order to achieve the most significant result. The operation was performed as follows:

$$f(i,j) = \begin{cases} 255 & (A(i,j) \neq 255) \bullet (B(i,j) \neq 0) \\ 0 & otherwise \end{cases} \tag{5.6}$$

where $f(i, j)$ is the pixel intensity of output image of integration, while $A(i, j)$ and $B(i, j)$ are pixel intensity of output of adaptive bi-level thresholding approach and edge-detection approach respectively. The i and j are the x-axis and y-axis position on the images.

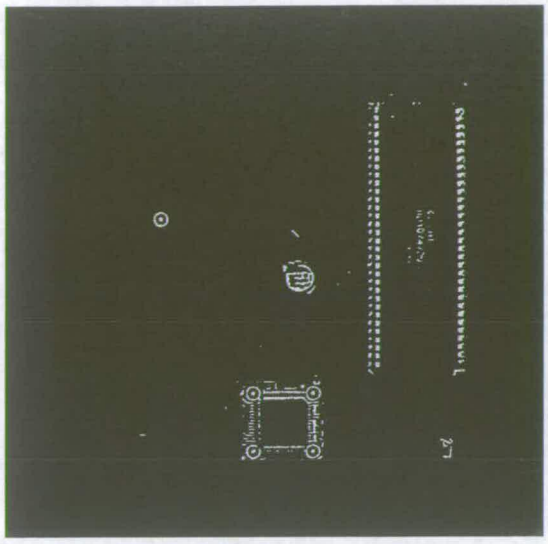

Figure 5.15: *image obtained from hybrid approach*

The hybrid approach successfully locates and recognises the missing components and open solder joints although there are still few speckles of noise as depicted by Figure 5.15. A good classification of type of defects based on recognised objects may easily omit these small sizes of noise. The detected open solder joints are very impressive performance by this approach although they have possibilities to be neglected as noise regarding the size. The approach has more advantages by employing two previous approaches especially in noise reduction and detecting small sizes of defects with very low computational time, which is less than 7 seconds. Since the segmentation operations are adaptive but reliable, this approach is suitable for any type of PCBs and any changes of lighting in inspection environment.

5.6.4 Composition approach

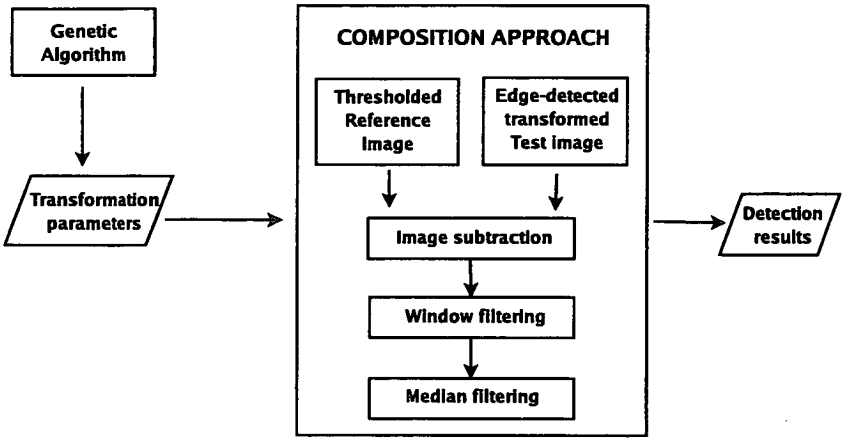

Figure 5.16: *Flow diagram of composition approach*

In this work, further defect detection operations are performed on output images from multi-thresholding and Sobel edge-detection operations. The reference image will experience multi-thresholding operation while Sobel edge-detection is performed on the test image. From here onwards, the thresholded reference image is known as the reference image and edge-detected test image is referred as the test image. This composition approach aims to compensate each other advantages and disadvantages in producing highly accurate segmented output to locate the differences to achieve efficient object detection with fault-free results.

In Figure 5.17, the reference image after multi-thresholding process is shown while the test image is segmented using Sobel edge-detection with factor of 0.3 depicted by Figure 5.18(a). Subtracted image shows the missing components clearly with very low level of noise in Figure 5.18(b). The window-filtering and median filter successfully remove all the remaining noise and produce a very

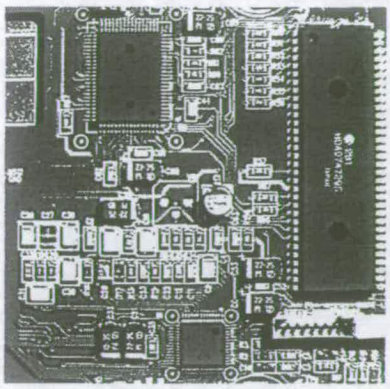

Figure 5.17: *Thresholded reference image using multi-thresholding*

clean image with all missing components detected. However, the approach fails to locate the open solder joints which are not found during image subtraction. This gives a deficiency to this approach although it performs very well in detecting other missing components with negligible noise. In this approach, the false alarms are not present and the level of noise is very low. Although the approach can capture detailed shape of absence defects, the approach lacks generality since the multi-thresholding operation relies on fixed values of threshold. The whole operation only takes less than 5 seconds to produce acceptable accuracy and nearly noise-free defect detection results.

5.7 Conclusions

In this chapter, a number of image processing operations which perform efficiently in detecting possible defects on completed PCBs for visual inspection process is discussed in detail. Segmentation methods using fixed global multi-thresholding, adaptive bi-level thresholding and Sobel edge-detection are presented with different parameter values to obtain the most powerful settings for this system. Effective segmentation techniques are very crucial to locate the differences in the reference and test PCB images in the image subtraction operation. Any differences detected have potentials to be recognised as defects while preventing false alarms by reducing the noise as low as possible. The occurrence of noise due to pixels movement during rotational operation and

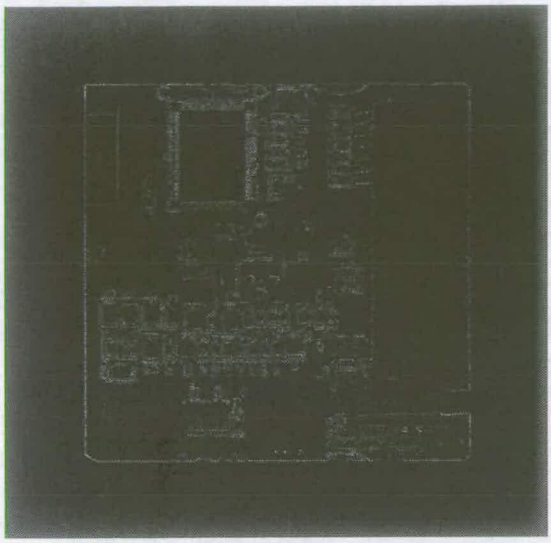

(a) After alignment correction and edge-detected

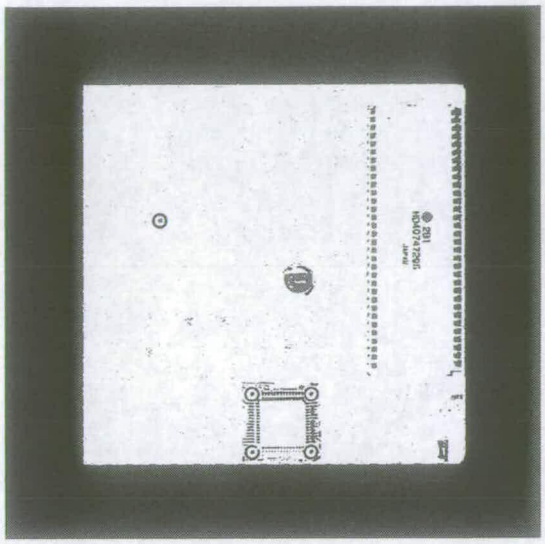

(b) After image subtraction

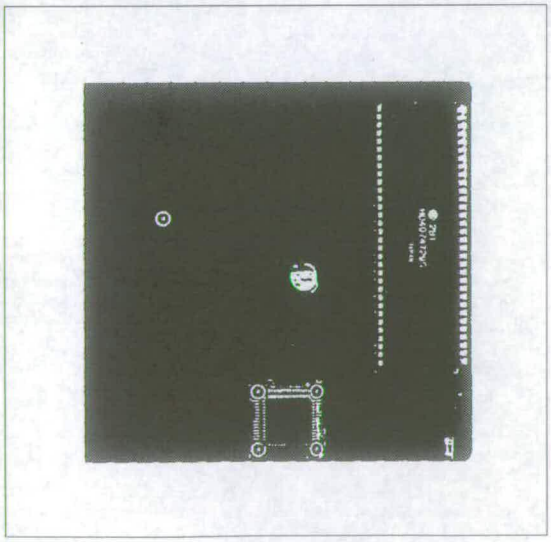

(c) After window filtering

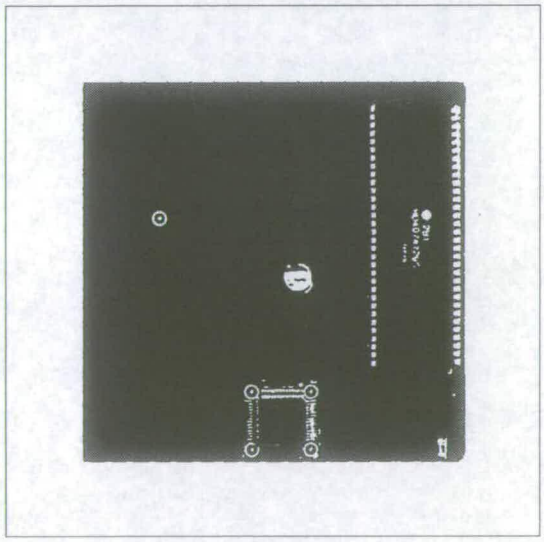

(d) After median filtering

Figure 5.18: *Images obtained from composition approach*

inaccurate segmentation caused by variance pixels intensity are eliminated using image noise filters. The window-filtering and median filter are employed as noise filters in this application.

The previously discussed image processing methods are incorporated in novel ways producing four main approaches which have their own specialities and also deficiencies. Both adaptive bi-level thresholding and edge-detection approaches are able to locate the defects in reasonable accuracy but are affected by the level of noise. They are also unsuccessful in detecting small size defects such as open solder joints although they operate with least computational cost.

The hybrid approach is the most efficient approach when it is able to detect all the artificial defects on the test image accurately with low level of noise. The adaptability in segmentation operators gives a big advantage to this approach to be implemented in a real inspection environment. However, it requires slightly more time than other approaches with regards to the complexity of the approach.

The last approach in this chapter combines the fixed global multi-thresholding and edge-detection and produces nearly identical performance with hybrid approach in detecting all defects except open solder joints. This approach is also very effective in reducing the noise level to the most minimum among all. However, this approach is not an adaptive operator since multi-thresholding approach uses a fixed values of threshold. This approach can be implemented in real inspection environments but it may require a manual setting of threshold level depending on the types of PCBs and lighting conditions.

The hybrid and composition approaches are both very effective and comparable, but the priority on noise reduction means that for this work the composition approach is implemented as the defect detection module in the complete framework, which will be presented in the next chapter. The defect detection module is integrated with the GA module in building a complete visual inspection system for completed PCBs. The completed system will be tested on more test samples from different types of board and varieties of artificial defects.

Chapter 6

Integration of Defect Detection within the GA

6.1 Introduction

Major constraints from typical PCB manufacturing lines today are variability in defects, variability in defect samples and pattern complexity in producing more complex but smaller size boards [119]. In the past, practical inspection systems have typically relied on embedding knowledge of the target inspection task in the algorithms especially for reference-based inspection [112]. CAD data is one of the prior knowledge that is usually required by the reference-based inspection. However, to-date, CAD-based vision techniques have not been very successful for the inspection of other than relatively simple parts because CAD models are not always available. Even if they do exist, too frequently the models are obsolete [120]. Due to the embedded knowledge, this creates limitation on reusability aspect of the system and is mostly operated by a vision expert.

An industrial vision system should be able to adapt itself automatically and achieve consistent high performance despite irregularities in illumination, marking or background conditions, and accommodate uncertainties in angles, positions etc [17]. A good example of an adaptive system is the artificial neural network embedded with automated inspection quality management system that has been developed by [121]. The system employs digital image processing and artificial neural network to identify the size and the location of the finished components on the manufactured products. It is also capable of detecting flaws and scratches on the surfaces of the products during manufacturing. The implementation of the content-based image retrieval has demonstrated that a powerful image query technique applied to the manufacturing environment is feasible including PCB manufacturing [122]. The system requires large storage media to store the vast databases of images and it needs consistent updates on the databases in order to inspect various defects.

The adaptation of the system is expected to be desirable for PCB inspection application due to the variability of types and sizes of PCB. Building a new setting for a new design of PCB is time-consuming and requires more allocation in total manufacturing cost. Our work focuses on image registration of inspected PCBs placed arbitrarily on a conveyor belt using GA and developing an efficient defect detection procedure using a special combination of image processing operations. This system will be flexible, accurate and will reduce the cost of visual inspection system.

This chapter presents a novel integrated system in which a number of image processing algorithms are embedded within a Genetic Algorithm (GA) based framework in order to provide a better quality analysis with less computational complexity while maintains flexibility to a broad range of defects. A specially tailored hybrid GA (HGA) previously discussed is used to estimate geometric transformation of arbitrarily placed Printed Circuit Boards (PCBs) on a conveyor belt without any prior information such as CAD data. An imaging procedure has been developed that consists of several image processing operations such as fixed multi-thresholding, Sobel edge-detection, image subtraction and noise filters. A novel approach under taken by compositing the edge-detection and the thresholding to complement each other's abilities has increased defect detection accuracy with low computational time.

This system is capable of performing real-time image processing tasks and identifies the possible defects on completed PCBs during inspection process. The advantages of the system are no calibration, no learning process is required and its ability to adapt to any type of PCB. The system will operate based on an image of reference (perfect) board that has been stored once and without the aid of CAD data.

The chapter is organised as follows: Section 6.2 will discuss the integration between HGA module and defect detection module, Section 6.3 explains the details on simulation environment while Section 6.4 will discuss the performance of the system. To sum it up, Section 6.5 will conclude the work based on performance.

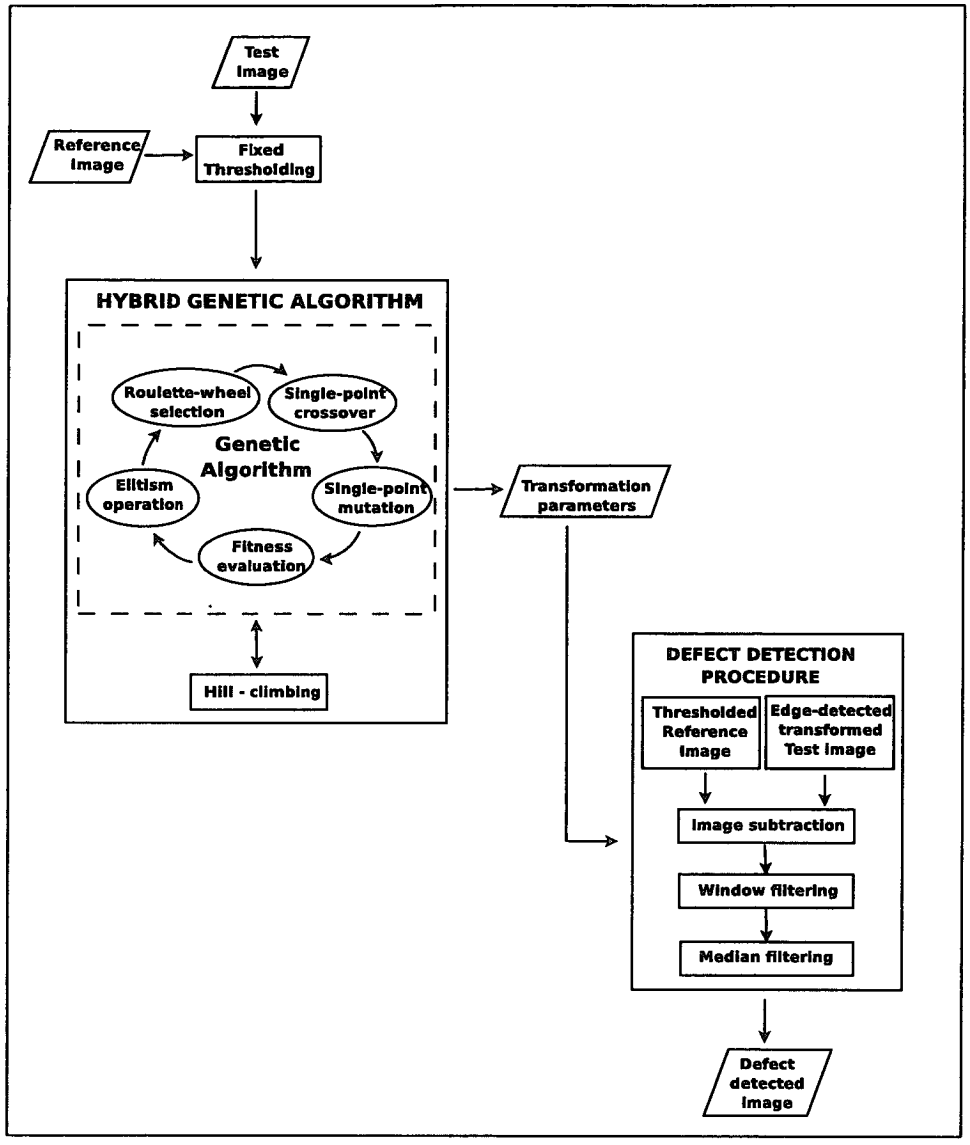

Figure 6.1: *Flow of system integration*

6.2 Full system implementation

The system is made up of two parts. The first part is an image registration module designed to find the correct transformation parameters of the inspected board in order to aid the defect detection process. The second part consists of a defect detection module supported by image processing elements, as outlined in Figure 6.1. The image registration module employed hybrid GA (HGA)

which contains conventional GA with elitism and hill-climbing operation as local optimisation agent. The defect detection procedure utilises a combination of image processing operations such as fixed multi-thresholding, Sobel edge detection, image subtraction and noise filtering. Every inspected board will undergo the full process of the system in order to produce defect-free completed PCB.

6.3 System testing

The geometric transformations considered in this work vary from 0 to 359 degrees while the displacement values are between -10 and 10 pixels at both axis. The reference images used in the simulation are shown in Figure 6.2. Twenty samples of test images are created from these reference images. A few samples of the test images are shown in Figure 6.3. All the test images are transformed with known values and some of them have artificial defects such as missing components and open solder joints. The simulation is repeated for 20 times for every test image. Test images of type 1 (T1), type 2 (T2) and type 3 (T3) are created from the reference images shown in Figure 6.2(a), 6.2(b) and 6.2(c) respectively. In the following experiment, the HGA parameters are: maximum generation is 200, population size is 50, crossover probability is 0.5, mutation probability is 0.01, 5 percent of elitism and hill-climbing's limit of generation, l is 10. The following result on mean value is determined by calculating the average value of 20 independent runs.

6.4 Performance analysis for real-time system

Based on Figure 6.4, the HGA successfully finds a mean of maximum fitness between 0.89 to 0.99 in all runs. Based on this finding, it is obvious that this specially-tailored HGA is well-suited to register high density PCBs accurately as produced by simulations on test images of type 1 and type 2.

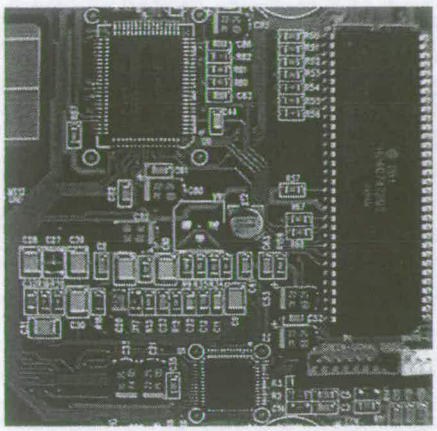

(a) Type 1

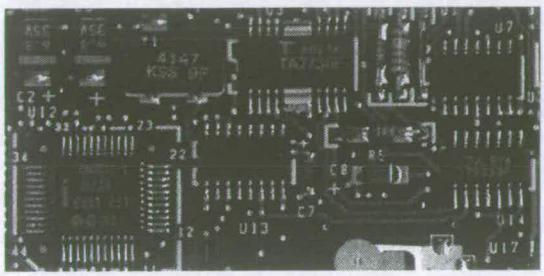

(b) Type 2

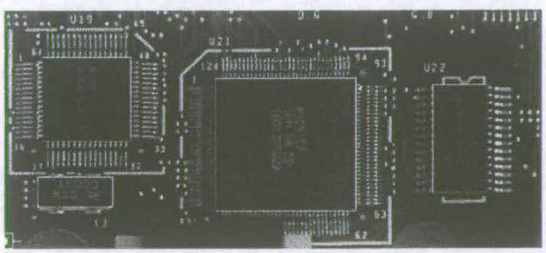

(c) Type 3

Figure 6.2: *Reference images of different types of PCB*

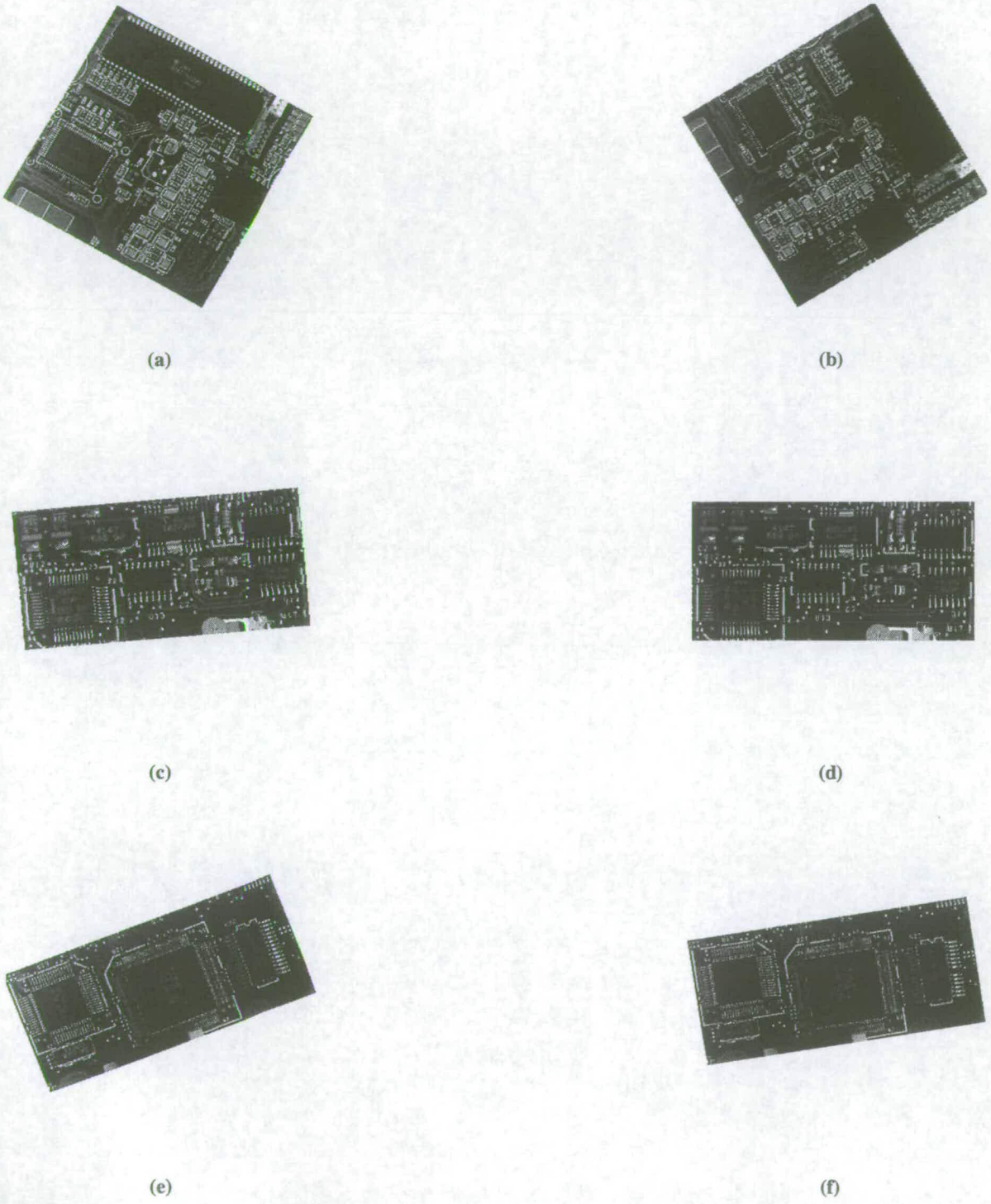

(a) (b)

(c) (d)

(e) (f)

Figure 6.3: *Samples of test images where each one is transformed using known values and some have artificial defect(s)*

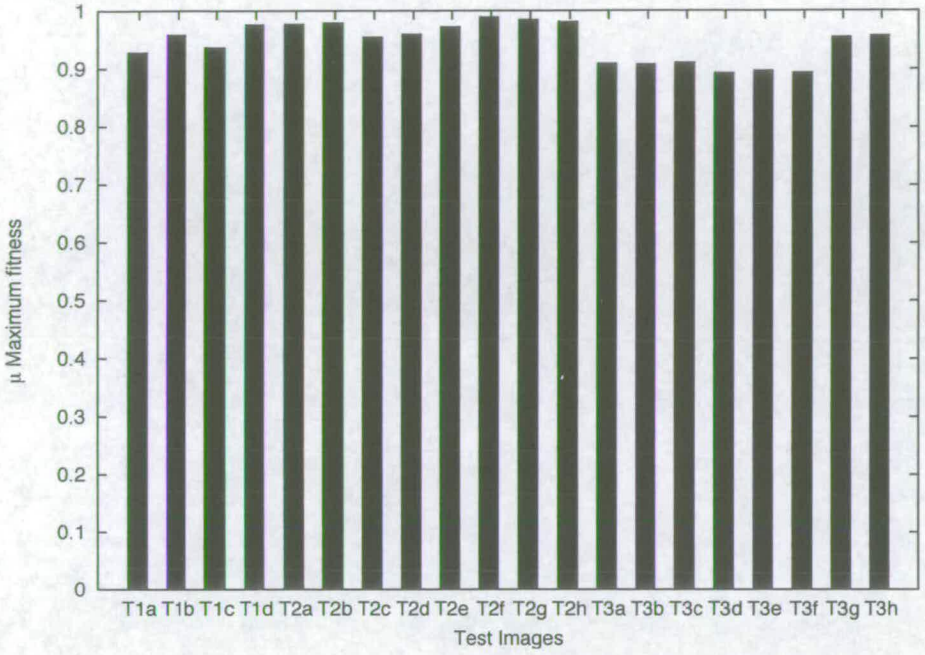

Figure 6.4: *Performance on mean, μ maximum fitness in each test image simulation*

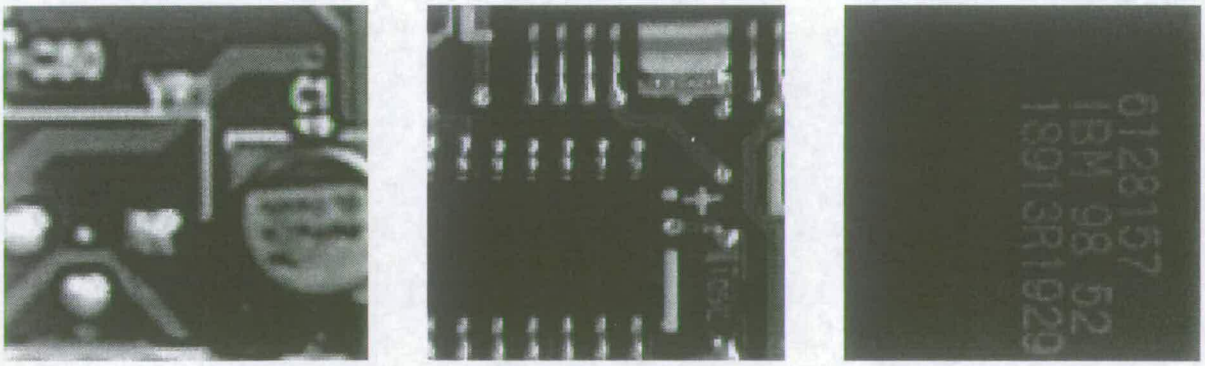

(a) Type 1 image (b) Type 2 image (c) Type 3 image

Figure 6.5: *Centre block image of every PCB type (40 x 40 pixels)*

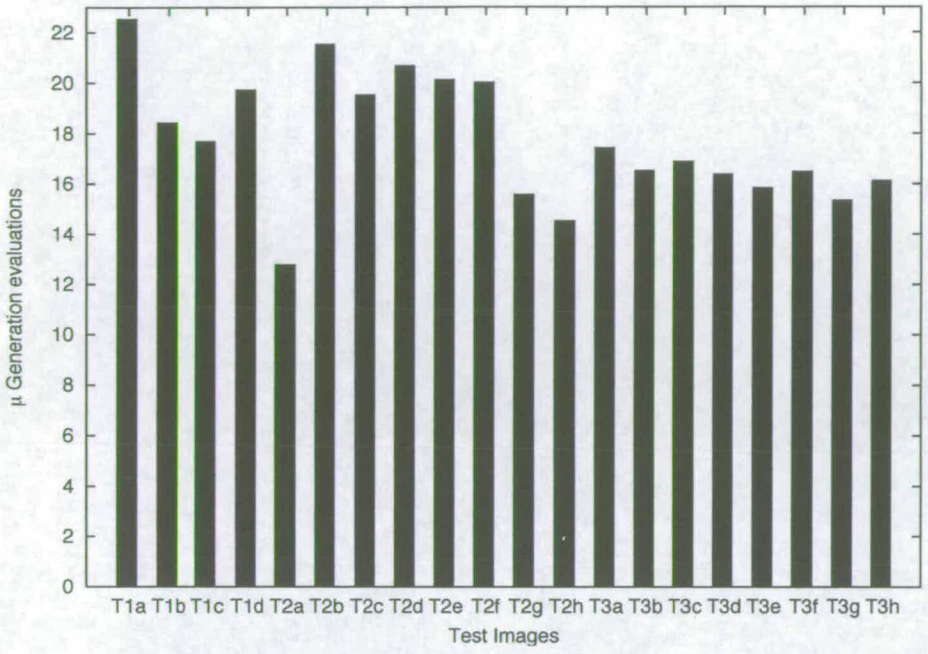

Figure 6.6: *Performance on mean, μ generation evaluations in each test image simulation*

Simulations on type 3 test images converge with slightly low fitness compared to other types of test images. This has been investigated and it has been discovered that the centre block of type 3 image that is used for fitness evaluations is lacking in features. The centre block image of every type of test images are shown in Figure 6.5. The image as shown in Figure 6.5(c) shows that the objects are too uniform compared to images in Figure 6.5(a) and Figure 6.5(b). It is known that a high-accuracy image registration will produce an image of overlapping area when the test image is subtracted from the reference image in defect detection procedure.

Figure 6.6 shows mean generation of the search convergence in every test image. This ranges between 13 to 23 generations. This implies a significant speed up when considering the amount of computation performed. Simulations on type 3 test images converges earlier compared to other test images and this may be one of the reasons for low maximum fitness found as presented earlier.

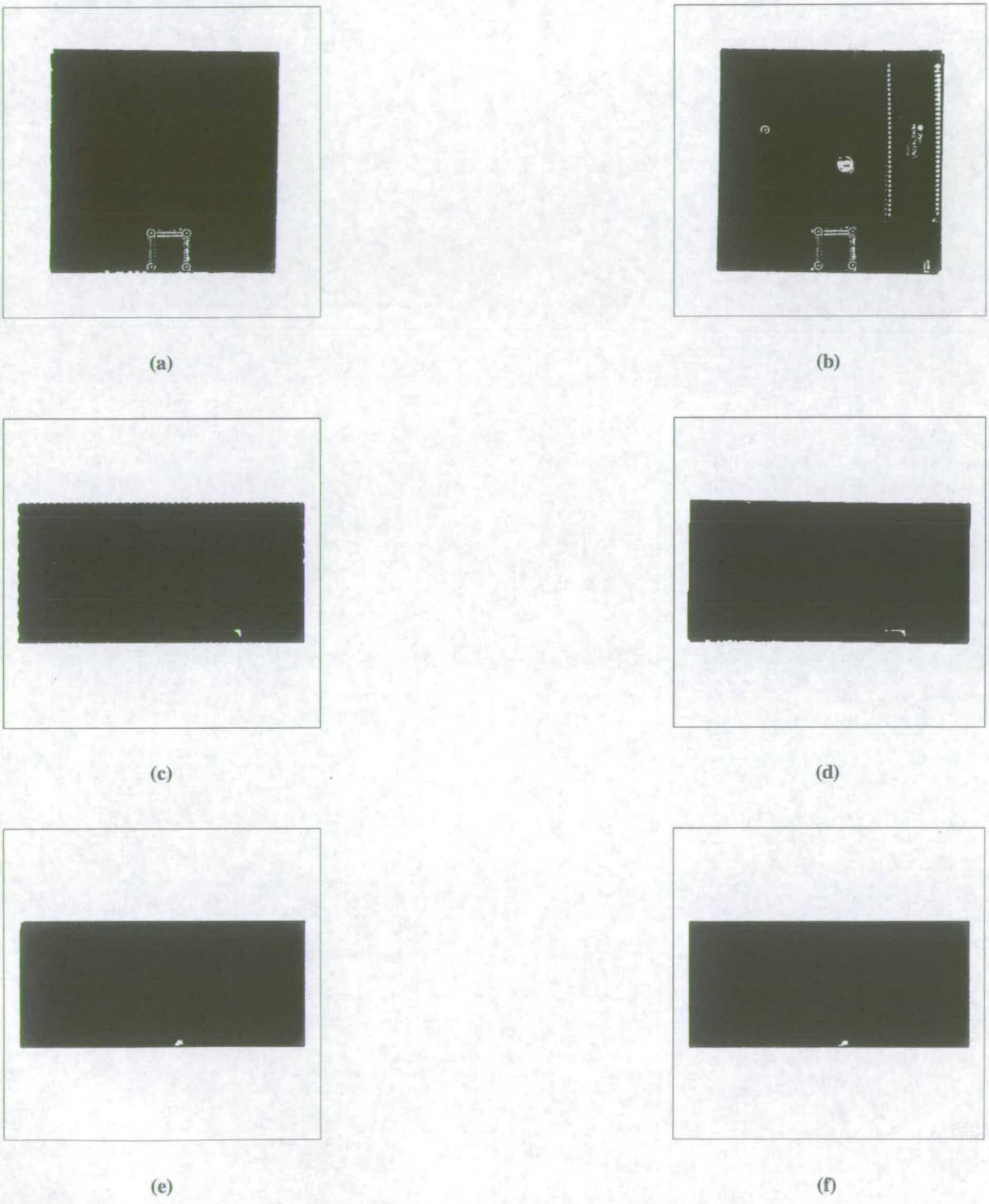

(a) (b)

(c) (d)

(e) (f)

Figure 6.7: *Samples of defect detected images after the whole operation respective to Figure 6.3. The overlapped area represented by the black area shows the accuracy of the image registration while the white objects detected are possible defects*

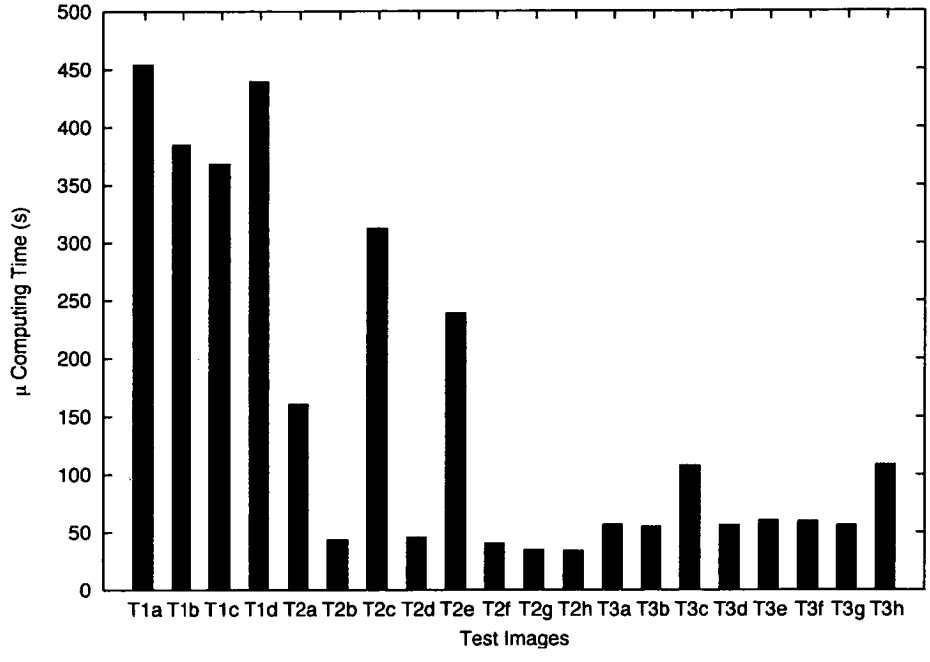

Figure 6.8: *Performance on mean, μ computational time in each test image simulation*

Figure 6.7 shows samples of defect detected images obtained from the simulation. The white objects are the possible defects of missing components and open solder joints. Possible defects in any shapes and sizes detected are very clear to recognise and free from noise as long as the image is registered with high precision. This shows that the system is robust enough to locate the possible defects accurately but it needs to refer the reference image in order to classify the type of defects that has been located. The image registration using HGA is successful when the reference image overlaps correctly on the test image after image subtraction operation as represented by the black area in samples of defect detected images. The above example shows good qualitative registration results. Later, quantitative analysis of the overall accuracy of the defect detection over these samples will be discussed.

Figure 6.8 depicts the mean computational time from 20 sets of simulations on every test image. Generally, every simulation consumes an acceptable computational time, which is suitable to be

Results (in percentage)	PCB Type 1	PCB Type 2	PCB Type 3
Correct defect detection	90	32	9
Correct defect detection with low false alarm	1	39	0
Correct defect detection with high false alarm	2	20	6
Wrong defect detection	6	9	85

Table 6.1: *Results of defect detection*

implemented in a real-time visual inspection system. The computational time ranges from 40 to 450 seconds. Type 1 test images take the longest time to register and to detect possible defects compared to type 2 and 3 due to the size of the image. Bigger images have more pixels to interpolate during image processing operations and this leads to longer processing time.

The percentage of the defect detection results on total runs of every type of PCBs are shown in Table 6.1. The results are categorised to four types of classifications based on visual interpretations on final output of every run. Correct defect detection category is the best and the most accurate results produced by the system, which makes it very easy to classify the types of defects. The rate of false alarm (i.e, accepted cases reported as non-accepted) is determined by the level of noise appear in the defect detected images. Low false alarm means the size of the noise is small and may be neglected during defect classification stage. More numbers and large sizes of noise are considered as high false alarm but will not affect the judgement in defect classification process. Wrong defect detection happens when the defect detected is inaccurate or the existing defects failed to be detected at all.

The analysis shows that the results from PCB type 1 yield the highest correct defect detection results and lowest failure percentage in locating the defects. PCB type 2 gives nearly similar percentage on correct defect detection with low false alarm. Another 20 percent of the runs successfully detect the defects in high false alarm. It failed to recognise the defects in small number of runs. It is obvious that the PCB type 3 produced the worst results by giving 85 percent of wrong defect detection outcomes. This poor performance has been caused by low accuracy of image registration by HGA which has been explained earlier.

These findings proved that this HGA-based inspection system with novel combination of image processing operations is powerful enough to produce high accuracy image registration and subsequently robust enough to locate the existence of possible defects on inspected PCBs with low computational time. The HGA converges in short generation time but is capable in obtaining very high maximum fitness, which gives an accurate transformation parameters. The defect detection procedure produces excellent results in locating the defects with low noise due to the successful search by HGA. However, system testing on PCB type 3 shows poor performance in quantitative analysis due to the low density of the PCB layout. Nevertheless this may be avoidable since the majority of the manufactured PCBs today are very complex yet small in size.

6.5 Conclusions

The combination of all of the above-mentioned disciplines result in the implementation of a PCB inspection system using HGA to register inspected images, which facilitates the defect detection procedure in real time. The system has been tested on various types of PCB with various missing components and open solder joints defects, giving satisfactory results with few exceptional conditions.

System testing in three types of PCB yield good overview of the developed system in terms of maximum fitness found by HGA, average generation time for HGA to converge, accuracy on defect detection and computational time required for the whole process to complete. Generally, HGA finds high maximum fitness in reasonable period of generation which gives high accuracy in image registration. HGA performed satisfactorily in image registration of PCB especially for high density PCB layout, which is placed arbitrarily on a conveyor belt during inspection. The registration process is crucial for the defect detection procedure that is based on pixel interpolation operations. Therefore, accurate image registration determine the success in defect detection procedure. The system operates in acceptable computing time which proves it can be implemented on real-time environment.

This adaptive system is suitable for any type of PCB, without aid of CAD data and learning process. However, the system needs classification process to recognise the type of defect for decision making by the system itself or human operator. Currently, the system is able to detect missing components and

open solder joints in any shapes and any sizes. The observation shows that the current block matching used in HGA is not very successful in low density PCB, which causes high number of failure in detecting the defects. Our main objective is to demonstrate that the feasibility and the functionality of this inspection system has been achieved by producing these results.

Chapter 7
Summary and Conclusions

7.1 Introduction

This thesis has considered the use of GA for image registration to inspect PCB placed arbitrarily on a conveyor belt during inspection process. A specially-tailored GA for this application has been developed and evaluated against accuracy, computational time and reliability constraints. Novel defect detection procedure has been produced by combining a number of image processing functions including thresholding, Sobel edge-detection, image subtraction and noise elimination operations. The integration between GA-based image registration module and defect detection module has proven that the integration system has potential to be applied on real-time inspection in PCB manufacturing industries.

The remainder of this chapter is organised as follows: Section 7.2 summarises the content of the thesis and identifies the contributions; in Section 7.3, the main achievements of this work is summarised; Section 7.4 draws conclusions from the work presented in this thesis, final remarks are described in Section 7.5 and limitations of this developed system is discussed in Section 7.6.

7.2 Summary of thesis

This thesis investigates the potential of a system integration of GA-based image registration and defect detection procedure that includes novel combination of image processing functions to be developed as a accurate, fast, reliable and flexible PCB inspection system.

Chapter 2 gives an overview and discussion in details on the main topics considered in this work such as existing techniques in PCB AOI, image registration, GA, image processing operations and

types of PCB defects that usually investigated. The literature reviews highlight the importance of a PCB inspection system to be flexible, reliable, fast, accurate and low cost. Therefore, these essential requirements give beneficial guidance in selecting every operation and parameter settings involved in GA and defect detection procedure. Discussion on several types of PCB defects gives an overview of the popular defects that need to be solved.

In Chapter 3, a basic framework of a specially-tailored GA-based image registration is presented. The structure and parameter settings of the GA is explained in detail with concise preliminary results are obtained using real PCB images. The experiments on this framework proves that GA has high potential in optimising image registration of whole PCBs placed arbitrarily on a conveyor belt during quality inspection in term of accuracy. However, the computational time is high which is impossible to be implemented in real time environment with regard to full image matching during fitness evaluation. The GA also needs an agent in local search space to speed up the search while improving the end solution. Hence, more enhancement work on the framework are needed in order to fulfil the main requirements of the expected PCB inspection system.

Chapter 4 emphasised the enhancement work on the GA framework to improve the performance of the image registration framework. Gray-coded mutation, integer encoding, elitist selection schemes and GA hybridisation are the major studies in improving the GA performance in the chapter. Block matching algorithm and conversion to rotate-by shear operation also contributed to the improved results in the experiments by speeding up the registration process and decrease the loss of pixel's original information during rotation operation. By implementing all these enhancement work, the framework has produced significant improvement in accuracy, consistency of the findings which caused the level of reliability and reduction of computational time. This statement is supported by performing experiments on 1000 test images from three different types of real PCB images.

Chapter 5 described the defect detection procedure based on a novel combination of image processing functions that developed specifically for this system. Four approaches have been tested with various segmentation techniques and different settings of image processing operations. Segmentation methods using fixed global multi-thresholding, adaptive bi-level thresholding and Sobel edge-detection are presented with different parameter values to obtain the most powerful settings for this application.

These four approaches are evaluated in terms of accuracy of defect detected with least image noise produced. Numerous types of component missing defects and open solder joint defects are tested using these four approaches. Experimental results demonstrate the ability of this novel defect detection procedure in detecting the tested types of defects correctly and in acceptable level of noise.

Chapter 6 discussed the system integration structure which consists of the improved framework of GA-based image registration and the defect detection procedure that employed the best approach. More experiments are performed on the system using more samples from three types of PCB images with artificial defects. The findings indicate that the system is accurate, flexible and fast enough to inspect absence component defect and open solder joint defect in any size and shape on any type of PCB. The system performs more successfully in high density layout PCB due to the block matching operation at the centre of an image. Additional advantages offered by this system are no requirement for learning process and prior information except the image of reference board.

7.3 Summary of achievements

The main achievement of this work is the development of a specially-tailored GA-based image registration for whole PCBs placed arbitrarily on a conveyor belt during inspection process. A special defect detection procedure is produced to aid the image registration framework, which successfully detects absence component defects including open solder joints in any size and shape with good accuracy and in reasonable computational time. This indicates that the system integration has good potential to be implemented in real-time environment. System flexibility also has been met when the system is able to register the images of whole PCB and locate the physical defects on any type of PCB that has been tested.

7.4 Conclusions

This thesis proposed a system integration using a specially tailored GA- based image registration and a novel defect detection procedure which is able to recognise the existence of missing component

defect and open solder joint defect.

From the work in Chapter 3, this thesis concludes that the GA has big potential in optimising the image registration of whole PCBs placed arbitrarily on a conveyor belt. The accuracy of transformation parameter estimation is high but the computational time gives a drawback to the framework to operate in real-time basis. The framework is developed based on a conventional GA which is suited for exploration capability but lacks in exploitation characteristics. Fitness evaluation using full image matching is also time consuming. Maximum fitness value is nearly impossible to be obtained corresponding to the high loss in pixels information of the studied images.

From the studies and experiments in Chapter 4, this thesis concludes that the enhancement work done on the image registration framework is successful in producing accurate, reliable and fast performance. Major reduction of time is achieved by employing block matching algorithm and by hybridising GA and E with local search technique such as HC. The hybridisation also contributes to the consistency of the system to deliver the accurate results in every experiment. This thesis therefore concludes that the enhanced image registration framework is suitable enough to be integrated with the defect detection procedure for producing high quality inspection results in real-time.

Based on the work presented in Chapter 5, this thesis concludes that a special combination of a number of image processing functions has good ability to detect missing component and open solder joint defect. It produces accurate location of the defect but not able to recognise the type of defect.

From Chapter 6, this thesis concludes that a system integration between GA-based image registration and this novel defect detection has a big potential to be developed in real-time inspection system and delivered results as expected.

7.5 Final remarks

This work represents a step forward in the area of quality control in manufacturing inspection process in general and of PCB inspection in particular. The system testing has demonstrated the functionality and big potential of the developed GA-based image registration on inspection system with aid of

image processing functions. Better system evaluation may be produced by testing the system on broader range of PCB samples.

7.6 Limitations

This work is limited by a number of issues that can be resolved in the future. With consistent precise alignment by the GA, this system will always find the accurate defect detection results and the defect detection procedure can be improved by employing adaptive image processing operations. Studies on more types of defects will give more highlights to this developed system in order to compete with other existing systems. This system also need a good classification algorithm in order to verify the detected defects without any error. Better illumination environment is also essential for this system in delivering expected results. For improved view on potential of this system, experiments on more types of PCB has to be investigated in order to evaluate the flexibility offered by the system.

References

[1] H.-H. Loh and M.-S. Lu, "Printed circuit board inspection using image analysis," *IEEE Transactions on Industry Applications*, vol. 35, no. 2, pp. 426–432, 1999.

[2] K. M. Chingping Han and N. Saravanan, "A printed circuit board system using artificial neural network," in *Twenty-Fifth Southeastern Symposium on System Theory, SSST '93*, pp. 238–242, 1993.

[3] Z. Ibrahim, Z. Aspar, S. Al-Attas, and M. M. Mokji, "Coarse resolution defect localization algorithm for an automated visual printed circuit board inspection," in *IEEE 28th Annual Conference of the Industrial Electronics Society, IECON02*, vol. 4, pp. 2629–2634, 2002.

[4] P. J. Besl, E. J. Delp, and R. Jain, "Automatic visual solder joint inspection," *IEEE Journal of Robotics and Automation*, vol. 1, no. 1, pp. 42–56, 1985.

[5] S. L. Bartlett, P. J. Besl, C. L. Cole, R. Jain, D. Mukherjee, and K. D. Skifstad, "Automatic solder joint inspection," *IEEE Transactions on Pattern Analysis and Machine Intelligence*, vol. 10, no. 1, pp. 31–43, 1988.

[6] D. W. Capson and S.-K. Eng, "A tiered-color illumination approach for machine inspection of solder joints," *IEEE Transactions on Pattern Analysis and Machine Intelligence*, vol. 10, no. 3, pp. 387–393, 1988.

[7] M. R. Driels and D. J. Nolan, "Automatic defect classification of printed wiring board solder joints," *IEEE Transactions on Components, Hybrids and Manufacturing Technology*, vol. 13, no. 2, pp. 331–340, 1990.

[8] Y. Matsuyama, T. Honda, H. Yamamura, H. Sasazawa, M. Nomoto, T. Ninomiya, A. Schick, L. Listl, P. Kollensperger, D. Spriegel, P. Mengel, and R. Schneider, "Automated solder joint inspection system using optical 3-D image detection," in *3rd IEEE Workshop on Applications of Computer Vision, WACV'96*, pp. 116–122, 1996.

[9] J. E. Mesbahi and M. Chaibi, "Printed circuit boards inspection using two new algorithms of dilation and connectivity preserving shrinking," in *Proceedings of the 1993 IEEE-SP Workshop Neural Networks for Signal Processing [1993] III*, pp. 527–536, 1993.

[10] M. Moganti and F. Ercal, "A subpattern level inspection system for printed circuit boards," *Computer Vision and Image Understanding*, vol. 70, no. 1, pp. 51–62, 1998.

[11] M. Ito and Y. Nikaido, "Recognition of pattern defects of printed circuit board using topological information," in *Eleventh IEEE/CHMT International Electronics Manufacturing Technology Symposium*, pp. 202–206, 1991.

[12] A. M. Darwish and A. K. Jain, "A rule based approach for visual pattern inspection," *IEEE Transactions on Pattern Analysis and Machine Intelligence*, vol. 10, no. 1, pp. 56–68, 1988.

[13] M. E. Zervakis, S. K. Goumas, and G. A. Rovithakis, "A bayesian framework for multilead SMD post-placement quality inspection," *IEEE Transactions on Systems, Man and Cybernetics*, vol. 34, no. 1, pp. 440–453, 2003.

[14] J. S. Park and J. T. Tou, "Automatic inspection of assembled PC board via highlight separation and dual channel processing," in *Proceedings of the IEEE International Conference on Robotics and Automation*, vol. 3, pp. 2702–2707, 1991.

[15] B. Raghunathan and S. T. Acton, "A content based retrieval engine for circuit board inspection," in *Proceedings. 1999 International Conference on Image Processing, ICIP 99.*, vol. 1, pp. 104–108, 1999.

[16] C. Charette, S. Park, R. Williams, B. Benhabib, and K. Smith, "Development and integration of a micro-computer based analysis system for automatic PCB inspection," in *International Conference on Computer Integrated Manufacturing*, pp. 129–135, 1988.

[17] E. N. Malamas, E. G. Petrakis, M. Zervakis, L. Petit, and J.-D. Legat, "A survey on industrial vision systems, applications and tools," *Image and Vision Computing*, vol. 21, pp. 171–188, 2003.

[18] Z. Michalewicz, *Genetic Algorithms + Data Structures = Evolution Programs*. Springer-Verlag Berlin Heidelberg New York, second ed., 1999.

[19] P. Chalermwat and T. El-Ghazawi, "Multi-resolution image registration using genetics," in *International Conference on Image Processing, ICIP 99*, vol. 2, pp. 452–456, 1999.

[20] B. C. H. Turton, T. Arslan, and D. H. Horrocks, "A hardware architecture for a parallel genetic algorithm for image registration," in *IEE Colloquium on Genetic Algorithms in Image Processing and Vision*, pp. 11/1–11/6, 1994.

[21] N.-H. Kim, J.-Y. Pyun, K.-S. Choi, B.-D. Choi, and S.-J. Ko, "Real-time inspection system for printed circuit boards," in *IEEE International Symposium on Industrial Electronics*, vol. 1, pp. 166–170, 2001.

[22] C. G. Drury, *Inspection Performance, G. Salvendy Edition, Handbook of Industrial Engineering*. New York: John Wiley and Sons, 2nd ed., 1992.

[23] M. Moganti, F. Ercal, C. H. Dagli, and S. Tsunekawa, "Automatic PCB inspection algorithms: A survey," *Computer Vision and Image Understanding*, vol. 63, no. 2, pp. 287–313, 1996.

[24] K. H. Chung, *Application of Augmented Reality to Dimensional and Geometric Inspection.* PhD thesis, Faculty of the Virginia Polytechnic Institute and State University, February 2002.

[25] J. Evans, *An Evolvable Hardware System for Automatic Optical Inspection.* PhD thesis, University of Edinburgh, March 2004.

[26] S. Tominaga and S. Okamoto, "Reflectance- based material classification for printed circuit boards," in *Proceedings of the 12th International Conference on Image Analysis and Processing (ICIAP'03)*, pp. 238–244, 2003.

[27] P. Mengel, "Automated inspection of solder joints on PC boards by supplementary processing of 3D and gray-level images," in *16th Annual Conference of IEEE Industrial Electronics Society, IECON '90*, vol. 1, pp. 786–791, 1990.

[28] Q.-Z. Ye and P. E. Danielsson, "Inspection of printed circuit boards by connectivity preserving shrinking," *IEEE Transactions on Pattern Analysis and Machine Intelligence*, vol. 10, no. 5, pp. 737–742, 1988.

[29] E. R. V. Dop and P. P. L. Regtien, "Multi-sensor recognition of electronic components," *Machine Vision and Applications*, pp. 213–222, 2001.

[30] M. H. Tatibana and R. D. A. Lotufo, "Novel automatic PCB inspection technique based on connectivity," in *Proceedings X Brazilian Symposium on Computer Graphics and Image Processing*, pp. 187–194, 1997.

[31] H. H. Loh and M. S. Lu, "Printed circuit board inspection using image analysis," *IEEE Transactions on industry applications*, vol. 35, no. 2, pp. 426–432, 1999.

[32] M. Ito, Y. Takeuchi, I. Fujita, M. Hoshinao, and T. Uchida, "Pattern analysis and evaluation of printed circuit boards," in *Proceedings of the Second International Conference on Document Analysis and Recognition*, pp. 798–801, 1993.

[33] J. F. Borba and J. Facon, "A printed circuit board automated inspection system," in *Proceedings of the 38th Midwest Symposium on Circuits and Systems, 1995*, vol. 1, pp. 69–72, 1995.

[34] T. Ninomiya, K. Yoshimura, M. Nomoto, and Y. Nakagawa, "Automatic screen-printed circuit pattern inspection using connectivity preserving image reduction and connectivity comparison," in *Proceedings of 11th International Conference on Pattern Recognition IAPR, Conference A: Computer Vision and Applications*, vol. 1, pp. 53–56, 1992.

[35] X. Lee and Y.-Q. Zhang, "A fast hierarchical motion-compensation scheme for video coding using block feature matching," *IEEE Transactions on Circuits and Systems for Video Technology*, vol. 6, no. 6, pp. 627–635, 1996.

[36] R. M. Armitano, R. W. Schafer, F. L. Kitson, and V. Bhaskaran, "Robust block-matching motion-estimation technique for noisy sources," in *IEEE International Conference on Acoustics, Speech and Signal Processing, ICASSP-97*, vol. 4, pp. 2685–2688, 1997.

[37] C.-H. Lin and J.-L. Wu, "Genetic block matching algorithm for video coding," in *Third IEEE International Conference on Multimedia Computing and Systems*, pp. 544–547, 1996.

[38] H. J. Kim, E. Y. Kim, J. W. Kim, and S. H. Park, "MRF model based image segmentation using hierarchical distributed genetic algorithm," *Electronics Letters*, vol. 34, no. 25, pp. 2394–2395, 1998.

[39] R. C. Gonzalez and R. E. Woods, *Digital Image Processing*. Prentice-Hall, Second ed., 2002.

[40] J. Fan, D. K. Y. Yau, A. K. Elmagarmid, and W. G. Aref, "Automatic image segmentation by integrating color-edge extraction and seeded region growing," *IEEE Transactions on Image Processing*, vol. 10, no. 10, pp. 1454–1466, 2001.

[41] M. H. F. Wilkinson, T. Wijbenga, G. D. Vries, and M. A. Westenberg, "Blood vessel segmentation using moving-window robust automatic threshold selection," in *International Conference on Image Processing, ICIP 2003*, vol. 2, pp. 1093–1096, 2003.

[42] A. E. Savakis, "Adaptive document image thresholding using foreground and background clustering," in *International Conference on Image Processing, ICIP 98*, vol. 3, pp. 785–789, 1998.

[43] J. Evans and T. Arslan, "Implementation of a robust image registration algorithm on an ARM system-on-chip platform," in *IEEE International Symposium on Circuits and Systems, ISCAS 2002*, vol. 2, pp. 269–272, 2002.

[44] J. Song, M. Cai, and M. R. Lyu, "Edge color distribution transform: An efficient tool for object detection in images," in *16th International Conference on Pattern Recognition*, vol. 1, pp. 608–611, 2002.

[45] D.-M. Tsai, "A fast thresholding selection procedure for multi-modal and unimodal histograms," *Pattern Recognition Letter*, vol. 16, no. 6, pp. 653–666, 1995.

[46] B. C. Jiang, Szu-Lang, and C.-C. Wang, "Machine vision-based gray relational theory applied to IC marking inspection," *IEEE Transactions on Semiconductor Manufacturing*, vol. 15, no. 4, pp. 531–539, 2002.

[47] A. E. Brito, E. Whittenberger, and S. D. Cabrera, "Segmentation strategies with multiple analysis for an SMD object recognition system," in *IEEE Southwest Symposium on Image Analysis and Interpretation*, pp. 59–64, 1998.

[48] M.-H. Perng and T.-C. Chen, "Optimal color segmentation with an application to the PCB industry," in *Proceedings of SPIE Applications of Digital Image Processing XXVII*, vol. 5558, pp. 604–615, 2004.

[49] W. Tarnawski, "Colour image segmentation algorithm in vectoral approach for automated optical inspection in electronics," *Opto-electronics Review*, vol. 11, no. 3, pp. 197–202, 2003.

[50] Z. Ibrahim, S. Al-Attas, and Z. Aspar, "Analysis of the wavelet-based image difference algorithm for PCB inspection," in *Proceedings of the 41st SICE Annual Conference, SICE 2002*, vol. 4, pp. 2108–2113, 2002.

[51] T. Seemann and P. Tischer, "Structure preserving noise filtering of images using explicit local segmentation," in *Fourteenth International Conference on Pattern Recognition*, vol. 2, pp. 1610–1612, 1998.

[52] P. S. Windyga, "Fast impulsive noise removal," *IEEE Transactions on Image Processing*, vol. 10, no. 1, pp. 173–179, 2001.

[53] Y. Hara, H. Doi, K. Karasaki, and T. Lida, "A system for pcb automated inspection using fluorescent light," *IEEE Transaction Pattern Analytical Machine Intelligent*, pp. 69–78, 1988.

[54] H. S. Alhichri and M. Kamel, "Image registration using virtual circles and edge direction," in *16th International Conference on Pattern Recognition*, vol. 2, pp. 969–972, 2002.

[55] L. G. Brown, "A survey of image registration techniques," *ACM Computing Surveys*, vol. 24, pp. 325–376, 1992.

[56] Y. Jianchao, "Image registration based on both feature and intensity matching," in *IEEE International Conference on Acoustics, Speech, and Signal Processing, ICASSP '01*, vol. 3, pp. 1693–1696, 2001.

[57] X. Dai and S. Khorram, "A feature-based image registration algorithm using improved chain-code representation combined with invariant moments," *IEEE Transactions on Geoscience and Remote Sensing*, vol. 37, no. 5, pp. 2351–2362, 1999.

[58] Z. Hu and S. T. Acton, "Morphological pyramid image registration," in *4th IEEE Southwest Symposium Image Analysis and Interpretation*, pp. 227–231, 2000.

[59] C. X. Zhong and Z. H. Liang, "A heuristic search algorithm for image registration," in *9th International Conference on Pattern Recognition*, vol. 2, pp. 733–735, 1988.

[60] R. Manduchi and G. Mian, "Accuracy analysis for correlation-based image registration algorithms," in *IEEE International Symposium on Circuits and Systems, ISCAS '93*, pp. 834 – 837, 1993.

[61] A. D. Mandalia, R. Sudhakar, K. Ganesan, and F. Hamano, "Low-level and high-level correlation for image registration," in *Conference Proceedings IEEE International Conference on Systems, Man and Cybernetics*, pp. 206–208, 1990.

[62] A. Efrat and C. Gotsman, "Subpixel image registration using circular fiducials," *International Journal of Computational Geometry and Applications, World Scientific Publishing Company*, vol. 4, no. 4, pp. 403–422, 1994.

[63] D. E. Goldberg, *Genetic Algorithms in Search, Optimization and Machine Learning*. Addison Wesley Longman Inc, Twentieth ed., 1999.

[64] J.-M. Rouet, J.-J. Jacq, and C. Roux, "Genetic algorithms for a robust 3-D MR-CT registration," *IEEE Transactions on Information Technology in Biomedicine*, vol. 4, no. 2, pp. 126–137, 2000.

[65] J. C. Rajapakse and B. Guojun, "Functional MR image registration using a genetic algorithm," in *6th International Conference on Neural Information Processing, ICONIP '99*, vol. 3, pp. 922–927, 1999.

[66] H. H. Ammar and Y. Tao, "Fingerprint registration using genetic algorithms," in *3rd IEEE Symposium on Application-Specific Systems and Software Engineering Technology*, pp. 148–154, 2000.

[67] C. K. Chow, H. T. Tsui, T. Lee, and T. K. Lau, "Medical image registration and model construction using genetic algorithms," in *International Workshop on Medical Imaging and Augmented Reality*, pp. 174–179, 2001.

[68] S. Loncaric and A. P. Dhawan, "3-D brain image registration using optimal morphological processing and iterative principal axis transform," in *Proceedings of the 16th Annual International Conference of the IEEE Engineering in Medicine and Biology Society, 1994. Engineering Advances: New Opportunities for Biomedical Engineers*, vol. 1, pp. 692–693, 1994.

[69] J.-J. Jacq and C. Roux, "Registration of successive DSA images using a simple genetic algorithm with a stochastic performance function," in *Proceedings of the 1993 IEEE Nineteenth Annual Northeast Bioengineering Conference*, pp. 223–224, 1993.

[70] G. M. Pagliari and J. R. Greene, "Image registration, parameter tuning and approximate function evaluation, using the genetic algorithm and digital image warping," in *IEEE AFRICON 4th*, vol. 2, pp. 536–541, 1996.

[71] K. Simunic and S. Loncaric, "A genetic search-based partial image matching," in *Proceedings of the 2nd IEEE International Conference on Intelligent Processing Systems*, pp. 119–122, 1998.

[72] M. Ahmed, S. Yamany, E. Hemayed, S. Ahmed, S. Roberts, and A. Farag, "3D reconstruction of the human jaw from a sequence of images," in *IEEE Computer Society Conference on Computer Vision and Pattern Recognition*, pp. 646–653, 1997.

[73] J. Inglada and F. Adragna, "Automatic multi-sensor image registration by edge matching using genetic algorithms," in *IEEE International Geoscience and Remote Sensing Symposium, IGARSS '01*, vol. 5, pp. 2313–2315, 2001.

[74] J. Fitzpatrick, J. Grefenstette, and D. V. Gucht, "Image registration by genetic search," in *Proceedings of IEEE Southeastcon'84*, pp. 460–464, 1984.

[75] B. Zitova and J. Flusser, "Image registration methods: a survey," *Image and Vision Computing*, pp. 977–1000, 2003.

[76] E. K. Teoh, D. P. Mital, B. W. Lee, and L. K. Wee, "An intelligent robotic vision system for inspection of surface mount PCBs," in *IEEE International Conference on Systems, Man, and Cybernetics, 1991. 'Decision Aiding for Complex Systems*, pp. 13–18, 1991.

[77] S. Hata, S. Hibi, and T. Gunji, "Assembled PCB visual inspection machine using image processor with DSP," in *15th Annual Conference of IEEE Industrial Electronics Society, IECON '89*, vol. 3, pp. 572–577, 1989.

[78] Y. J. Roh, W. S. Park, and H. Cho, "Correcting image distortion in the x-ray digital tomosynthesis system for PCB solder joint inspection," *Image and Vision Computing*, pp. 1063–1075, 2003.

[79] S. Mashohor, J. R. Evans, and T. Arslan, "Genetic algorithm based printed circuit board inspection system," in *IEEE International Symposium on Consumer Electronics*, pp. 519–522, September 2004.

[80] J. Evans and T. Arslan, "The implementation of an evolvable hardware system for real time image registration on a system-on-chip platform," *Proceedings of the 2002 NASA/DOD Conference on Evolvable Hardware (EH'02) IEEE*, pp. 142–146, 2002.

[81] A. Mahajan, A. Pilch, and T. Chu, "Intelligent image correlation using genetic algorithms for measuring surface deformation in the autonamous inspection of structures," in *Proceedings of the American Control Conference*, vol. 1, pp. 460–461, 2000.

[82] J. Xin, D. Liu, H. Liu, and Y. X. Yang, "GA-based object recognition in a complex noisy environment," in *Proceedings of the First International Conference on Machine Learning and Cybernetics*, pp. 1586–1589, 2002.

[83] G. Harik and F. Lobo, "A parameter-less genetic algorithm," in *Proceedings of the Genetic and Evolutionary Computation Conference*, vol. 1, pp. 258–265, 1999.

[84] A. E. Eiben, R. Hinterding, and Z. Michalewicz, "Parameter control in evolutionary algorithms," *IEEE Transactions on Evolutionary Computation*, vol. 3, no. 2, pp. 124–141, 1999.

[85] M. Srinivas and L. M. Patnaik, "Adaptive probabilities of crossover and mutation in genetic algorithms," *IEEE Transactions on Systems, Man and Cybernetics*, vol. 24, no. 4, pp. 656–667, 1994.

[86] A. Peacock, *Information Fusion for Improved Motion Estimation.* PhD thesis, School of Engineering and Electronics, University of Edinburgh, May 2001.

[87] E. Izquierdo and M. Ghanbari, "Nonlinear gaussian filtering approach for object segmentation," in *IEE Proceedings-Vision, Image and Signal Processing*, vol. 146, pp. 37–143, 1999.

[88] L. Silva, O. R. Bellon, P. F. Gotardo, and K. L. Boyer, "Range image registration using enhanced genetic algorithms," in *International Conference on Image Processing, ICIP03*, vol. 2, pp. 711–714, 2003.

[89] K. E. Mathias, L. D. Whitley, C. Stork, and T. Kusuma, "Staged hybrid genetic search for seismic data imaging," in *Proceedings of the First IEEE Conference on Evolutionary Computation*, vol. 1, pp. 356–361, 1994.

[90] D. Thierens, "Selection schemes, elitist recombination and selection intensity," in *International Conference of Genetic Algorithm*, pp. 152–159, 1997.

[91] S. Legg, M. Hutter, and A. Kumar, "Tournament versus fitness uniform selection," in *Congress on Evolutionary Computation CEC2004*, vol. 2, pp. 2144–2151, 2004.

[92] D. Quagliarella and A. Vicini, "A genetic algorithm with adaptable parameters," in *Proceedings of International Conference on Systems, Man and Cybernetics*, vol. 3, pp. 598–603, 1999.

[93] M. Srinivas and L. M. Patnaik, "Genetic algorithms: A survey," *Computer*, vol. 27, no. 6, pp. 17 – 26, 1994.

[94] U. K. Chakraborty and C. Z. Janikow, "Binary and gray encoding in univariate marginal distribution algorithm, genetic algorithm, and stochastic hillclimbing," in *Proceedings of Genetic and Evolutionary Computation Conference*, pp. 8–14, 2003.

[95] A. S. Wu, R. K. Lindsay, and M. D. Smith, "Studies on the effect of non-coding segments on the genetic algorithm," in *Proceedings of Sixth International Conference on Tools with Artificial Intelligence*, pp. 744–747, 1994.

[96] W. Venables, D. Smith, and the R Development Core Team, *An Introduction to R*, May 2002 ed.

[97] A. W. Paeth, "A fast algorithm for general raster rotation," *Graphics Gems*, p. 179, 1990.

[98] E. Yariv, "High quality image rotation (rotate by shear)." www.codeproject.com/bitmap/rotatebyshear.asp, January 2000.

[99] D. Whitley, S. Rama, and R. Heckendom, "Representation issues in neighborhood search and evolutionary algorithms," *Genetic Algorithms and Evolution Strategy in Engineering and Computer Science*, pp. 39–67, 1997.

[100] S. K. Sharma and G. W. Irwin, "Fuzzy coding of genetic algorithms," *IEEE Transactions on Evolutionary Computation*, vol. 7, no. 4, pp. 344–355, 2003.

[101] I. Rojas, H. Pomares, J. Gonzalez, P. Gloesekotter, J. Diestuhl, and K. Goser, "Multideme evolutionary algorithm based approach to the generation of fuzzy systems," in *IEEE International Fuzzy Systems Conference*, pp. 1412–1415, 2001.

[102] J.-M. Renders and H. Bersini, "Hybridizing genetic algorithms with hill-climbing methods for global optimization: Two possible ways," in *Proceedings of the First IEEE Conference on Evolutionary Computation*, vol. 1, pp. 312–317, 1994.

[103] F. G. Lobo and D. E. Goldberg, "Decision making in a hybrid genetic algorithm," in *IEEE International Conference on Evolutionary Computation*, pp. 121–125, 1997.

[104] B. Henderson *et al.*, *User manual for Netpbm*, April 2005.

[105] S. Mashohor, J. R. Evans, and T. Arslan, "Elitist selection schemes for genetic algorithm based printed circuit board inspection system," in *IEEE Congress on Evolutionary Computation*, vol. 2, pp. 974–978, 2005.

[106] Z. Ibrahim, S. Al-Attas, O. Ono, and M. Mokji, "A noise elimination procedure for wavelet-based printed circuit board inspection system," in *2004 5th Asian Control Conference*, vol. 2, pp. 875–880, 2004.

[107] T. Taniguchi, D. Kacprzak, S. Yamada, and M. Iwahara, "Wavelet-based processing of ECT images for inspection of printed circuit board," *IEEE Transactions on Magnetics*, vol. 37, no. 4, pp. 290–2793, 2001.

[108] D. Demir, S. Birecik, F. Kurugollu, M. Sezgin, I. Bucak, B. Sankur, and E. Anarim, "Quality inspection in PCBs and SMDs using computer vision techniques," in *20th International Conference on Industrial Electronics, Control and Instrumentation, IECON'94*, vol. 2, pp. 857–861, 1994.

[109] T. F. Cootes, C. J. Taylor, D. H. Cooper, and J. Graham, "Active shape models- their training and application," *Computer Vision and Image Understanding*, vol. 61, no. 1, pp. 38–59, 1995.

[110] J. J. Hong, K. J. Park, and K. G. Kim, "Parallel processing machine vision system for bare PCB inspection," in *Proceedings of the 24th Annual Conference of the IEEE Industrial Electronics Society, IECON '98*, vol. 3, pp. 1346–1350, 1998.

[111] H. G. Langbotham, P. Yan, H. N. Kothari, and J. Zhou, "Nondestructive reverse engineering of trace maps in multilayered PCBs," in *Conference Record AUTOTESTCON '95. 'Systems Readiness: Test Technology for the 21st Century'*, pp. 390–397, 1995.

[112] J. J. Hunter, J. Graham, and C. J. Taylor, "User programmable visual inspection," *Image and Vision Computing*, vol. 13, pp. 623–628, 1995.

[113] H. R. Myler and A. R. Weeks, *The Pocket Handbook of Image Processing Algorithms in C*. Prentice Hall, first ed., 1993.

[114] M. Robert, J. P. Bonnaure, M. Paindavoine, and S. Hafdi, "Design of an image processing integrated circuit for real time edge detection," in *Proceedings Euro ASIC '92*, pp. 280–283, 1992.

[115] M. Basu, "Gaussian-based edge-detection methods—a survey," *IEEE Transactions on Systems, Man and Cybernetics*, vol. 32, no. 3, pp. 252–260, 2002.

[116] H. Feng, F. Ercal, and F. Bunyak, "Systolic algorithm for processing RLE images," in *IEEE Southwest Symposium on Image Analysis and Interpretation*, pp. 127–131, 1998.

[117] A. M. Ahmad, D. Y. Chen, and S. Y. Lee, "Robust object detection using cascade filter in MPEG videos," in *Proceedings of the IEEE Fifth International Symposium on Multimedia Software Engineering (ISMSE'03)*, pp. 196–203, 2003.

[118] G. Deng and L. W. Cahill, "An adaptive gaussian filter for noise reduction and edge detection," in *IEEE Conference Record. Nuclear Science Symposium and Medical Imaging Conference*, vol. 3, pp. 1615–1619, 1993.

[119] A. R. Rao, "Future directions in industrial machine vision: a case study of semiconductor manufacturing applications," *Image and Vision Computing*, vol. 13, no. 1, pp. 3–19, 1996.

[120] J. A. Noble, "From inspection to process understanding and monitoring: a view on computer vision in manufacturing," *Image and Vision Computing*, vol. 13, no. 3, pp. 197–214, 1995.

[121] C. H. Kung, M. J. Devaney, C. M. Huang, C. M. Kung, and Y. J. Wang, "The development of an artificial neural network embedded automated inspection quality management system," in *IEEE Instrumentation and Measurement Technology Conference*, vol. 2, pp. 865–868, 2001.

[122] K. W. Tobin, T. P. Karnowski, and R. K. Ferrell, "Image retrieval in the industrial environment," in *SPIE's 11th Annual Symposium on Electronic Imaging Science and Technology, San Jose Convention Center*, vol. 3652, pp. 184–92, 1999.